NOTICE

The quality of this microform is heavily dependent upon the quality of the original thesis submitted for microfilming. Every effort has been made to ensure the highest quality of reproduction possible.

If pages are missing, contact the university which granted the degree.

Some pages may have indistinct print especially if the original pages were typed with a poor typewriter ribbon or if the university sent us an inferior photocopy.

Reproduction in full or in part of this microform is governed by the Canadian Copyright Act, R.S.C. 1970, c. C-30, and subsequent amendments.

AVIS

La qualité de cette microforme dépend grandement de la qualité de la thèse soumise au microfilmage. Nous avons tout fait pour assurer une qualité supérieure de reproduction.

S'il manque des pages, veuillez communiquer avec l'université qui a conféré le grade.

La qualité d'impression de certaines pages peut laisser à désirer, surtout si les pages originales ont été dactylographiées à l'aide d'un ruban usé ou si l'université nous a fait parvenir une photocopie de qualité inférieure.

La reproduction, même partielle, de cette microforme est soumise à la Loi canadienne sur le droit d'auteur, SRC 1970, c. C-30, et ses amendements subséquents.

ISBN 0-315-53299-8

Canada

DIFFUSION COEFFICIENTS OF DISSOLVED GASES IN LIQUIDS

by

Chi-Fun Wong

This Thesis is Submitted to the School of Graduate Studies and Research in Partial Fulfillment of the Requirements for the Degree of Ph. D. in Chemical Engineering

UNIVERSITY OF OTTAWA

ABSTRACT

Diffusion is a very important phenomenon in all mass transfer operations. From practical considerations, the molecular diffusivity is an important transport property for the design of a separation process. From theoretical considerations, a knowledge of molecular diffusivity in liquids is useful in understanding the mechanism of diffusive transport in liquids and the structure of liquids.

In this study, an apparatus based on Taylor dispersion phenomenon was constructed for measuring diffusion coefficients of gases in liquids. The diffusion coefficients of propene were measured in the solvents n-butanol, chlorobenzene, ethylene glycol and n-octane between 298.15 K and 348.15 K and between 101.3 kPa and 6891 kPa. These data were considered new in the literature. It was generally found that the diffusivity tended to decrease with increasing pressure. However, the effect of pressure on the diffusivity was relatively small from 101.3 to 6891 kPa, and the effect became more significant at higher temperatures.

The rough hard sphere (RHS) theory was utilized to analyse the experimental data and develop a predictive equation for gas-liquid systems. Methods for estimating the parameters needed to predict the diffusivity from the RHS theory were provided.

The steady-state capillary cell method was also employed to measure the diffusivities of propene in the solvents acetic acid, acetone, n-butanol, chlorobenzene, N,N dimethyl formamide, ethyl acetate and n-octane between 278.15 K and 323.15

K and at atmospheric pressure. The solvents used in this investigation have different polarities and tendencies for molecular association. It was found that the diffusivities were reduced in associating solvents.

In this study, three new empirical correlations have been proposed for prediction of diffusivities for specified solute-solvent systems. The first is for the n-alkane systems, the second correlation is for dissolved gases in organic solvents, and the last one is for dissolved gases in water. It was found that all these correlations gave lower average absolute errors when it compared with the available correlations in the literature.

Finally, in addition to the molecular diffusivities, the gas solubilities, densities and viscosities of all eight solvents used in this study, were measured by different techniques.

ACKNOWLEDGMENTS

I wish to thank my thesis supervisor, Professor Walter Hayduk, for allowing me to work with him on this project. His guidance has fostered independent thinking and individual initiative, yet he has always been available for consultation and guidance. Words cannot express my appreciation of his help.

The help received from the technical personnel of the Chemical Engineering Department has made the experimental work possible and is gratefully acknowledged.

Finally, I wish to thank my family, especially my parents, for their love and support.

TABLE OF CONTENTS

LIST OF TABLES

LIST OF FIGURES

NOMENCLATURE

A_1, A_2, A_3	constants in the Antoine equation (4.6)
A_u, A_l	cross-sectional areas of the upper and lower capillary tubes
A_p	calibration constant in equation (5.24)
a, b	constants in equation (2.18)
B	second virial coefficient
C	constant in equation (4.3)
C_A	concentraton of solute (mass/volume)
C_m	mean concentration of solute
$C(.....)$	correction term in equation (2.9)
D	diffusion coefficient
D_{AB}	mutual diffusion coefficient (m^2/s)
D_{AB}^{SHS}	mutual diffusion coefficient for smooth hard spheres
D_{AB}^{HSG}	mutual diffusion coefficient for a low density hard sphere gas
D_{AB}^{o}	mutual diffusion coefficient at infinite dilution
D_{AW}^{o}	mutual diffusion coefficient of solute (A) in water at infinite dilution
D_{BB}	self-diffusion coefficient of solvent (B)
De	Dean number
E	constant in equation (6.2)
E_D	free activation energy for diffusion process
E_μ	free activation energy for viscous process
E_{AA}^{j}, E_{BB}^{j}	activation energies of jumping for the solute and solvent
f	constant in equation (2.32)
F	correction term in equation (2.9)
F_D, F_D^*	partition functions for equilibrium and activated state for diffusion process

F_μ, F_μ^*	partition functions for equilibrium and activated state for viscous process
$g(\sigma_{AB})$	radial distribution function in equation (2.9)
G	constant in equation (6.2)
ΔG_D	difference in Gibbs energy between the molecules in equilibrium state and those in activated state for diffusion process
ΔG_μ	difference in Gibbs energy between the molecules in equilibrium state and those in activated state for viscous process
h	Planck's constant
H	plate height
$\Delta H_A, \Delta H_B$	latent heats of vaporization for solute and solvent at normal boiling point (cal/mole)
I, J	calibration constants in equation (5.1)
j_A	mass flux of solute from diffusion process
L	length of the dispersion column
L_d	diffusion path in the capillary cell
k_1, k_2	calibration constants in equation (5.26)
k	Boltzmann constant
K	Taylor diffusion coefficient
m	mass of solute in the sample injected
m_A, m_B	molecular masses of solute and solvent
M	molecular weight
M_A, M_B	molecular weights of solute and solvent
MV	molar volume
MV_A, MV_B	molar volumes of solute and solvent
n	number density (molecules/volume)
n_A, n_B	number densities of solute and solvent
n_A^m, n_B^m	mass fluxes of solute and solvent in equation (5.8)
n_t	total flux
N	Avagadro number

N_A, N_B	numbers of carbon atoms in solute and solvent
OST	Ostwald coefficient
p_A	partial pressure of solute gas
p_p	partial pressure of solute gas at pressure, P
P	pressure
P_A, P_B	parachors of solute and solvent ($g^{1/4}cm^3/sec^{1/2}mole$)
P_c	critical pressure
P_r	reduced pressure
p_i^s	saturated vapor pressure of substance i
r	radial distance measured form the axis of tube
r_A	radius of solute molecule
Q	constnat in equation (6.4)
R	radius of the tube
R_A, R_B	radius of gyration for solute and solvent (nm)
R_c	helix radius
R_g	gas constant
Re	Reynolds number
ROB	constant in equation (5.15)
S	constant in equation (6.4)
S_i	surface tension of substance i
Sc	Schmidt number
SLP	constant in equation (5.4)
SSR	sum of square of the residuals
t	time
t_R	residence time
T	absolute temperature (K)
T'	temperature (^oF)
T_r	reduced temperature
u_x	velocity at x_m frame of reference
v_m	average velocity
v_x	velocity at x frame of reference

V	molar volume
V_1, V_p	molar volumes at one atm. and at pressure, P
V_{bA}, V_{bB}	molar volumes of solute and solvent at normal boiling point
V_{CA}, V_{CB}	critical volumes of solute and solvent
V_D	molar volume at which the diffusion is frozen
VC	volume of the capillary cell reservoir
V_i	molar volume of substance i
V_o	closed-packed hard sphere volume
V_s	rate of the gas-saturated solvent bead travelling down the capillary tube
$W_{1/2}$	the width at half the peak height
x	axial coordinate
x_m	new axial coordinate moving with the average fluid velocity
x_1, x_p	mole fractions of solute at one atm. and at pressure, P
x_l, x_r	distances of LHS and of RHS from the curve to the center line of the peak
x_A, x_B	mole fractions of solute and solvent
x_A^{ideal}	ideal gas solubility
y	direction of diffusion in equation (5.9)
z	r/R
Z	compressibility factor
Z_c	critical compressibility

Greek Letter

β	coefficient of sliding friction
γ	constant in equation (2.18)
ϵ_A	the number of solvent molecules around the central solute molecule
ε, ζ	constants in equation (2.26)
η	constant in equation (2.32)

κ	coefficient of compression
κ_1, κ_2	constants in equation (3.1)
κ_3, κ_4	constants in equation (3.2)
λ	jump distance for rate process
λ_1	distance between two adjacent layers
λ_2	distance between two neighboring molecules in a layer perpendicular to the direction of motion
λ_3	distance between two neighboring molecules in a layer in the direction of motion
μ	viscosity of solution
μ_B	viscosity of solvent (B)
μ_W	viscosity of water
ν	constnat in equation (2.38)
ξ	frictional coefficient
ϖ	constant in equation (6.11)
ρ	density, total mass concentration
ρ_B	density of solvent (B)
ρ_1, ρ_p	densities at one atm and pressure, P
ρ_C	critical density
ρ_{Al}	effective mass concentration of solute (A) in solution
σ_A, σ_B	molecular diameters of solute and solvent
σ_{AB}	average collision diameter of the solute and solvent molecules
τ	variance
ϕ	ratio of the helix radius to the tube radius
Φ	association parameter in Wilke and Chang correlation
φ, χ	constants in equation (4.1)
ψ	packing factor for hard sphere assemblies
Ω	period of oscillation
ω	Pitzer's Acentric factor
ω_A	mass fraction of solute
ω_{Ao}	mass fraction of solute at $L_d = 0$

ω_{AL_d}	mass fraction of solute at L_d

Chapter 1

INTRODUCTION

Molecular diffusion refers to the net transport of material within a single phase which results strictly from the random thermal motion of molecules, and excludes mixing caused by any mechanical means whatsoever or by convection. Molecular diffusion is caused by a gradient in chemical potential, which results in the diffusion of a species from a region of higher chemical potential to a region of lower chemical potential. Since the gradient of chemical potential is difficult or impossible to measure experimentally, the concentration gradient is usually utilized in diffusion equations. When a concentration gradient occurs in a solution, it causes a diffusive flux which acts to bring the solution to a uniform concentration. Based on the Fick's first law, the proportionality constant between the diffusive flux and the concentration gradient is called the diffusion coefficient or diffusivity.

Diffusion plays a decisive role in many chemical processes involving mass transfer, such as distillation, solvent extraction, absorption, chemical reaction etc.. In all the mass transfer operations, mass transfer occurs between two phases separated by an interface through which material passes by the mechanism of molecular

diffusion. For instance, distillation involves the vapor and liquid phases, liquid extraction involves two immiscible liquid phases and absorption involves the gas and liquid phases. In each case, a concentration gradient is the driving force for the molecular diffusion. Diffusion is also important in many other fields, as for example, in biological systems, in certain aspects of pollution control, and in the separation of isotopes.

From practical considerations, the molecular diffusivity is an important transport property for predicting the mass transfer coefficient for the design of a separation process. From theoretical considerations, a knowledge of molecular diffusivity in liquids is useful in understanding the mechanism of diffusive transport in liquids and the structure of liquids. It is noted that the study of diffusion processes in the gas phase are also important in the chemical process industries, particularly in the analysis of transfer rates in microporous catalysts of catalytic reactors. However, this research is limited to diffusion processes in liquids, and more particularly to diffusion processes for dissolved gases in liquids, to reduce the scope of this research for practical reasons.

There are two general classifications of diffusion coefficients, with special types within each classification. The nomenclature used in the literature is often confusing; therefore, the definitions of the various classes of diffusion coefficients will be summarized below. The first general class of diffusion coefficients are called inter-diffusion or mutual diffusion coefficients which can be explained based on the following experiment. When two liquid solutions containing the same species but

at different concentrations are put in contact with each other, the components will diffuse to eleminate any concentration gradients. A net flux of the various components can be observed. The diffusion coefficients which pertain in this situation are called inter-diffusion or mutual diffusion coefficients. Diffusion coefficients at infinite dilution are a special type of inter-diffusion coefficients determined for a system in which the solute species is present only in very low concentrations. The determination and correlation of diffusion coefficients at infinite dilution are the subject of this study. In this work, we shall refer to the diffusion coefficients at infinite dilution simply as diffusion coefficients or diffusivities, and shall use the notation D°_{AB} to represent them. The diffusivities at infinite dilution of each of the components in a solution represent a limiting case for the inter-diffusion coefficients.

The second general classification of diffusion coefficients are termed intra-diffusion or tracer diffusion coefficients. When there exists a solution of uniform composition, no net mass flux can be observed. However the molecules are still in dynamic motion. If it is possible to label a group of otherwise similar molecules (for example, by radioactive isotopic substitution) and observe their motion, one can obtain the intra-diffusion coefficient which describes the motion of molecules within an essentially uniform environment. The self-diffusion coefficients are a special type of intra-diffusion coefficients for a system that consists of only one chemical component, and represent a limiting case for the intra-diffusion coefficients.

Diffusion coefficients in liquids are important in many theoretical and engineering calculations. Experimental diffusion coefficient data are used whenever they are

available. However, comparatively few such data have been published. In particular, there are few data at high temperatures and pressures because of the difficulties and the cost of experimentally determining them. Molecular diffusion of dissolved gases in liquids forms a special class of molecules of small size in the broad category of liquid diffusion. The first objective of this work was to measure the diffusion coefficients of propene gas in various solvents at different temperatures and pressures. The diffusivity data for these solute-solvent pairs are considered new in the literature; therefore, the measurements are intended to broaden the available data base.

The solute-solvent pairs investigated in this study are chosen for the following reasons. First, these systems are useful in industrial chemical processing. Second, the use of these diffusivity data allows one to investigate the diffusion process over a wide range of molecular sizes, shapes and masses. Third, there are no such diffusivity data available in the literature.

Diffusion in liquids is more difficult to understand than in either solids or low-density gases, because of the additional complexities introduced from different types of molecular association in liquids, a variety of molecular motion and intermolecular forces. At present, no completely theoretical equation for predicting the diffusion coefficients in liquids is available. Thus empirical and semi-empirical correlations for predicting diffusion coefficients play an important role in design calculations and for other purposes in engineering. However, the predictions based on these correlations sometimes may differ from the experimental values by more than 50%,

and most of the correlations were designed for moderate temperature range and for atmospheric pressure. It is clear that the available correlations are only partially successful, and thus the problem of accurate prediction of diffusion coefficients at different conditions still remains to be solved. The second objective of this study was to examine available predictive equations and develop correlations for predicting diffusion coefficients for some specific solute-solvent systems. Finally, the effect of pressure on diffusivity of gases in liquids has been a major component of this study.

In addition to the primary goal of data acquisition and interpretation, some contribution in the area of experimental techniques for measuring the diffusivity for a broad range of conditions was made. An apparatus was constructed for the measurement of diffusivities at high pressures and temperatures. In addition to diffusivity measurements, gas solubilities, as well as densities and viscosities of the solvents used in this study, were also measured.

Chapter 2

LITERATURE SURVEY

This chapter contains a brief review of the literature that is relevant to this study. There are three sections in this chapter. In the first section, the broad classification of diffusivity measurement methods is discussed and the critical techniques involved are reviewed. In the second section, three theories for the diffusion process in liquids which are used for analysis of the experimental data obtained in this study, are reviewed. In the last section, some important correlations for the prediction of diffusivities based on selected data from the literature, are discussed.

There is only one comprehensive review for diffusion of dissolved gases in liquids in the literature and it is by Himmelblau [1]. In this review, some of the theories and correlations which were developed at that time were discussed. Many different techniques for measuring the diffusivities of dissolved gases in liquids were also described. The author also summarized the gas-liquid diffusivity data available in the literature up to 1964.

2.1 Experimental Techniques and Devices

Different techniques have been employed for the measurement of diffusion coefficients of dissolved gases in liquids as reported in the literature. It is noted however that the diffusivity data reported in the literature show large variations, in certain instances, depending on which technique or device is used. This fact indicates that at least some of the devices used do not give reliable diffusivity results.

The most widely used methods to determine molecular diffusion coefficients of dissolved gases in liquids are to measure the mass transfer rate of gas into or out of a liquid phase, or to measure concentration gradients along the path of diffusion. Almost all the methods employ Fick's first and/or second laws as a basis for determining the diffusion coefficients. The difference between the methods lies mainly in the boundary conditions and in the analytical procedures used. Difficulties encountered during measurement have often arisen because of convection currents or bulk movement of the test solution due to vibration, or temperature fluctuation.

2.1.1 Methods for the Measurement of Diffusivities of Dissolved Gases in Liquids

Diffusivity measurement techniques can be classified depending on whether the solvent is flowing or is stagnant. The various techniques are further classified as follows:

A. Liquid in motion

I. gas absorption in laminar flow systems

1. laminar jet

2. wetted wall column

3. flow over a wetted sphere

II. Taylor dispersion in a capillary tube

B. Quiescent liquid

I. diaphragm cell technique with diffusion through pores of the diaphragm

II. open-tube technique with non-steady state absorption rate determined volumetrically through the gas-liquid interface

III. techniques utilizing capillaries

1. diaphragm consisting of multiple capillaries

2. steady-state capillary cell

3. single open-ended capillary cell operated in a transient desorption mode

IV. bubble dissolution technique with gas absorption from gas bubble

1. bubble adhering to a flat surface

2. for a constant bubble size

For all the techniques mentioned above, the concentration gradient falls into one of three categories: (1) steady-state, corresponding to a concentration gradient which,

once established, is time independent; (2) pseudo-steady state, which shows some time variation, but closely approximates a steady-state process and (3) non-steady state, which is time dependent or transient. Various methods have been utilized for generating the necessary concentration gradients for the various measurement techniques. Some of the experimental techniques will now be described in more detail in the following sections.

2.1.2 Description of Experimental Techniques

Gas absorption in laminar flow systems

Several different techniques have been devised for determining diffusion coefficeints of gases in liquids by measuring gas absorption rates in solvents which are in laminar flow under precisely controlled conditions. In these methods, if the absorption rate can be independently measured and the velocity profile in the liquid can be accurately described, the rate of molecular diffusion into the exposed liquid surface can be determined. A commonly used device involves the laminar flow of solvent in the form of a jet of circular cross-section [2] - [11], another involves a wetted-wall column [12] - [15] and a third device involves the flow of a thin film over a sphere [16]. All these techniques have a non-steady state concentration gradient at the solvent surface, and they have the advantages of being fast and being relatively insensitive to mechanical vibrations as well as to minor fluctuations in temperature and/or minor changes in the concentration gradient. Unfortunately, end effects are often very significant in these devices because they cause some uncertainty in the

velocity profiles at the inlet and outlet. The uncertainty in hydrodynamics results in deviations from the idealized hydrodynamic models which are used for calculation of the diffusion coefficients. The other limitation of these techniques is that the accuracy of the measured diffusivity depends greatly upon the accuracy of the gas solubility data which pertains. An error of 1% in the gas solubility will introduce an error of about 2% in the calculated diffusivity.

Taylor dispersion technique

In this technique, a small sample of a dilute solution is introduced as a pulse into a solvent which is in steady laminar flow through a capillary tube. According to the analyses of Taylor [17,18] and Aris [19], the combination of flow in the axial direction and molecular diffusion in the radial direction causes the injected pulse of solute to disperse axially. At the far end of the capillary tube, the concentration distribution along the tube is considered to be gaussian, and the variance to be inversely proportional to the diffusion coefficient of the solute in the solvent. The Taylor dispersion technique was first used for measurement of diffusivities in the gas phase [20], then a number of workers modified this technique to determine diffusivities of dissolved gases in liquids [21]-[28]. The application of the Taylor dispersion technique to high temperatures and pressures has been demonstrated in a number of recent papers [28]-[32]. This technique has several advantages: (1) no gas-liquid interface is present, (2) no calibration is necessary, (3) a knowledge of gas solubility is not required, (4) it is a relatively fast method, and (5) it is

easily adaptable to extremes of temperature and pressure. This is the experimental technique utilized in this study for diffusivity measurements at elevated pressures, and a detailed description will be given in Chapter 5.

Diaphragm cell technique

A diaphragm cell consists of two chambers filled with different concentrations of solute, separated by a porous sintered-glass or metal diaphragm. When a steady-state rate of diffusion occurs across the diaphragm, then the diffusion coefficient can be determined by accurately measuring the changes in concentration on each side of the diaphragm over a specified period of time. Since the dimensions of the channels for diffusion cannot be determined by direct measurement, each cell has to be calibrated by means of a solute-solvent pair of known diffusivity. However, the cell constant is a function of viscosity and concentration of the solution involved, and therefore, the calibration must be performed using a solution having physical properties similar to the one under investigation. This is a disadvantage of the diaphragm cell technique. With sparingly soluble gases there is an inherent difficulty in measuring small concentration changes in the solutions and ensuring that there is no loss of gas on sampling the solution. A number of workers have used this techniques to measure the diffusivities of dissolved gases in liquids [33] - [38], and McCool and coworkers [39,40,41] extended this technique to measure the self-diffusion coefficients in liquids at elevated pressures.

Open-tube technique

In the open-tube technique, the diffusion ceofficient is determined by measuring the transient rate of absorption of gas through the gas-liquid interface. The experimental methods described in the literature differ mainly in the size and shape of the gas-liquid interface [42,43]. Reamer, Sage and coworkers [44] - [49] used the open-tube method to measure diffusion coefficients of methane, ethane and n-butane in liquid hydrocarbons under pressure.

Techniques utilizing multiple capillaries

Ross and Hildebrand [50] measured diffusion coefficients of gases in liquids by using a modified diaphragm cell. The 'diaphragm' consisted of a large number of capillary-sized holes drilled in a plate. Nakanishi et. al. [51] modified the 'diaphragm' so that it contained a bundle of hypodermic tubes imbedded in a solder plug. These cells required no prior calibration since the diffusion path dimensions were known; thus the diffusivity could be calculated directly from a knowledge of the gas absorption rates.

Recently, Comb and Field [52,53] proposed a technique which combined the open-tube technique and the multiple-capillary diaphragm technique, for measuring diffusion coefficients of gases in liquids. In this method, the gas solubilities and diffusion coefficients can be simultaneously determined.

Steady-state capillary cell technique

The steady-state capillary cell techinque for measuring diffusion coefficients of gases in liquids was developed by Hayduk and coworkers [54] - [61]. A column of degassed solvent is confined in a capillary, one end of which is connected to a reservoir of degassed solvent and the other is exposed to dissolving gas. The flux of gas is measured by observing the movement of a gas-saturated solvent bead in the capillary. Based on the gas solubility and the shrinkage rate of gas inside the capillary, the diffusion coefficient can be determined. This technique does not require any chemical analysis and the structure of the cell and the experimental procedure are relatively simple. Therefore, it is employed for the measurement of diffusion coefficients at atmospheric pressure in this study, and a detailed description will be presented in Chapter 5.

Open-ended capillary cell technique

The open-ended capillary cell technique involves the transient effusion of solute from a capillary into a much large volume of solvent. The technique becomes disfavour because of the analytical difficulty of determining the exact amount of solute in an extremely small volume of solution, and also because the end effects of this technique were found to be significant introducing errors in the results. The use of the open-ended capillary cell technique for self-diffusion and mutual diffusion coefficients measurements had been extended to high pressures by Hildebrand and coworkers [62,63]. Naghizadeh and Rice [64] utilized the same method to measure

self-diffusivities of several liquidified gases at elevated pressures.

Gas bubble dissolution technique

The gas bubble dissolution technique involves suspending a small gas bubble in a degassed solvent and measuring the rate of shrinkage of the bubble which is equivalent to measure the gas absorption rate. The gas bubble dissolution technique is assumed to obey a pseudo steady-state boundary condition. This technique is attractive because it gives a direct measurement of the gas absorption rate, it is rapid, and it is also relatively easy to analyse because of the essentially spherical geometry of the liquid surrounding the bubble. However, this technique is very sensitive to vibration and other sources of convection. A number of workers used this technique for the measurement of diffusivities [65]-[72]. De Blok and Fortuin [73] reduced convection resulting from the shrinking effect in the gas bubble dissolution technique by maintaining the gas bubble at a constant size. This was made possible by adding gas through a syringe needle.

This concludes a brief survey of the measurement techniques for diffusion coefficients of dissolved gases in liquids.

2.2 Theories Concerning Diffusion in Liquids

The structure of liquids is complicated by the dense packing of the molecules; the time-average distance between molecules in liquids is very small so that intermolecular forces are significant. However, the effects of these intermolecular forces

cannot be easily taken into account mathematically, because the molecules are not confined to fixed lattice sites as they are in solids. Therefore, the diffusion in liquids is more difficult to understand than in either solids or dilute gases. Various theoretical models of the diffusion process in liquids have been reported. However, none of these theoretical approaches has yielded equations that can predict diffusion coefficients with satisfactory accuracy for all systems. The most important contribution of these theoretical models is to provide a basis for correlation and extrapolation of data. In this section, three theoretical approaches for diffusion in liquids are presented, namely, the hydrodynamic theory, the Eyring rate theory, and the kinetic theory of rough hard spheres. These three approaches will be used in Chapter 6 in the interpretation of experimental results.

2.2.1 Hydrodynamic Theory

For a single particle moving in a fluid medium, Brownian motion theory shows that for the case where there is no correlation of molecular motions, the diffusion coefficient is inversely proportional to the frictional coefficient ξ.

$$D_{AB} = \frac{kT}{\xi} \tag{2.1}$$

The above equation is also known as the Nernst-Einstein equation and is the starting point for the hydrodynamic theory.

It was shown that the ξ can be calculated for a rigid sphere of radius r_A, moving

through medium B having shear viscosity of μ_B, from classical hydrodynamics [74]:

$$\xi = 6\pi\mu_B r_A \left(\frac{2\mu_B + r_A\beta}{3\mu_B + r_A\beta}\right) \tag{2.2}$$

In the above equation, β is the coefficient of sliding friction between the diffusing molecule and its surroundings. There are two possible limiting forms, namely:

1. When there is no tendency for the fluid to slip over the surface of the sphere, $\beta = \infty$ for this situation; therefore equation (2.1) becomes

$$D_{AB} = \frac{kT}{6\pi\mu_B r_A} \tag{2.3}$$

   This is the well known Stokes-Einstein equation and is known to apply for the case where the size of the solute molecules is very large compared to the size of the solvent molecules.

2. When the fluid slips over the surface of the sphere, then $\beta = 0$, and the equation (2.1) reduces to:

$$D_{AB} = \frac{kT}{4\pi\mu_B r_A} \tag{2.4}$$

   This equation may be expected to give a better correlation for data for solute-solvent pairs for which the molecular sizes are comparable.

There have been many attempts to develop a rigorous hydrodynamic approach to diffusion, but the problems involved are many, both conceptually and computationally. For example, the Stokes-Einstein equation applies, at best, only for the case where the size of solute molecules is much larger than those of the solvent; that is not true for the gas-liquid systems investigated in this work. In this research,

the size of solute molecules was slightly smaller than those of the solvents. Also, if the solute is not spherically symmetrical, then three frictional coefficients instead of one are required [75].

Although the hydrodynamic approach is based on an over-simplification of liquid structure, it has provided the starting point for many empirical correlations, such as Wilke-Chang correlation.

2.2.2 Eyring Rate Theory

The Eyring rate theory attempts to explain diffusion and other transport phenomena in a way analogous to the activated state approach to kinetic reaction rate constants. The development is based on the hole theory of the liquid state which describes diffusion as a process in which molecules move from a given position into an adjacent hole in the liquid structure.

The first application of the rate theory to diffusion process was given by Eyring [76]. By assuming that the liquid maintains a lattice type structure, it is possible to express the diffusion coefficient as [77]:

$$D_{AB} = \frac{F_D^{\bullet}}{F_D} \lambda^2 \frac{kT}{h} \exp\left(\frac{-\Delta G_D}{R_g T}\right) \tag{2.5}$$

In this equation, λ is a jump distance, and ΔG_D is the difference in Gibbs energy between the "normal" molecules and those in the activated state. This approach has had success as the basis of several predictive equations, such as that of Olander [78] and Akgerman and Gainer [79,80], because the diffusion coefficient is observed to

follow the exponential dependence of equation (2.5) over a fairly wide temperature range.

The chief use of the Eyring rate theory arises when it is combined with Eyring's expression for viscosity:

$$\mu = \frac{F_\mu}{F_\mu^*} \frac{\lambda_1}{\lambda_2 \lambda_3 \lambda^2} h \exp\left(\frac{\Delta G_\mu}{R_g T}\right) \tag{2.6}$$

In the above expression, λ_1 is the distance between two adjacent layers, λ_2 and λ_3 are the distances between two neighboring molecules in a layer perpendicular to, and in the direction of motion, respectively. Combining equations (2.5) and (2.6), the result is:

$$D_{AB} = \frac{kT}{\mu} \frac{F_D^*}{F_D} \frac{F_\mu}{F_\mu^*} \frac{\lambda_1}{\lambda_2 \lambda_3} \exp\left(\frac{\Delta G_\mu - \Delta G_D}{R_g T}\right) \tag{2.7}$$

By assuming that (1) the processes of diffusive and viscous flows are identical, so $F_D = F_\mu$, $F_D^* = F_\mu^*$ and $\Delta G_D = \Delta G_\mu$, and (2) the intermolecular distance can be related to the molar volume as:

$$\lambda_1 = \lambda_2 = \lambda_3 = \left(\frac{V}{N}\right)^{1/3}$$

Thus, equation (2.7) becomes:

$$D_{AB} = \frac{kT}{\mu} \left(\frac{N}{V}\right)^{1/3} \tag{2.8}$$

There is experimental evidence suggesting that values predicted utilizing Eyring's approach in the form of equation (2.8) are not accurate. Thus, equation (2.8) only gives value of diffusivity, of the correct order of magnitude.

2.2.3 Rough Hard Sphere Theory

The rough hard sphere (RHS) approach to diffusion and other transport properties is one specific result in the broad field of kinetic theories. In compact form, the RHS mutual diffusion coefficient is obtained as the product of four terms:

$$D_{AB} = D_{AB}^{HSG} \frac{1}{g(\sigma_{AB})} C(\sigma_A, \sigma_B, m_A, m_B, V) F \tag{2.9}$$

The rough hard sphere approach begins with an analytical expression for diffusion in a dilute gas, scales this expression to the moderately dense region with the radial distribution function $g(\sigma_{AB})$, then applies two more correction terms, C and F, accounting for correlated motions and exchanges of rotational and kinetic energies. The terms in equation (2.9) are discussed briefly:

The first term D_{AB}^{HSG} is the mutual diffusion coefficient for a low density hard sphere gas. The expression for D_{AB}^{HSG} was derived by Chapman and Enskog [82] with the following assumptions:

1. molecules are spherically symmetrical and smooth.
2. the mean free path is large compared to the diameters of the molecules.
3. all collisions are binary.
4. the collisions are perfectly elastic and instantaneous.
5. there is no correlation between position and velocity vectors of molecules.
6. there are no force fields affecting the molecules on their flight between collisions.

For the above conditions, the expression of D_{AB}^{HSG} can be written as [82]:

$$D_{AB}^{HSG} = \frac{3}{8n\sigma_{AB}^2}\left[\frac{kT}{2\pi}\left(\frac{m_A + m_B}{m_A m_B}\right)\right]^{1/2} \tag{2.10}$$

In the above expression, n is the number density (molecules/volume), σ_{AB} is the average collision diameter of the solute and solvent molecules and m_A and m_B are the molecular masses of solute and solvent.

As the density of the fluid increases, the assumptions of no correlation between position and velocity vectors of molecules and binary collisions are not applicable for real molecules. Enskog [82] showed that:

$$\frac{nD_{AB}}{(nD_{AB}^{HSG})^{\circ}} = \frac{1}{g(\sigma_{AB})} \tag{2.11}$$

In this equation, nD_{AB} is the number density times the diffusivity at moderate density, and $(nD_{AB})^{\circ}$ is the same quantity at low density, and $g(\sigma_{AB})$ is the radial distribution function for hard spheres evaluated at a particular contact distance. The effect of $g(\sigma_{AB})$ is to correct the dilute gas diffusivity for the increased frequency of collision in the denser gas.

The radial distribution function $g(\sigma_{AB})$ can be considered as a correction term relating diffusivities in dilute gas to that in moderately dense gas. This function depends on the composition and molar volume of the mixture and on the diameters of the constituent molecules. For an infinitely dilute solution, $g(\sigma_{AB})$ can be obtained by using the following expression [83]:

$$g(\sigma_{AB}) = \frac{1}{1-\psi} + \frac{3\psi\sigma_A}{(1-\psi)^2(\sigma_A + \sigma_B)} + \frac{\psi^2\sigma_A}{2(1-\psi)^3\sigma_B} \tag{2.12}$$

In the above expression, ψ is the packing factor for hard sphere assemblies. For the infinitely dilute case ($n_A = 0$), ψ can be obtained by using the following expression [83]:

$$\psi = \frac{\pi n_B \sigma_B^3}{6} \tag{2.13}$$

At liquid densities, it is found that the assumption of uncorrelated velocities breaks down completely. The diffusion coefficients calculated from the first two terms of equation (2.9) were found to differ significantly from experimental values. The deviation from the Chapman-Enskog theory is considered to result from two phenomena, namely backscattering and vortex motion. At high densities ($\rho > 1.5\rho_c$) and for low solute to solvent mass ratios, the diffusion coefficient is decreased by backscattering. It is considered that the solute is temporarily trapped in a "cage" for a time corresponding to several collisions before it can move on. At somewhat lower liquid densities ($\rho < 1.5\rho_c$) and of higher solute to solvent mass ratios, it has been shown that a vortex of neighbor molecules forms around the diffusing molecule, acting to increase its diffusion coefficient (and velocity) above that predicted by Chapman-Enskog theory [28]. The term $C(\sigma_A, \sigma_B, m_A, m_B, V_B)$ in equation (2.9) corrects the Enskog theory for densities in the region of liquid densities for backscattering and vortex formation. The factor C is defined as:

$$C(\sigma_A, \sigma_B, m_A, m_B, V) = \frac{D_{AB}^{SHS}}{(D_{AB}^{HSG}/g(\sigma_{AB}))} \tag{2.14}$$

In the above expression, D_{AB}^{SHS} represents the diffusion coefficient of smooth hard-spheres. The factor C cannot be obtained analytically. Chen et. al. [25] reported

the values of C for various solute-solvent mass and size ratios at various specific volumes by interpolating or extrapolating from existing computer simulation results on hard-sphere fluids.

In collisions between polyatomic molecules, it is possible that kinetic and rotational energy can be exchanged, violating the smoothness assumption of the Enskog theory. Chandler [84] has discussed this phenomenon and has shown that a roughness factor F should be introduced to account for this. The effect of coupling between rotational and kinetic energy is to reduce the diffusion coefficient, so that:

$$0 \leq F \leq 1 \tag{2.15}$$

The constant, F, is essentially independent of density and temperature. Several workers [83,84] proposed values of F for different systems.

Dymond [85] has shown that computer calculations for self-diffusion coefficients of hard sphere molecules can be fitted accurately to the following expression:

$$D = \frac{2.306 \times 10^{-5}(T/M)^{1/2}}{V_o^{2/3}}(V - 1.384V_o) \tag{2.16}$$

In this equation, M is the molecular weight, V is the molar volume of the liquid solution and V_o is the closed-packed hard sphere volume defined as:

$$V_o = \frac{N\sigma_B^3}{\sqrt{2}} \tag{2.17}$$

Based on Dymond's result, Chen et. al. [26] and Matthews [28] have introduced an expression which is equivalent to equation (2.9) in terms of the molar volume of

the solution.

$$\frac{D_{AB}}{\sqrt{T}} = \frac{const.}{\sigma_{AB}^2}\left(\frac{m_A + m_B}{m_A m_B}\right)^{1/2}[a(V - bV_o)] = \gamma[V - V_D] \qquad (2.18)$$

In the above expression, a is a constant for a given solute-solvent pair and the constant b has been found empirically to be 1.358 [75]. For infinite dilution diffusion coefficients, the constant, V_D, should depend only on the solvent. The constant, γ, will depend on both the solute and the solvent, and should be inversely proportional to the σ_{AB}^2 and the square root of the reduced mass $(m_A + m_B)/m_A m_B$.

The RHS theory has been shown to be useful in interpreting diffusivity data in a number of systems. The physical approach of the RHS theory, while imperfect, is perhaps more sound than those for the hydrodynamic or Eyring rate theories.

2.3 Correlations for Prediction of Diffusion Coefficients at Infinite Dilution

In the absence of a satisfactory theory of the liquid state, it is not possible to provide any exact picture of the diffusion phenomenon in liquids. Therefore, no completely successful theoretical equation for predicting diffusivities in liquids has yet been developed. A large number of correlations are found in the literature for prediction of diffusion coefficients in liquids, however, most of these correlations are either semi-empirical or entirely empirical in nature, and they all have certain limitations regarding the classes of liquids and/or the temperature ranges in which they can be applied. Most of the correlations are based on properties that can be readily measured or estimated such as viscosity, molar volume etc.. Ghai, Ertl and

Dullien [86,87], Reid et. al. [88,89], and Hayduk [90] reviewed the correlations that were developed for predicting diffusivities at infinite dilution.

The diffusion coefficient of a solute at infinite dilution in a solvent implies that each solute molecule is in an environment of essentially pure solvent. In engineering work, a diffusion coefficient at infinite dilution, D^{o}_{AB}, is considered to be applicable for concentrations of solute of up to 5, or perhaps 10 mole percent.

Some of the important or recently developed correlations for prediction of diffusivities at infinite dilution are reviewed in this section and are discussed under the following headings:

1. general correlatons for all types of solutes in all types of solvents.

2. correlations for dissolved gases in liquids.

3. correlations for liquid n-alkane systems.

4. correlations for water as solvent.

The purpose for making the different classifications is that correlations devised for a limited amount of data for chemically similar systems usually yield a lower error of prediction, or are simplier in form, than those for general case that includes widely different solvent and solute properties. To keep the correlations in their original forms, the units of the diffusivity are retained as cm^2/s, of the viscosity as cp, and of the molar volume as $cm^3/mole$ and are used for the correlations presented in the following subsection.

2.3.1 General Correlations for Prediction of Diffusivities at Infinite Dilution in Liquids

Wilke and Chang correlation

Wilke and Chang [91] developed a classic correlation which is one of the most widely used and referred to in the literature. The Wilke-Chang equation is an empirical modification of the Stokes-Einstein equation. The correlation can be expressed by the general equation as:

$$D^{\circ}_{AB} = 7.4 \times 10^{-8} \frac{(\Phi M_B)^{1/2} T}{\mu V_{bA}^{0.6}} \tag{2.19}$$

In the above equation, μ is viscosity of solution in centipoise, and Φ is the association parameter. The authors proposed that $\Phi = 1.0$ for non-associated solvents, $\Phi = 2.6$ for water, $\Phi = 1.9$ for methanol, and $\Phi = 1.5$ for ethanol, and defined ΦM_B being the 'effective molecular weight' with respect to the diffusion process.

Hayduk and Laudie [59] examined the literature data for diffusion in aqueous solution at 298.15 K. They proposed that a revised association parameter for water of 2.26 instead of 2.6 improves the accuracy of the Wilke-Chang equation for diffusivities in water. An average error of about 10% was noted when 285 data were tested by the authors. However, it has been found that this correlation should not be used when the solute is water and for highly viscous solvents.

King, Hsueh and Mao correlation

King, Hsueh and Mao [92] presented a correlation which was based upon the empirical observation that $D\mu/T$ was nearly constant for self-diffusion. They utilized the latent heats of vaporization as a measure of the intermolecular forces involved. The expression is:

$$D^{\circ}_{AB} = 4.4 \times 10^{-8}\left(\frac{T}{\mu_B}\right)\left(\frac{V_{bB}}{V_{bA}}\right)^{1/6}\left(\frac{\Delta H_B}{\Delta H_A}\right)^{1/2} \tag{2.20}$$

This correlation has worked satisfactorily for solutes which have a small molecular size or are polar, but it still results in serious error for polar solvents of high viscosity. Also, it is found generally inaccurate for diffusion coefficients in aqueous systems.

Tyn and Calus correlation

Based on Stokes-Einstein equation, Tyn and Calus [93] utilized the ratios of the molecular sizes and of the parachors as measures of molecular interaction and they proposed the following correlation:

$$D^{\circ}_{AB} = 8.93 \times 10^{-8}\left(\frac{V_{bA}}{V_{bB}^2}\right)^{1/6}\left(\frac{P_B}{P_A}\right)^{0.6}\left(\frac{T}{\mu_B}\right) \tag{2.21}$$

The parachor is related to the liquid surface tension as follows:

$$P_i = V_i S_i^{1/4} \tag{2.22}$$

In the above expression, S_i is the surface tension in $dynes/cm$, and V_i is the molar volume in cm^3/mol, both measured at the same temperature. It has been found that over a moderate temperature range, the parachor is essentially constant.

When using the Tyn-Calus correlation, several specific rules are noted: (1) The correlation should not be used for diffusion in viscous solvents ($\mu_B > 20cp$); (2) If the solute is water diffusing in organic solvents, the water is considered to be a dimer so that appropriate values of V_A and P_A should be used; (3) If the solute is an organic acid and the solvent is other than water, methanol or butanol, the acid should be considered as a dimer with double the values of V_A and P_A; (4) For nonpolar solutes diffusing in monohydroxy alcohols, the value of V_B and P_B should be multiplied by a factor equal to $8\mu_B$,where μ_B is the solvent viscosity in centipoise.

This correlation was tested by Reid et. al. [89] for a number of systems. They concluded that this equation gave estimates of diffusivity with errors normally less than 10%.

Hayduk and Minhas correlation

Hayduk and Minhas [94] modified the Tyn and Calus correlation to get slightly improved results. Their correlation based on the parachor values is:

$$D^{o}_{AB} = 1.55 \times 10^{-8} T^{1.29} \mu_B^{-0.92} V_{bB}^{-0.23} P_A^{-0.42} P_B^{0.5} \tag{2.23}$$

The same authors also used the molecular radius of gyration, R, to describe the effects of molecular size and shape on the diffusion process in liquids and proposed an equation as follow:

$$D^{o}_{AB} = 6.916 \times 10^{-10} T^{1.7} \mu_B^{-0.8} R_A^{-0.4} R_B^{0.2} \tag{2.24}$$

Equation (2.23) was tested for 756 data and average error of 13.9% was reported by the authors. It is important to note that when using the Hayduk-Minhas correlation, the same specific rules apply as in the Tyn-Calus correlation.

Siddiqi and Lucas correlation

Siddiqi and Lucas [95] developed a correlation based on the assumption that the viscosity of the solvent and the molecular volumes at the boiling point of the solute and solvent are adequate measures for the intermolecular forces associated with the diffusion process. The working equation for organic liquid mixtures is :

$$D^{\circ}_{AB} = 9.89 \times 10^{-8} T \mu_B^{-0.907} V_{bA}^{-0.45} V_{bB}^{0.265} \tag{2.25}$$

This equation was tested for 1275 data points and an average error of 13.1% was reported by the authors.

2.3.2 Correlations for Prediction of Diffusivities of Dissolved Gases in Liquids

Hayduk and Cheng correlation

Hayduk and Cheng [56] proposed a hypothesis that diffusivity of a solute in a dilute solution depended only on the solvent viscosity. A relation of the following form has been found to apply to systems in which there is no association or complexing.

$$D^{\circ}_{AB} = \varepsilon \mu_B^{\zeta} \tag{2.26}$$

In the above equation, ε and ζ are constants which are only dependent on the solute properties. This equation is useful to predict diffusivities of a solute in various solvents if diffusivity values are known in at least two solvents of known viscosities.

Akgerman and Gainer equation

Akgerman and Gainer [79,80] developed an equation for prediction of diffusion coefficients of dissolved gases in liquids. This correlation was based on the absolute rate theory of Eyring, and the working equation is:

$$D^{o}_{AB} = \frac{kT}{\epsilon_A \mu_B}\left(\frac{N}{V_{bB}}\right)^{1/3}\left(\frac{M_B}{M_A}\right)^{1/2}\exp\left(\frac{E_\mu - E_D}{R_g T}\right) \tag{2.27}$$

In the above equation, ϵ_A is the number of solvent molecules around the central solute molecule A, and it was defined by the authors as:

$$\epsilon_A = 6\left(\frac{V_{bA}}{V_{bB}}\right)^{1/6} \tag{2.28}$$

The activation energy difference is calculated from the jump energies associated with different molecules.

$$E_\mu - E_D = E^j_{BB}\left[1 - \left(\frac{E^j_{AA}}{E^j_{BB}}\right)^{\frac{1}{\epsilon_A+1}}\right] \tag{2.29}$$

In the above expression, E^j_{AA} and E^j_{BB} are the jump energies for solute and solvent respectively, and these are calculated from the following equations:

$$E^j_{BB} = -\frac{R_g \ln\left(\frac{\mu_2}{\mu_1}\right) + \frac{R_g}{2}\ln\left(\frac{T_1}{T_2}\right)}{\frac{1}{T_1} - \frac{1}{T_2}} \tag{2.30}$$

$$E^j_{AA} = 5875.3 M_A^{-0.186} \tag{2.31}$$

This equation can be used for small gas molecules such as hydrogen and helium and for solvents having high viscosities ($\mu_B > 5cp$).

Sovová correlations

Sovová [96] applied the hypothesis proposed originally by Hayduk and Cheng [56] to develop correlations. The general working equation is:

$$D^{\circ}_{AB} = 14.8 \times 10^{-5} \frac{f \mu_B^{\eta}}{V_A^{0.6}} \tag{2.32}$$

In the last expression, f=1.0 and η=-1.15 for water as solvent, f=1.8 and η=-1.15 for solvents of aromatic hydrocarbons and their derivatives and f=2.28 and η=-0.50 for solvents of aliphatic hydrocarbons and alcohols.

Sridhar and Potter correlation

Sridhar and Potter [97] combined Hildebrand's expression for gas-liquid diffusion and Dullien's expression for self-diffusion; they came up with a correlation for diffusivities of gases in liquids. The expression is:

$$D^{\circ}_{AB} = 0.088 \frac{V_{CB}^{4/3}}{N^{2/3}} \frac{R_g T}{\mu_B V^{*}} \frac{1}{V_{CA}^{2/3}} \tag{2.33}$$

The value V^{*} is determined as follows:

$$V^{*} = 0.31 V_{CB} \tag{2.34}$$

This correlation should not be used for gases like hydrogen and helium.

Umesi and Danner correlation

Umesi and Danner [98] developed a correlation for predicting diffusivities of hydrocarbon gases in nonpolar solvents. Those authors ulitized the radius of gyration to define the size-shape relationship which was considered to be the predominant factor in determining the diffusivity. The expression is:

$$D^{\circ}_{AB} = 2.75 \times 10^{-8} \frac{T}{\mu_B} \left[\frac{R_B}{R_A^{2/3}} \right] \tag{2.35}$$

The equation can be extended to the cases of dilute nonpolar or polar solutes diffusing in nonpolar solvents.

2.3.3 Correlations for Prediction of Diffusivities of n-Alkane Systems

Lo correlation

Lo [99] studied the binary systems of several n-alkanes. He gave the following relationship between mutual diffusion coefficient at infinite dilution and self-diffusion coefficient of the solvent (D_{BB}).

$$D^{\circ}_{AB} = D_{BB} + \frac{1}{0.1964 - 0.06785 N_B} \times 10^{-5} \log \frac{N_A}{N_B} \tag{2.36}$$

In this equation, N_A and N_B are the numbers of carbon atoms in the solute and in the solvent respectively. This correlation is limited for prediction of diffusivity to substance for which the self-diffusivity is known as a function of temperature. A shortage of the necessary data in the literature for self-diffusion coefficients greatly

limits the application of this correlation. An average error of 3.46% was reported by the authors based on 27 systems.

Hayduk and Minhas correlation

Hayduk and Minhas [94] developed a correlation from a viscosity-diffusivity 'map' for n-alkanes. The following correlation was proposed:

$$D^{\circ}_{AB} = 13.3 \times 10^{-8} T^{1.47} \mu_B^{\frac{10.2}{V_{bA}} - 0.791} V_{bA}^{-0.71} \tag{2.37}$$

The above equation was tested by means of 58 data for solutes ranging from pentane to dotriacontane and for solvents ranging from pentane to hexadecane. An average error of 3.4% was reported by the authors.

Chen and Chen correlation

Chen and Chen [100] proposed an empirical correlation for binary systems involving long-chain hydrocarbons. The correlation was:

$$D^{\circ}_{AB} = 1.0 \times 10^{-9} \frac{T}{\mu_B} V_{bB}^{2/3} \nu \left(\frac{11.96}{V_{bA}^{1/3}} - 0.8796 \right) \tag{2.38}$$

In the above equation, ν is a parameter depending on the group of solutes and solvents. For example, it is equal to one for n-alkane solvents. The authors reported that the average error was 5.8 % for n-alkane systems based on 84 data points.

Matthews correlation

Matthews [28] proposed a correlation for diffusivities for n-alkane systems based on the RHS theory. The working equation is:

$$\frac{D^{\circ}_{AB}}{\sqrt{T}} = 15.8 \times 10^{-9} M_A^{-1.56} \left(\frac{\sigma_A}{\sigma_B}\right)^{2.99} (V_B - V_D) \tag{2.39}$$

The constant, V_D, is estimated as follows:

$$V_D = 0.308 V_{CB} \tag{2.40}$$

In the above equation, D°_{AB} is in m^2/s, T is in K and molar volumes are in $\times 10^{-6} m^3/mol$. An average error of 5.5% was reported by the author.

2.3.4 Correlations for Prediction of Diffusivities in Water

Othmer and Thakar correlation

Othmer and Thakar [101] developed a correlation for predicting diffusion coefficients of various solutes in dilute water solutions based on the Eyring rate theory. The expression is:

$$D^{\circ}_{AW} = \frac{14.0 \times 10^{-5}}{\mu_W^{1.1} V_{bA}^{0.6}} \tag{2.41}$$

Hayduk and Laudie [59] modified the Othmer and Thakar equation as follows:

$$D^{\circ}_{AW} = \frac{13.26 \times 10^{-5}}{\mu_W^{1.14} V_{bA}^{0.589}} \tag{2.42}$$

Those authors reported that equation (2.42) gave better results than equation (2.41)

.

Hayduk and Minhas correlation

Hayduk and Minhas [94] proposed a correlation for predicting diffusivities of various solutes in water solvent. The correlation is:

$$D^{\circ}_{AW} = (1.25V_{bA}^{-0.19} - 0.365) \times 10^{-8} \mu_W^{\frac{9.58}{V_{bA}}-1.12} T^{1.52} \tag{2.43}$$

An average error of 9.4% was reported by the authors based on 237 data points.

Siddiqi and Lucas Correlation

Siddiqi and Lucas [95] proposed a correlation for aqueous solutions including dissolved gases. The proposed equation is:

$$D^{\circ}_{AW} = 2.98 \times 10^{-7} T \mu_W^{-1.026} V_{bA}^{-0.5473} \tag{2.44}$$

An average absolute error of 19.7% for 658 data points was reported by the authors.

This concludes a brief review of the correlations for diffusion coefficients at infinite dilution for specified systems as available in the literature.

Chapter 3

DEVELOPMENT OF NEW CORRELATIONS

Investigations in which changes of only one physical variable at a time, such as temperature, pressure, or concentration of solute during measurement of diffusion coefficients are considered as fundamental tests of these particular variables on the diffusion process. These fundamental investigations are useful for understanding the diffusion process and for developing models for the diffusion process.

In this work, only diffusion coefficients at infinite dilution are considered. Thus the effect of concentration of solute on the diffusion coefficient can be considered negligible because the concentration of the solute is relatively low in every case. The correlations proposed in this chapter are for the prediction of diffusivities in liquids at atmospheric pressure, thus the effect of pressure on diffusivity is not considered at this stage. Therefore, of the variables mentioned, only the effect of temperature on diffusivity is discussed in this chapter.

Also in this chapter, three new correlations are presented for the prediction

of diffusivities for specific type of solutes and/or solvents in each case. The first correlation is for the n-alkane systems, the second is for dissolved gases in organic solvents, and the third correlation is for dissolved gases in water. These correlations are discussed and compared with correlations found in the literature. The reasons for developing correlations for specific solute-solvent systems instead of a single general correlation are that these correlations usually give better predictions of diffusivity and are simplier in form.

3.1 Effect of Temperature on Diffusivity in Liquid

Most equations developed to predict diffusivities in liquids contain the temperature-dependent variable, the liquid viscosity. Because the viscosity of liquid is highly dependent upon temperature, a test of these equations for changes of only the temperature is not possible. In the literature, only two equations can be found relating diffusivity to temperature without involving any temperature-dependent variable. The first one describes the temperature dependence of diffusivity by utilizing a form of the Arrhenius equation:

$$D = \kappa_1 \exp\left(\frac{-\kappa_2}{T}\right) \tag{3.1}$$

In the expression above, κ_1 and κ_2 are constants, and the κ_2 can be identified with E_D/R_g in which the term E_D is the free activation energy for diffusion. Equation (3.1) is based on the linear relationship observed in the plot of logarithm of diffusivity versus the reciprocal of absolute temperature. The second equation, slightly

different in form, also describes the temperature dependence of diffusivity:

$$D = \kappa_3 T \exp\left(\frac{-\kappa_4}{T}\right) \tag{3.2}$$

In this equation, κ_3 and κ_4 are also constants. Equation (3.2) is based on the work of Eyring rate theory.

In this study, the applicability of the two equations shown above was tested by means of experimental data found in the literature. The data consisted of mutual and self-diffusion coefficients at infinite dilution involving many different solute-solvent systems; for each system there were data for at least three different temperatures. Totally 296 systems (2325 diffusivity data) for gas and liquid solutes in liquid solvents were tested. The temperature range of the data was from 194.65 K to 561.65 K.

The parameters in equation (3.1) and equation (3.2) were estimated for each system by using the nonlinear least squares criterion. A computer package named NLIN from SAS library at University of Ottawa was utilized for nonlinear regression analysis, and Marquardt's method was employed in NLIN. There was no evidence of lack of fit based on the observation of residual plots. Therefore, it is considered that both equations (3.1) and (3.2) can describe the effect of temperature on diffusivity for most of the solute-solvent systems for which data are available.

Since these two equations contain the same number of parameters (two), the models can be compared by means of the sum of squares of residuals (SSR). The comparison shows that equation (3.1) gives smaller values of SSR for 156 systems, and equation (3.2) gives smaller values of SSR for 140 systems. However, the

differences of the values of SSR between two models are small; they are always less than 3% from the average values of SSR's. Therefore, there is no clear indication as to which equation is better. Figure 3.1 is a semi-logarithm plot of diffusivity versus the reciprocal of absolute temperature for self-diffusion of n-heptane at atmospheric pressure. It shows that the curves representing equations (3.1) and (3.2) give values which are very similar for temperatures between 273.15 K and 373.15 K. However, because most of the experimental data used in this test lie in the temperature range mentioned above, it is difficult to indicate which model is the better of the two based on the test performed. The other systems tested in this work gave, more or less, the same result as that shown in Figure 3.1. Therefore, it is concluded that for temperature between 273.15 K and 373.15 K both equations describe the temperature dependence of diffusivity equally well. The shortage of reliable data at extremely low and extremely high temperatures makes it difficult to evaluate the effect of temperature on diffusivity for wide ranges of temperature. Earlier, Simons and Pontor [74] examined the above two equations extensively and came to the same conclusion.

3.2 New Correlation for Prediction of Diffusivities at Infinite Dilution in n-Alkane Solutions

Diffusion in normal alkane systems is comparatively simple because the solute and solvent are not associated, and there are no complex intermolecular forces between the molecules. Hayduk and Buckley [57] stated that the mechanism of

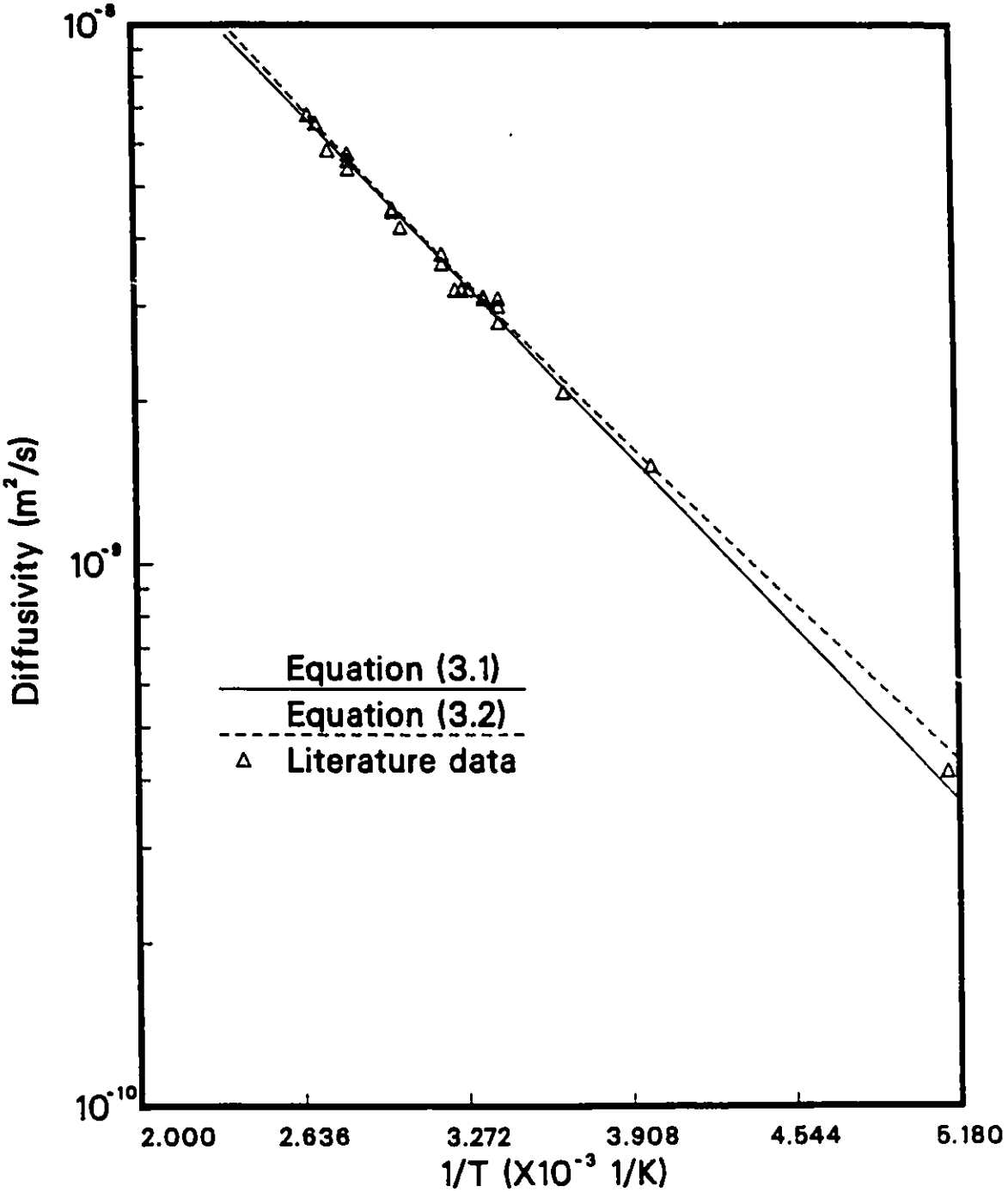

Figure 3.1: Plot of ln D°_{AB} versus 1/T for self-diffusion of n-heptane at atmospheric pressure

diffusion for long-chain hydrocarbon molecules was expected to be different from that for spherical molecules; it was considered that for long-chain molecules diffusion consisted of multiple displacements of chain segments rather than of molecules as a whole. Most of the currently available correlations were developed based on either the hydrodynamic theory or the kinetic theory; however, these diffusion theories were derived on a basis of spherical molecules. Therefore, some of the available correlations may be inadequate for n-alkane systems for which the molecules are far from spherics. It is considered possible to develop a correlation specifically for the n-alkane systems which is an improvement over existing correlations.

A new empirical correlation for prediction of mutual and self-diffusion coefficients of n-alkane solutions at infinite dilution is proposed here. This correlation was developed by using a diagnostic technique and an iterative model-building procedure.

One hundred and four data of mutual and self-diffusion coefficients for n-alkane systems at infinite dilution were collected from the literature. A listing of the references for the solute-solvent pairs used in this correlation is presented in Appendix A. The temperature range for the data was from 273.15 K to 373.15 K. All diffusivity data were measured at atmospheric pressure. The solutes ranged from pentane to dotriacontane, and the solvents ranged from pentane to octadecane. The values of the diffusivity data were from 0.32×10^{-9} to 7.30×10^{-9} m^2/s.

The correlation was started by using a form of equation equivalent to equation (3.1) for the effect of temperature on diffusivity. By examining the plot of $\ln D^{\circ}_{AB}$

at 298.15 K versus $\ln M_A$ for the n-alkane systems as shown in Figure 3.2, a linear relationship is observed within experimental error for each of the individual solutes and this linear relationship can be represented by:

$$D^{o}_{AB} = \alpha_1 M_A^{\alpha_2} \tag{3.3}$$

Therefore, the basic model form for the correlation was made up by combining equations (3.1) and (3.3), which resulted in the following expression:

$$D^{o}_{AB} = \beta_1 \exp\left(\frac{\beta_2}{T}\right) M_A^{\beta_3} \tag{3.4}$$

The diagnostic technique for model building was applied to equation (3.4). In this technique, a statistical analysis is applied to the estimated parameters rather than to the observation directly. The parameters in equation (3.4) were estimated by means of the nonlinear regression analysis for groups of data of various solutes diffusing in a specified solvent, for which the following relationships were obtained:

$$\beta_1 = a + bM_B \tag{3.5}$$

$$\beta_2 = c + dM_B \tag{3.6}$$

$$\beta_3 = e + fM_B \tag{3.7}$$

Combining equations (3.4) and (3.6), yields the result:

$$D^{o}_{AB} = \gamma_1 \exp\left(\frac{\gamma_2 + \gamma_3 M_B}{T}\right) M_A^{\gamma_4} \tag{3.8}$$

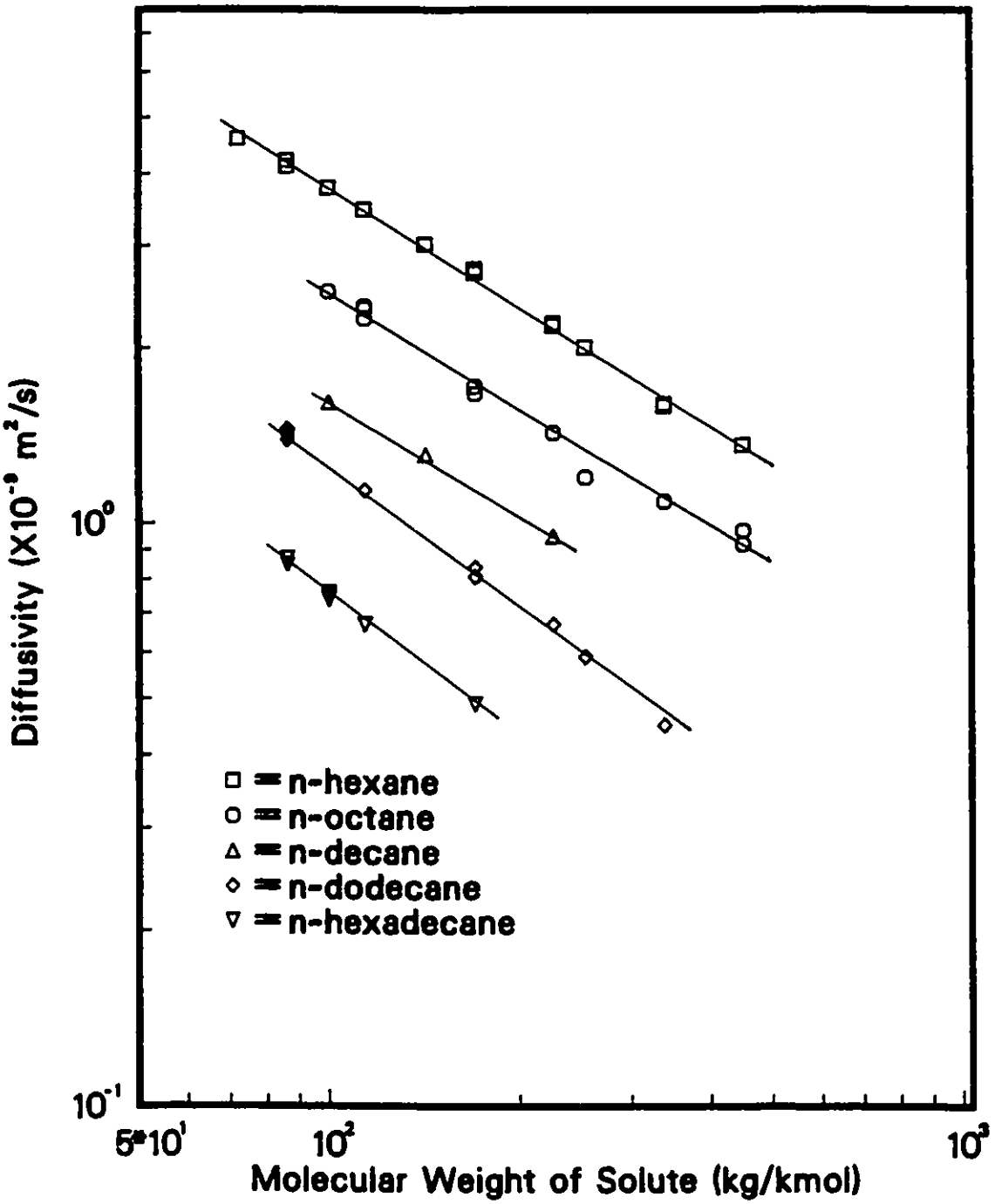

Figure 3.2: Plot of $\ln D^{\circ}_{AB}$ versus $\ln M_A$ at 298.15 K for n-alkane systems

The parameters in equation (3.8) were estimated by using the nonlinear least squares criterion based on 104 data; again the NLIN package from the SAS library was utilized.

The iterative procedure was employed for model-building at this stage. This procedure involves three basic steps, namely, identification, fitting and diagnostic checking. The procedure starts by identifying the model form, then uses an appropriate estimation criterion to fit the model, and finally, the model is checked by utilizing a lack of fit test. If the model is inadequate, then the iteration is continued until an adequate model is obtained. By following the basic steps of the iterative model-building procedure, the final expression of the correlation is:

$$D^{\circ}_{AB} = \theta_1 M_B \exp\left(\frac{\theta_2 + \theta_3 M_B + \theta_4 M_B^2}{T}\right) M_A^{\theta_5 + \theta_6 M_B} \tag{3.9}$$

The constants in the above expression are $\theta_1 = 0.000318 \pm 0.000024$, $\theta_2 = -483.81 \pm 60.03$, $\theta_3 = -8.317 \pm 0.656$, $\theta_4 = 0.0166 \pm 0.001$, $\theta_5 = -0.504 \pm 0.041$ and $\theta_6 = -0.0017 \pm 0.0005$. In the above correlation, D°_{AB} is in cm^2/s, M_A and M_B are in $g/mole$, and T is in K. The detailed development of this correlation can be found in reference [102].

The plots of residuals of 104 data against predicted responses and all independent variables for equation (3.9) were examined, and all residuals were found to be randomly distributed in those plots. No correlation between the residuals was detected. Therefore, there was no evidence for lack of fit of the proposed correlation equation (3.9). The predicted diffusivities from the equation (3.9) are compared with the experimental data as shown in Figure 3.3. It shows that the predicted

results are very close to the experimental data.

Equation (3.9) was compared with the Hayduk-Minhas (2.37), Chen-Chen (2.38) and Matthews equations (2.39) for n-alkane systems by means of the average absolute percent error, defined as follows:

$$absolute\ \%\ error = \frac{|\ expt'l\ data - predicted\ result\ |}{expt'l\ data} \times 100\% \qquad (3.10)$$

The comparison, as reported in Table 3.1, shows that the proposed correlation has the smallest average absolute percent error (2.78%) based on 104 data. Although the improvement of prediction based on the proposed correlation is small when compared with the existing correlations, a significant advantage of the proposed correlation is that only values of temperature and molecular weights of solute and solvent are required for the prediction of diffusivities. The molecular weights are easy to obtain and are known exactly. Thus the proposed correlation is easier to use than any of the existing correlations in the literature. However, the proposed correlation is an empirical model so that extrapolation cannot be made with confidence.

3.3 New Correlation for Prediction of Diffusivities of Dissolved Gases in Organic Solvents at Infinite Dilution

Molecular diffusion of dissolved gases in liquids forms a special class of molecules of small size in the broad category of liquid diffusion. A new empirical correlation for diffusion coefficients of dissolved gases in organic solvents at infinite dilution has

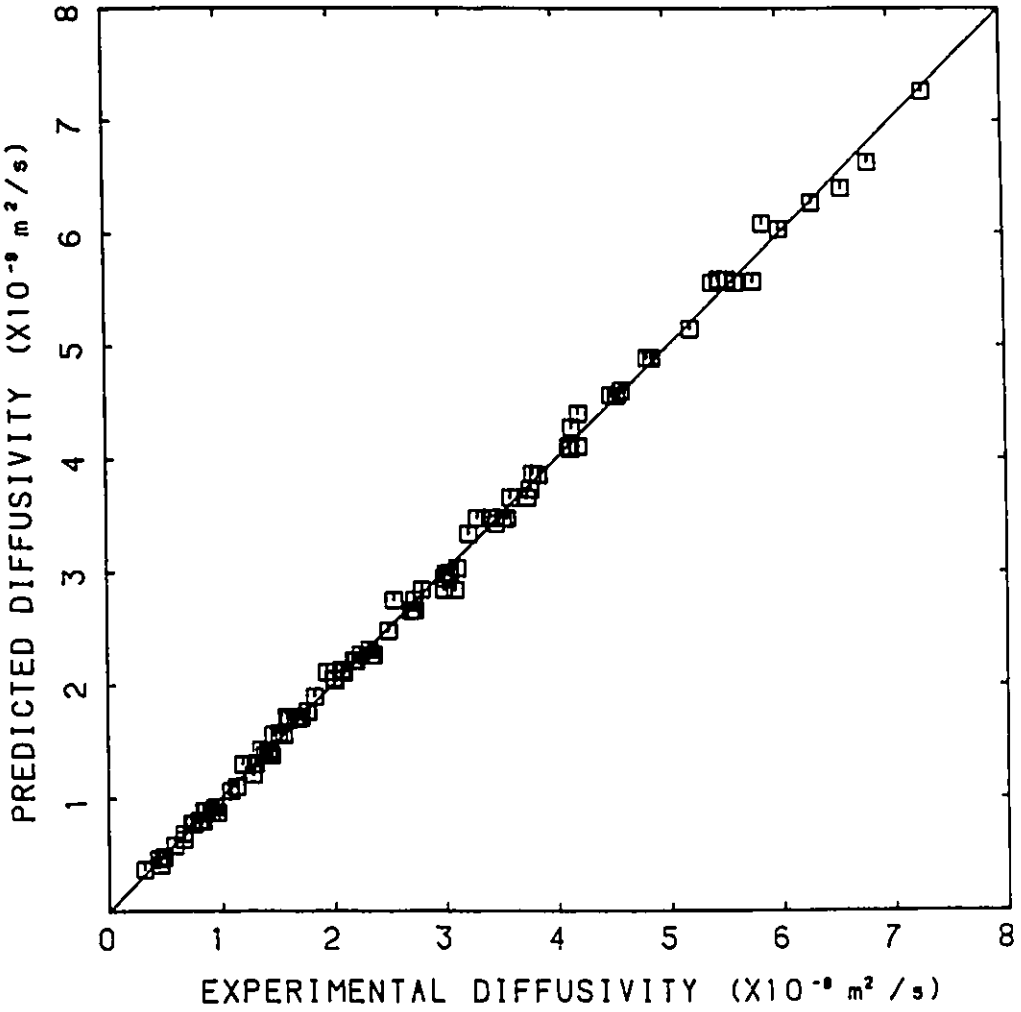

Figure 3.3: Comparison of experimental data and predictive results from equation (3.9) based on 104 data

CORRELATION	AVERAGE ABSOLUTE PERCENT ERROR (%)
Proposed equation (3.9)	2.78
Hayduk and Minhas (2.37)	3.39
Chen and Chen (2.38)	4.65
Matthews (2.39)	5.02

Table 3.1: Comparison of the average absolute percent error from the four correlations for n-alkane systems based on 104 data

been proposed in this work. The correlation utilizes the viscosity of the solvents, the critical volumes and molecular weights of the solutes and solvents as measures of the size, shape effects and of the intermolecular forces associated with the diffusion process.

Three hundreds and fifty two diffusivity data have been collected from the literature. A listing of the sources for the solute-solvent pairs utilized in this development is given in Appendix B. The data do not include those for hydrogen and helium as solutes because the reported data for those solutes, while available in the literature, are very inconsistent. The diffusivity data were reported for a temperature range from 273.15 K to 433.15 K. All the data were reported for atmospheric pressure. The values of the diffusivities were from 2.79×10^{-10} to 1.88×10^{-8} m^2/s. For use in the correlation, the viscosity data were taken from the literature, and the range was from 2.07×10^{-4} to 3.92×10^{-2} $kg/m.s$. The critical volumes were estimated by

Lydersen's method [88], if the data could not be found in the literature. The range of the critical volume for the solutes was from 7.34×10^{-2} to 3.01×10^{-1} $m^3/kmol$, and that for the solvents was from 1.18×10^{-1} to 9.20×10^{-1} $m^3/kmol$.

The correlation was started by using an equation having the form of equation (3.1) for describing the temperature dependence of the diffusivity. Based on the empirical observation from the plots of diffusivity versus various physical properties of solutes and solvents, a seven-parameter model was initially tested. The original form was as follows:

$$D^o_{AB} = \beta_1 \exp\left(\frac{\beta_2}{T}\right) \mu_B^{\beta_3} V_{CA}^{\beta_4} V_{CB}^{\beta_5} M_A^{\beta_6} M_B^{\beta_7} \tag{3.11}$$

The parameters in equation (3.11) were estimated by the nonlinear regression analysis; again the NLIN package from the SAS library was utilized. The final correlation was simplified to the form of:

$$D^o_{AB} = \gamma_1 \exp\left(\frac{\gamma_2}{T}\right) \mu_B^{\gamma_3} \left(\frac{V_{CB}}{V_{CA}^{1.64}}\right)^{\gamma_4} (M_A M_B^2)^{\gamma_5} \tag{3.12}$$

In this equation, $\gamma_1 = 0.0025 \pm 0.00068$, $\gamma_2 = -514.81 \pm 45.09$, $\gamma_3 = -0.607 \pm 0.032$, $\gamma_4 = 0.358 \pm 0.030$ and $\gamma_5 = -0.152 \pm 0.014$. In the above equation, D^o_{AB} is in cm^2/s, M_A and M_B are in $g/mole$, μ_B is in cp, V_{CA} and V_{CB} are in $cm^3/mole$ and T is in K. The residual plots based on 352 data showed that the residuals were randomly distributed. Thus there was no evidence for lack of fit of the proposed correlation. The results predicted by means of equation (3.12) are compared with the experimental data in Figure 3.4; it shows that the proposed correlation can be used for reasonably accurate predictions for most of the systems.

The proposed correlation as expressed by equation (3.12), was compared with four correlations for dissolved gases in liquids found in the literature and included those of: Akgerman and Gainer (2.27), Umesi and Danner (2.35), Sridhar and Potter (2.33) and Sovová (2.32). The parameter compared, was the average absolute percent error as mentioned in the last section. The comparison is shown in Table 3.2. Based on the same set of data, the proposed correlation has an average absolute percent error of 15.82%, which is the lowest among all the correlations. It can be concluded that the proposed correlation gives better predictions of the diffusivity of dissolved gases in organic solvents than any of the existing correlations. The proposed correlation is an empirical model so that confidence for extrapolation is limited.

3.4 New Correlation for Prediction of Diffusivities of Dissolved Gases in Water at Infinite Dilution

It has been found that diffusivities for dissolved gases in water and for dissolved gases in organic solvents may not be correlated using a single equation due to a significantly lower diffusion rate in water of essentially all gases. The reason for the lower rate of diffusion in water is probably the result of the formation of complexes of the diffusing solute with water and/or the result of self-association of the water molecules. A simple empirical correlation for prediction of diffusion coefficients of dissolved gases in water at infinite dilution has been developed. The correlation

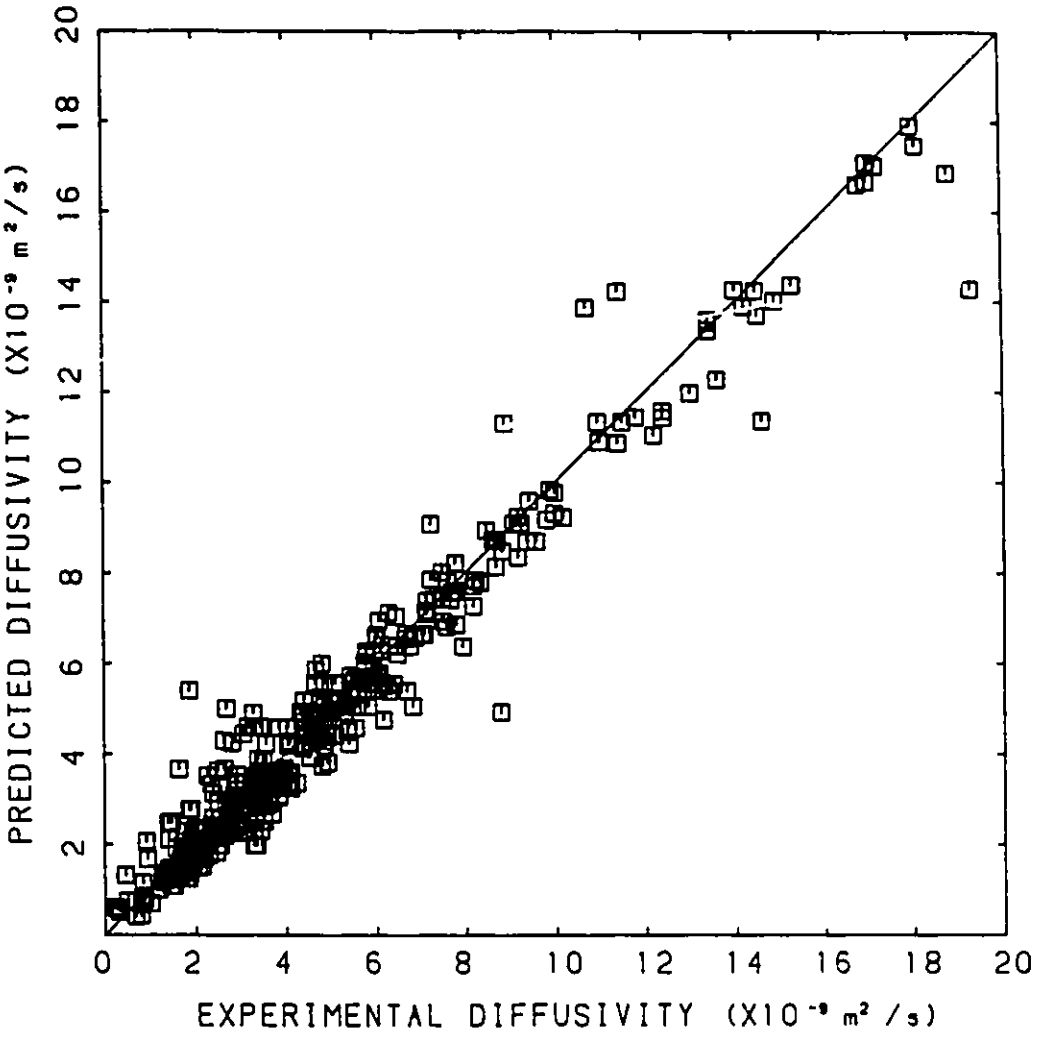

Figure 3.4: Comparison of experimental data and predictive results from equation (3.12) based on 352 data

CORRELATION	NO. OF DATA	AVERAGE ABSOLUTE PERCENT ERROR (%)
Proposed equation (3.12)	352	15.82
	299	14.14
Akgerman and Gainer (2.27)	352	33.77
Umesi and Danner (2.35)	299	29.28
Sridhar and Potter (2.33)	352	30.62
Sovová (2.32)		
(group 2)	107	31.42
(group 3)	212	22.83
average	319	25.71

Table 3.2: Comparison of the average absolute percent error from the correlations for dissolved gases in liquids

utilizes critical volumes of solute to represent the effects of the size or mobility of the solute molecules.

Three hundreds and nine diffusivity data were collected from the literature. A listing of the sources for the data utilized in this development is given in Appendix C. Again the data do not include hydrogen and helium as solutes because the experimental data for those solutes are very inconsistent. The temperature range for the data was from 273.15 K to 348.15 K, and all the data were measured at atmospheric pressure. The range of the diffusivity data was from 3.75×10^{-10} to $1.36 \times 10^{-8}\ m^2/s$. The critical volumes were estimated by Lydersen's method [88], if the data could not be found in the literature The range of the critical volumes for the solutes was from 4.17×10^{-2} to $2.25 \times 10^{-1}\ m^3/kmol$.

The correlation was again started by using an equation of the same form as equation (3.1) for describing the effect of temperature on diffusivity. A three-parameter model was utilized:

$$D^o_{AB} = \alpha_1 \exp\left(\frac{\alpha_2}{T}\right) V_{CA}^{\alpha_3} \tag{3.13}$$

The parameters in equation (3.13) were estimated by the nonlinear regression analysis; again the NLIN package from the SAS library was utilized. The estimated parameters in the above equation are: $\alpha_1 = 2.348 \pm 2.402$, $\alpha_2 = -2531.67 \pm 264.02$, and $\alpha_3 = -0.704 \pm 0.130$. In the above correlation, D^o_{AB} is in cm^2/s, V_{CA} is in $cm^3/mole$, and T is in K. There was no evidence for lack of fit of the proposed correlation based on the observation of the residuals plots. The diffusivities predicted using equation (3.13) are compared with the experimental data as shown in Figure

3.5 which shows that the proposed correlation gives a good prediction for most of the systems except the systems involving butene and nitric oxide in water. These data were reported by Unver and Himmelbau [4] and Wise and Houghton [68], and it is considered that these data may not be reliable.

The proposed correlation (3.13) was compared with seven correlations for dissolved gases in liquids in the literature and included those of: Akgerman and Gainer (2.27), Umesi and Danner (2.35), Sridhar and Potter (2.33), Sovová (2.32), Othmer and Thakar (2.41), Hayduk and Minhas (2.43), and Siddiqi and Lucas (2.44). The comparison was on the basis of the average absolute percent error. The result is reported in Table 3.3. Based on the same set of data (309 data), the proposed correlation has an average absolute percent error of 13.51%; it is the lowest among all the correlations. However, the improvement of prediction from the proposed correlation is marginal when compared with the Othmer and Thaker equation (13.63%) and the Sovová correlation (13.71%). Therefore, it is considered that those three correlations can be used for predicting the diffusivities of dissolved gases in water with essentially the same result. Again the proposed correlation is an empirical model so that confidence for extrapolation is limited.

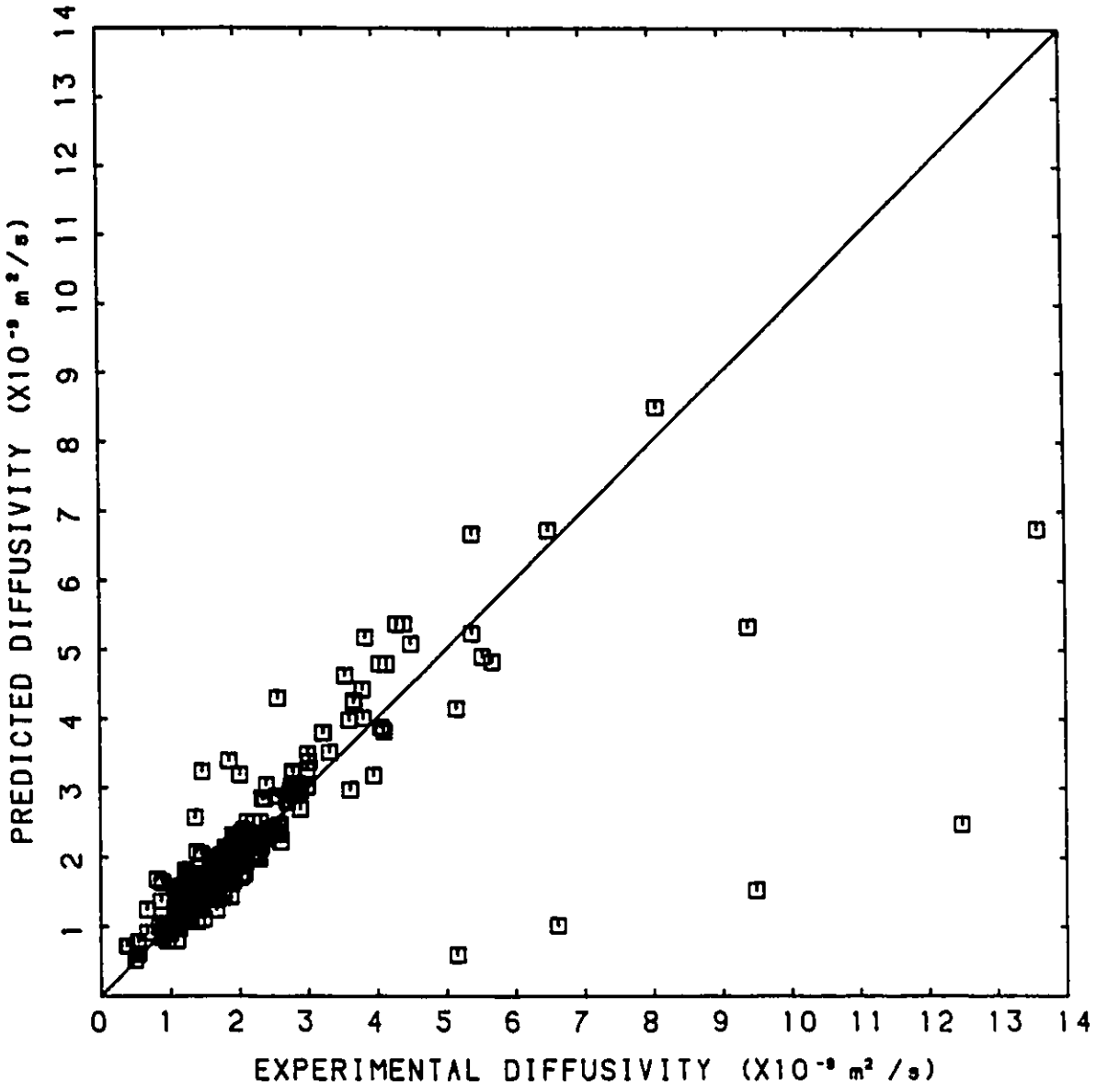

Figure 3.5: Comparison of experimental data and predictive results from equation (3.13) based on 309 data

CORRELATION	NO. OF DATA	AVERAGE ABSOLUTE PERCENT ERROR (%)
Proposed equation (3.13)	309	13.51
Othmer and Thakar (2.41)	309	13.63
Hayduk and Minhas (2.43)	309	17.16
Siddiqi and Lucas (2.44)	309	27.37
Akgerman and Gainer (2.27)	309	24.07
Umesi and Danner (2.35)	299	29.28
Sridhar and Potter (2.33)	309	14.28
Sovová (2.32)	309	13.71

Table 3.3: Comparison of the average absolute percent error from the eight correlations for dissolved gases in water

Chapter 4

PROPERTIES OF MATERIALS

The chemicals used in this investigation were obtained from different companies. The solute gas, propene, was purchased from Air Product. The specified purity of the gas was 99%. The useful physical properties of propene are listed in Table 4.1. All the solvents (acetic acid, acetone, n-butanol, chlorobenzene, N,N dimethyl formamide, ethyl acetate, ethylene glycol and n-octane) were obtained from the Aldrich Chemical Company. The specified purities and the physical properties of these solvents are presented in Tables 4.2, 4.3, 4.4 and 4.5.

The molar volumes of propene gas at different temperatures were calculated by means of the second virial coefficient except for the value at 278.15 K. The experimental data for the second virial coefficients of propene from the literature could be fitted by the following equation [103]:

$$B = \varphi T^{\chi} \tag{4.1}$$

In the above equation, B is the second virial coefficient, φ and χ are the constants characteristic of the substance, and T is the absolute temperature in K. The values

of φ and χ were determined by an optimization technique utilizing a computer, and the results were $\varphi = -1.012 \times 10^8$ and $\chi = -2.209$. The temperature range of the experimental data used was from 280.15 to 500.15 K [103]. The second virial coefficient obtained from equation (4.1) was then substituted into the truncated form of the virial equation of state.

$$Z = \frac{PV}{R_g T} = 1 + \frac{B}{V} \tag{4.2}$$

In the above equation, P, V, R_g and T are the pressure, the molar volume, the gas constant and the absolute temperature, respectively. Then the molar volume was calculated by the following equation:

$$V = \frac{C + \sqrt{C^2 + 4BC}}{2} \tag{4.3}$$

where

$$C = \frac{R_g T}{P} \tag{4.4}$$

The molar volume of propene gas at 278.15 K was calculated by means of Pitzer three-parameter correlation [104].

$$Z = Z^{(0)}(T_r, P_r) + \omega Z^{(1)}(T_r, P_r) \tag{4.5}$$

It was because this temperature was outside the temperature range used for the correlation for the second virial coefficients. The calculated values of molar volumes of propene gas at different temperatures are listed in Table 4.6.

Saturated vapor pressures of all solvents were calculated by the Antoine equation [105].

$$\ln \frac{p_i^s}{P_c} = A_1 - \frac{A_2}{T' + A_3} \tag{4.6}$$

PROPERTIES	PROPENE
molecular weight ($kg/kmol$)	42.081
normal freezing point (K)	87.90
normal boiling point (K)	225.40
critical temperature (K)	365.00
critical pressure (kPa)	4619.28
critical volume ($m^3/kmol$)	0.181
critical compressibility [Z_c]	0.275
Pitzer's Acentric factor [ω]	0.148
dipole moment (debyes)	0.40
heat of vaporization at n.b.p. ($cal/kmol$)	4.40×10^6

Table 4.1: Physical properties of propene gas

In this equation, p_i^s is the saturated vapor pressure of substance i, P_c is the critical pressure in psi, T' is temperature in $^\circ F$, and A_1, A_2 and A_3 are constants characteristic of the substance. The values of A_1, A_2 and A_3 for the solvents used in this study are listed in Table 4.7.

Densities and viscosities of all solvents were measured at different temperatures. Thus the methods utilized in the measurements of densities and viscosities and the measured results will be presented in Chapter 5 and Chapter 6.

PROPERTIES	ACETIC ACID	ACETONE
purity	99.8%	99.9+%
molecular weight ($kg/kmol$)	60.052	58.080
normal freezing point (K)	289.80	178.20
normal boiling point (K)	391.10	329.40
critical temperature (K)	594.40	508.10
critical pressure (kPa)	5784.23	4700.32
critical volume ($m^3/kmol$)	0.171	0.209
critical compressibility [Z_c]	0.200	0.232
Pitzer's Acentric factor [ω]	0.454	0.309
dipole moment (debyes)	1.30	1.90
heat of vaporization at n.b.p. ($cal/kmol$)	5.66×10^6	6.96×10^6
refractive index at 293.15 K	1.3716	1.3588

Table 4.2: Physical properties of acetic acid and acetone

PROPERTIES	N-BUTANOL	CHLOROBENZENE
purity	99.9+%	99.9+%
molecular weight ($kg/kmol$)	74.123	112.559
normal freezing point (K)	183.90	227.60
normal boiling point (K)	390.90	404.90
critical temperature (K)	562.90	632.40
critical pressure (kPa)	4416.68	4517.98
critical volume ($m^3/kmol$)	0.274	0.308
critical compressibility [Z_c]	0.259	0.265
Pitzer's Acentric factor [ω]	0.590	0.249
dipole moment (debyes)	1.80	1.60
heat of vaporization at n.b.p. ($cal/kmol$)	1.03×10^7	8.74×10^6
refractive index at 293.15 K	1.3985	1.5241

Table 4.3: Physical properties of n-butanol and chlorobenzene

PROPERTIES	DMF	ETHYL ACETATE
purity	99.9+%	99.9+%
molecular weight ($kg/kmol$)	73.095	88.107
normal freezing point (K)	212.72	189.60
normal boiling point (K)	426.15	350.30
critical temperature (K)	596.55	523.20
critical pressure (kPa)	5216.95	3829.14
critical volume ($m^3/kmol$)	0.249	0.286
critical compressibility [Z_c]	——	0.252
Pitzer's Acentric factor [ω]	——	0.363
dipole moment (debyes)	——	1.90
heat of vaporization at n.b.p. ($cal/kmol$)	9.16×10^6	7.70×10^6
refractive index at 293.15 K	1.4305	1.3720

Table 4.4: Physical properties of N,N dimethyl formamide and ethyl acetate

PROPERTIES	ETHYLENE GLYCOL	N-OCTANE
purity	99.0+%	99.0+%
molecular weight ($kg/kmol$)	62.069	114.232
normal freezing point (K)	260.20	216.40
normal boiling point (K)	470.40	398.80
critical temperature (K)	645.00	568.80
critical pressure (kPa)	5216.95	3829.14
critical volume ($m^3/kmol$)	0.186	0.492
critical compressibility [Z_c]	0.270	0.259
Pitzer's Acentric factor [ω]	——	0.394
dipole moment (debyes)	2.20	0.00
heat of vaporization at n.b.p. ($cal/kmol$)	1.26×10^7	8.23×10^6
refractive index at 293.15 K	1.4318	1.3974

Table 4.5: Physical properties of ethylene glycol and n-octane

TEMPERATURE (K)	MOLAR VOLUME ($m^3/kmole$)
278.15	22.39270
288.15	23.26059
293.15	23.68526
298.15	24.10912
323.15	26.21832
348.15	28.31437

Table 4.6: Calculated values of molar volume of propene gas

SUBSTANCE	A_1	A_2	A_3
Acetic acid	7.203594	7376.157	410.1814
Acetone	6.244412	5356.715	397.5290
N-butanol	6.303186	5235.324	274.4291
Chlorobenzene	5.888080	6222.905	372.2756
N,N dimethylformamide	5.298043	5665.834	313.2540
Ethyl acetate	6.330700	5440.049	373.4800
Ethylene glycol	7.258288	8088.817	311.8854
N-octane	6.414100	5947.491	360.2600

Table 4.7: Constants for the Antoine vapor pressure equation (4.6)

Chapter 5

EXPERIMENTAL EQUIPMENT AND PROCEDURE

In this study, several different experimental devices were used for the measurements. The densities of the pure solvents were measured at atmospheric pressure and elevated pressures by means of two Anton Paar densitometers, one for low pressures, the other for high pressures. The viscosities of the pure solvents were determined at atmospheric pressure by means of Cannon-Fenske viscometers. The solubilities of propene gas in various solvents were measured by an apparatus which was similar to that used by Asatani [106]. The diffusivities of propene gas in various solvents were measured at atmospheric pressure by means of the steady-state capillary cell method. The apparatus used in this study was similar to the one employed by Hayduk and Cheng [56]. Some modifications were made to the original apparatus in the interest of simplifying the experimental procedure. For the measurements of diffusivities at elevated pressures, an apparatus based on the Taylor despersion phenomenon was developed.

5.1 Density Measurements of Pure Solvents at Atmospheric pressure

For the precise measurements of solvent densities, an Anton Paar densitometer was utilized. This densitometer consisted of two components. One was the sensing unit, DMA601 which contained a U-shape sample tube connecting to a glass reed oscillator. The other component, DMA60 was a frequency counter and displayed the period of oscillation of the reed characteristic of the liquid or gas in the sample tube. The sample tube was enclosed in a circulating chamber where the temperature of the sample could be controlled to within ±0.01 K by means of constant temperature fluid.

The density was determined by means of the following equation relating the density with the period of oscillation (Ω):

$$\rho = I(\Omega^2 - J) \tag{5.1}$$

In the above equation, I and J are apparatus constants which are determined by calibration. The calibration is performed by measuring the periods of oscillation for two samples of known densities, usually dried air and distilled water. Let the densities of two reference samples be ρ_1 and ρ_2, and the corresponding periods of oscillation obtained from DMA60 be Ω_1 and Ω_2. The constants I and J can be determined by the following equations:

$$I = \frac{\rho_2 - \rho_1}{\Omega_2^2 - \Omega_1^2} \tag{5.2}$$

$$J = \Omega_2^2 - \frac{1}{I}\rho_2 \tag{5.3}$$

After the apparatus constants I and J were obtained, equation (5.1) was used to calculate the densities of the samples. In this study, dried air and distilled water were used as reference fluids for the calibration, and the densities of both substances were obtained from Weast [107]. The detailed procedure for density measurements can be referred to in the instruction manual for the Anton Paar densitometer.

5.2 Viscosity Measurements of Pure Solvents at Atmospheric Pressure

The viscosities of the pure solvents were measured by Cannon-Fenske viscometers immersed in a constant temperature bath. The Cannon-Fenske viscometer is classified as a gravity type viscometer. In this type of viscometer, the liquid under test is allowed to flow through a capillary tube, and the kinematic viscosity can be obtained by timing the position of the liquid meniscus as it passes between two marks. All the viscometers used were obtained from Induchem Lab Glass Co., and were calibrated by the Cannon Instrument Co.. The detailed procedure for using the Cannon-Fenske viscometer can be referred to in the instruction sheet for the viscometer.

5.3 Degassing Apparatus and Procedure

A diagram of the degassing apparatus used for deaerating the solvent is shown in Figure 5.1. The degassing apparatus consisted of a solvent flask and a solvent accumulation column connected to a vacuum pump. A tape heater around the solvent flask supplied the heat for boiling. The bottom of the solvent accumulation column was filled with glass beads, and the lower outlet was bent. The glass beads provided greater surface area for solvent as it filled the column exposing it to the vacuum that aided the complete degassing of the solvent.

The procedure for degassing the solvent involved charging the solvent flask with a suitable amount of solvent and then applying heat and vacuum. After a boiling time of about 20 to 30 minutes had elapsed, the solvent was allowed to flow into the solvent accumlation column where further degassing was performed.

5.4 Solubility Measurements at Atmospheric Pressure

For the steady state capillary cell method, a knowledge of the gas solubility is required for calculation of the diffusivity. However, gas solubilities for some of the systems under the present investigation are not available in the literature. Therefore, the solubilities of propene gas were measured in acetic acid, acetone, n-butanol, chlorobenzene, N,N, dimethyl formamide, ethyl acetate, ethylene glycol and n-octane at different temperatures.

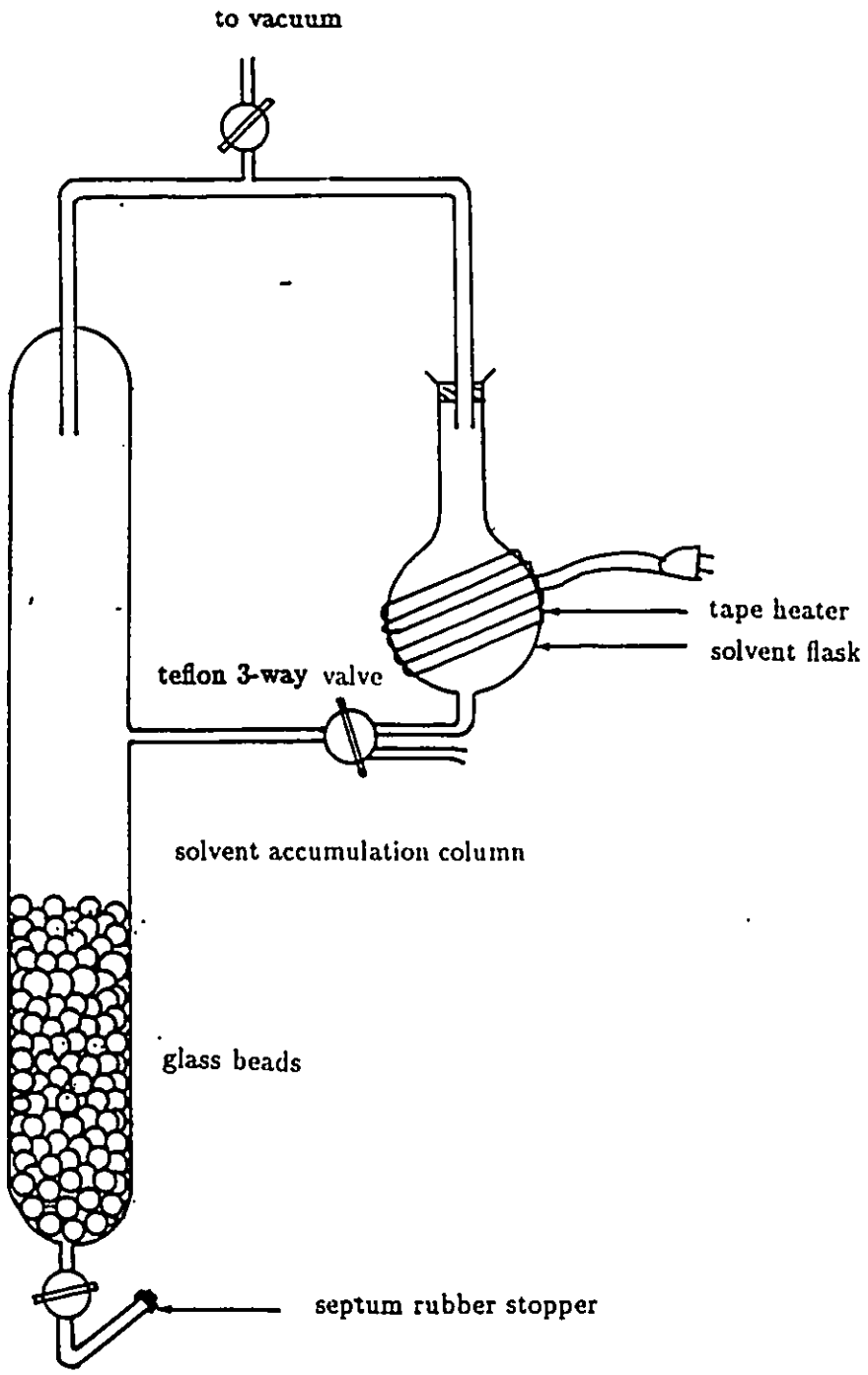

Figure 5.1: Degassing apparatus for deaerating the solvent

The apparatus used to measure gas solubilities at atmospheric pressure was the same design as that described by Asatani [106]. This technique involved measuring the rate of dissolution of the gas by a constant flow of deaerated solvent passing through a spiral coil. A diagram of the apparatus for gas solubility measurements is shown in Figure 5.2.

The apparatus consisted of a gas burette, a spiral coil, a miniature capillary U-tube manometer and a solution collecting burette. All these were enclosed inside a cylindrical glass jacket through which a fluid at constant temperature was circulated. The lower end of the gas burette was connected to the mercury levelling bottle which could be raised by means of a variable speed motor. For most experiments, the solubility apparatus used had a 2.5×10^{-5} m^3 (25.0 ml) gas burette. For measuring lower solubilities such as that for propene in ethylene glycol, a second apparatus equipped with a 1.0×10^{-5} m^3 (10.0 ml) gas burette was used. The top end of the spiral coil was closed with a rubber septum. The degassed solvent was brought into the system through the rubber septum by means of a syringe attached to a syringe pump. A heat exchanger for the solvent syringe was installed in which the solvent was brought to the experimental temperature before it went into the spiral coil. The solvent syringe used was a 5.0×10^{-6} m^3 (5.0 ml) gas-tight Hamilton syringe, and the syringe pump was a Harvard infusion-withdrawal pump, model 1100 which operated with a interchangeable constant speed motor. For most experiments, motor speeds of 1/10 rpm and 1/20 rpm were used and the corresponding solvent infusion rates were 2.95×10^{-10} m^3/s and 1.47×10^{-10} m^3/s

1. gas burette
2. spiral tube
3. capillary U-tube manometer
4. solution collecting burette
5. glass jacket
6. syringe heat exchanger
7. syringe pump
8. mercury levelling bottle
9. variable speed motor

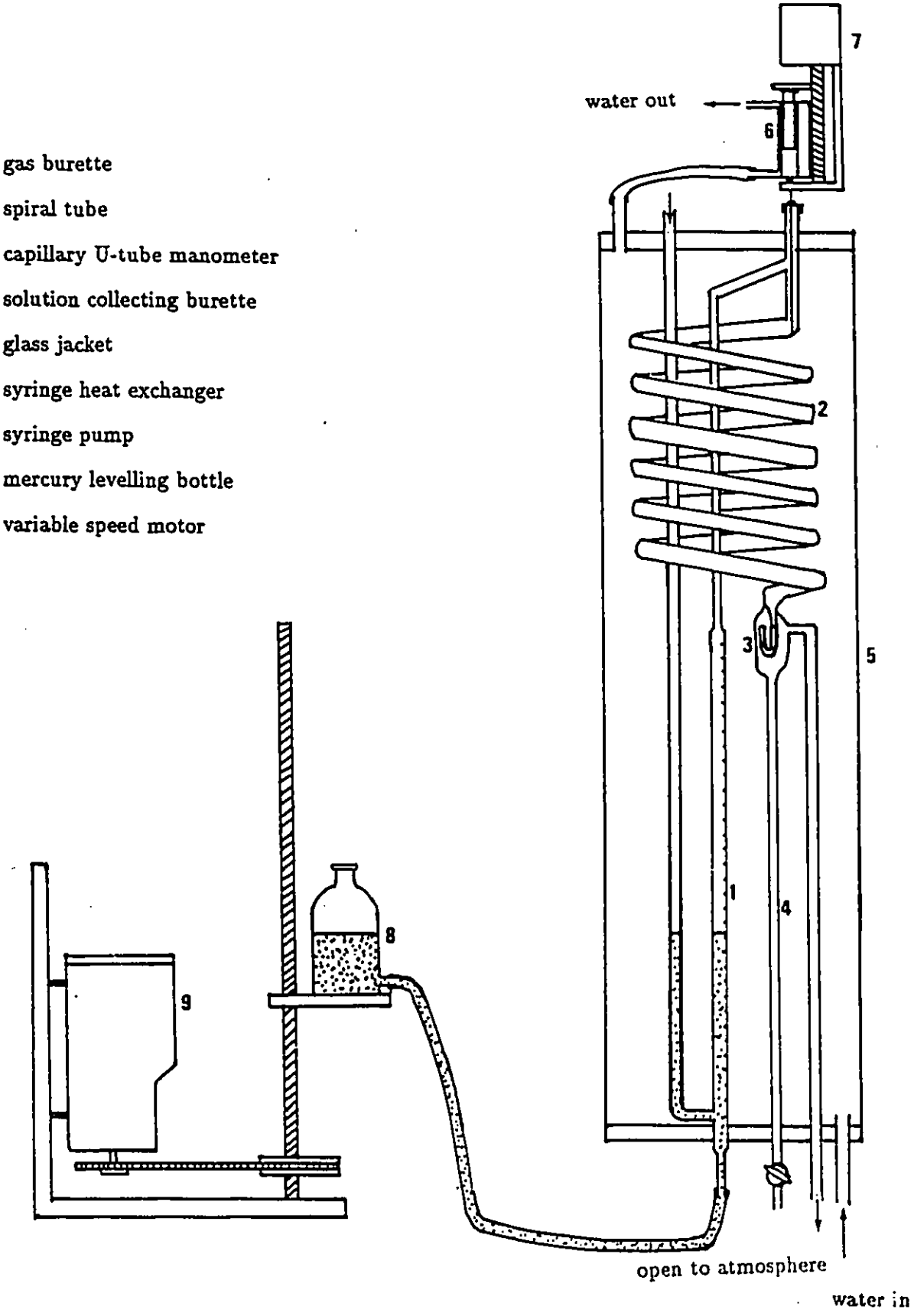

Figure 5.2: Apparatus for gas solubility measurements at atmospheric pressure

respectively. The volumetric infusion rates were determined accurately by weighing the quantity of distilled water delivered in a given period of time.

The experimental procedure for solubility measurements will be briefly described. While the solvent was being degassed, the solubility apparatus was purged with solute gas. Then the syringe filled with degassed solvent was attached to the syringe heat exchanger and then to the syringe pump. The needle of the syringe was inserted into the spiral coil through the rubber septum. It was confirmed that the tip of the needle actually touched the wall of the spiral coil in order to ensure a continuous supply of solvent. The stopcock at the outlet of the solvent collecting burette was closed, and the syringe pump was switched on. The solubility apparatus was left with the solute gas slowly flowing through it until gas-saturated solution appeared in the capillary U-tube manometer, one end of which was open to the atmosphere. Then the flow of the solute gas was shut off, and the mercury level in the gas burette was slowly and continuously raised by raising the position of the mercury levelling bottle. In this way the liquid in the capillary U-tube manometer remained at a constant level indicating a constant gas pressure in the solubility apparatus. The gas volume in the gas burette which was replaced by the mercury was identical to the volume of solute gas dissolved in the solvent, and was recorded at regular time intervals. With the knowledge of volumes of dissolved gas and of degassed solvent supplied to the apparatus, the solubility could be calculated.

5.5 Treatment of Data for Gas Solubility Measurements at Atmospheric Pressure

The volumes of dissolved gas as measured at fixed time intervals are always found to be directly proportional to the volume of degassed solvent supplied. The gas solubility is based on the slope of the straight line in a plot of volume of dissolved gas versus volume of solvent supplied.

Let the slope of the straight line be (SLP) and the liquid phase mole fractions of solute gas and solvent be x_A and x_B respectively, the ratio of the mole fractions of solute to solvent can be written as:

$$\frac{x_A}{x_B} = (SLP)\frac{MV_B}{MV_A} \tag{5.4}$$

In the above equation, MV_A, and MV_B, are molar volumes of solute, and solvent, respectively. The molar volume of solute gas is calculated by the methods described in Chapter 4, and the molar volume of solvent is calculated from the mass density.

The gas solubility, $x_A(P,T)$, at an atmospheric pressure of P and the temperature, T, is then obtained by means of the following equation:

$$x_A(P,T) = \frac{\frac{x_A}{x_B}}{1+\frac{x_A}{x_B}} \tag{5.5}$$

It is conventional to convert the gas solubility measured at atmospheric pressure, P, to the gas solubility for which the partial pressure of solute gas is one atmosphere (101.3 kPa). Assuming Henry's law and Raoult's law are valid, the gas solubility

at a gas partial pressure of 101.3 kPa can be expressed as:

$$x_A(101.3kPa, T) = x_A(P, T) \times \frac{101.3}{P - p_B^s[1 - x_A(P, T)]} \tag{5.6}$$

In the above equation, p_B^s is the vapor pressure of the solvent at temperature T, and it is calculated from the Antoine equation as mentioned in Chapter 4.

5.6 Diffusivity Measurements at Atmospheric Pressure

The diffusivities of propene gas were measured in acetic acid, acetone, n-butanol, chlorobenzene, N,N dimethyl formamide, ethyl acetate and n-octane at different temperatures by means of the steady-state capillary cell method which was originally described by Malik and Hayduk [54]. This method is relatively simple because it does not require any complicated analysis, and the capillary cell is easy to construct. Furthermore, the diffusion process of the steady-state capillary cell method can be accurately described mathematically. However, a knowledge of gas solubility is required for the calculation of the diffusion coefficient.

A diagram of a capillary cell is shown in Figure 5.3. The capillary cell consisted of a glass capillary sealed in a closed reservoir which could be filled with degassed solvent by means of two stopcocks. The upper stopcock was connected at an angle which made the filling procedure more easy. The capillary stem was made of two capillary tubes of different inside diameters which were permanently joined together. The upper capillary had an inside diameter of 6.13×10^{-4} m and was at least 0.20 m long. The lower capillary had an inside diameter of 1.016×10^{-3} m and was at

least 0.05 m long. The end of the lower capillary which was positioned inside the reservoir was conically ground to aid dissipation of solute. The capillary tubes with small inside diameters could prevent any convection during the diffusion process. The reason for joining two capillaries of different diameters was to magnify the change in volume of the gas confined in the capillaries resulting from absorption and diffusion. The capacity of the reservoir was about $2.0 \times 10^{-5}\ m^3$. The glass capillary tubes were purchased from Wilmad Glass Company Inc., Buena, New Jersey, with a manufacturer's tolerance for the bore of $\pm 3.8 \times 10^{-5}\ m$. The diameters of these capillaries were verified by a mercury displacement method assuming the inside diameters of the capillaries to be uniform.

A schematic diagram of the apparatus for diffusivity measurements is shown in Figure 5.4. The apparatus consisted of a constant temperature bath with glass windows, a propene gas cylinder, a bubbling device, a capillary cell and a cathetometer. The temperature bath was a Neslab Model TMV70DD which could maintain constant temperature to within ± 0.01 K by means of a build-in temperature controller. For measurements at low temperature, a Neslab bath cooler (PBC-75II) was used for cooling, and water-glycol solution replaced water in the temperature bath to prevent freezing. Propene gas was obtained from Air Product (99 % purity, CP grade). The gas flow rate was controlled by a rotameter and a regulator. The gas was saturated with the solvent in the bubbling device before it contacted the degassed solvent. As a result of the simplicity in construction and the relatively long period of time required to achieve steady state, two capillary cells were used

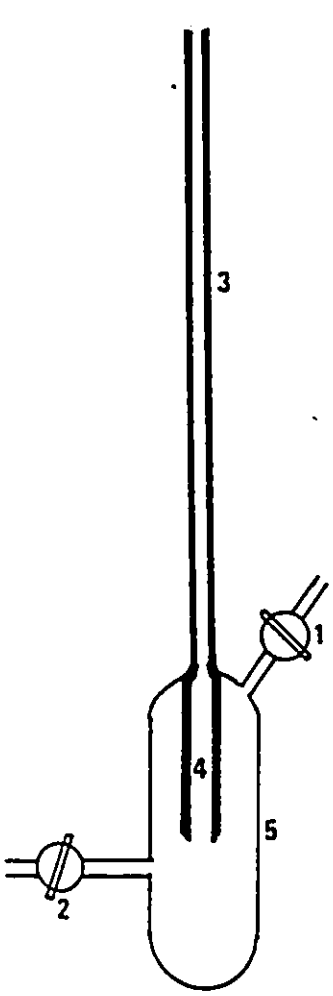

1. upper Teflon stopcock
2. lower Teflon stopcock
3. upper capillary tube, $i.d. = 0.613 \times 10^{-3} m$
4. lower capillary tube, $i.d. = 1.016 \times 10^{-3} m$
5. solvent reservoir

Figure 5.3: capillary cell used for steady-state capillary cell method

simultaneously at a time for the diffusivity measurements.

The experimental procedure will be briefly described. Prior to use, the capillary cell was cleaned by means of chromic acid solution and distilled water; then it was rinsed with acetone and dried with dry air. The stopcocks were greased using a small amount of water resistant silicine grease. About 1.20×10^{-4} m^3 solvent under investigation was degassed by means of the degassed apparatus. While the solvent was being degassed, the capillary cell was purged with propene gas for about 20 minutes to ensure there was no air trapped inside the cell. After the degassing was completed, the degassed solvent was introduced into the reservoir through the lower stopcock until the reservoir was completely filled with the degassed solvent. More than 6.0×10^{-5} m^3 of additional degassed solvent was used to flush out the cell so that any solvent which had been even briefly in contact with the gas was adequately purged. The capillary cell was then immersed in the temperature bath. The height of the diffusion path in the lower capillary was adjusted to about 0.02 m by adjusting the two stopcocks. The reason for setting the diffusion path to at least 0.02 m was to eliminate any end effects [54]. A small stream of propene gas was permitted to flow continually through the system to maintain an atmosphere of propene gas at the upper end of the capillary cell. The thermal equilibrium could be attained after an elapsed time of about an hour. However, it took a much longer time for obtaining a steady-state concentration profile along the diffusion path. The

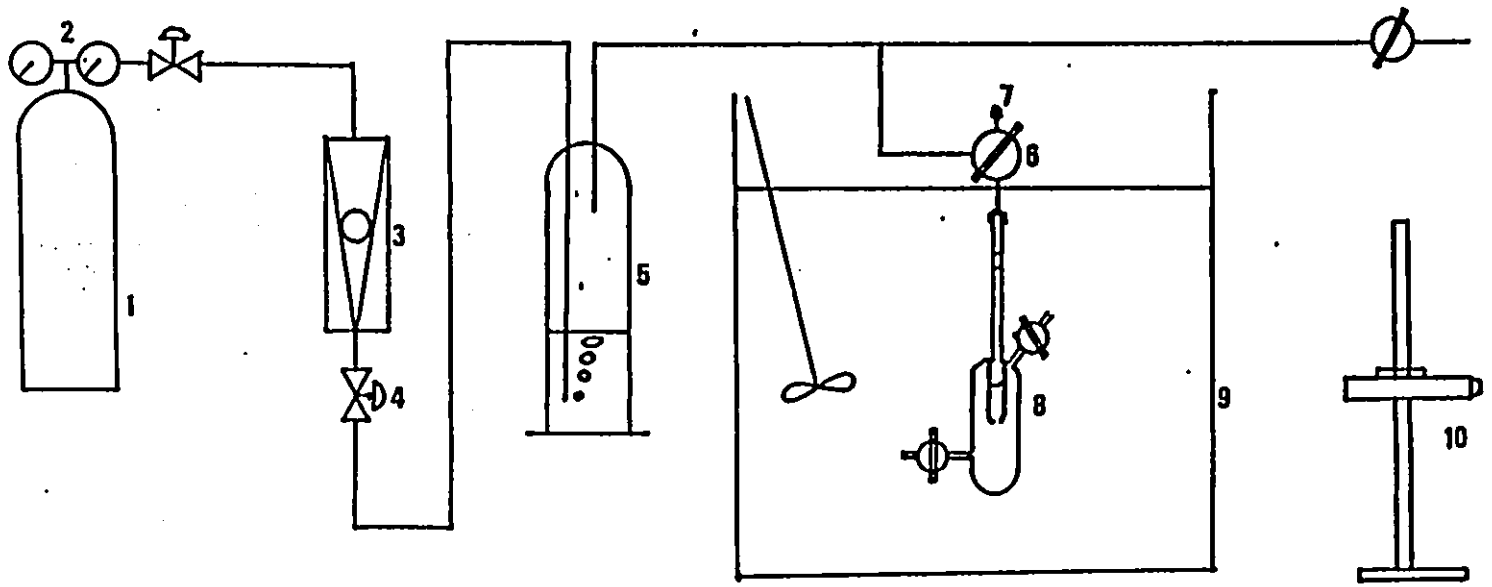

(1) gas cylinder, (2) regulator, (3) rotameter, (4) control valve, (5) bubbling device, (6) 3-way valve, (7) septum rubber stopper, (8) capillary diffusion cell, (9) temperature bath, (10) cathetometer

Figure 5.4: A schematic diagram of the steady-state capillary cell method for measurements of diffusion coefficients

length of time required was estimated, using the equation given by Crank [108] as:

$$\frac{D_{AB}t}{L_d^2} = 0.45 \tag{5.7}$$

In this expression, D_{AB} is the diffusion coefficient, t is the time required to achieve steady state and L_d is the diffusion path length. In general, at least 1.2 times the estimated time t was allowed for development of a steady state concentration profile. After steady state was obtained, a bead of gas saturated solvent was injected by a syringe through a three-way valve and was placed in the top section of the upper capillary. The solvent used for the bead was initially saturated by bubbling with the solute gas at room temperature. The position of the liquid bead was observed by means of the cathetometer. The liquid bead positions and the corresponding times were recorded at regular time intervals. The skrinkage rate of the gas in the capillary could be related to the flux of gas at the gas-liquid interface and then to the diffusivity.

5.7 Theory of the Steady-State Capillary Cell Method

For the derivation of the appropriate equation to describe the steady-state capillary cell method, several necessary assumptions are stated:

1. that a steady-state concentration profile was established along the diffusion path.

2. that end effects were negligible.

3. that the concentration of solute in the reservoir was very low and constant during the experiment.

4. that the total mass concentration in the liquid phase was nearly constant.

The general diffusion equation for species A (solute) relative to a stationary axis is given by:

$$n_A^m = j_A + n_t\omega_A = j_A + (n_A^m + n_B^m)\omega_A \tag{5.8}$$

In the equation, n_A^m and n_B^m are the mass fluxes of A and B, n_t is the total flux, ω_A is the mass fraction of A and j_A is the mass flux resulting from diffusion. By using Fick's first law:

$$j_A = -D_{AB}\rho\frac{d\omega_A}{dy} \tag{5.9}$$

In Fick's law equation, ρ is the total mass concentration and y is the direction of diffusion.

The volume increases in solution as solute gas is absorbed in the system, is equal to the volumetric upward displacement of column of liquid. Therefore, it follows that:

$$\frac{n_A^m}{\rho_{Al}} = -\frac{n_t}{\rho} \tag{5.10}$$

In the above equation, ρ_{Al} is the effective mass concentration of A in solution. Combining equations (5.8) and (5.10), the following equation is obtained:

$$n_A^m = -D_{AB}\rho\frac{d\omega_A}{dy} - \frac{\rho}{\rho_{Al}}n_A^m\omega_A \tag{5.11}$$

Separating the variables and integrating yields the required result:

$$\int_0^{L_d} n_A^m dy = -D_{AB}\rho \int_{\omega_{Ao}}^{\omega_{AL}} \frac{d\omega_A}{1+\frac{\rho}{\rho_{Al}}\omega_A} \tag{5.12}$$

$$D_{AB} = \frac{n_A^m L_d}{\rho_{Al}} \frac{1}{\ln \frac{1+\frac{\rho}{\rho_{Al}}\omega_{Ao}}{1+\frac{\rho}{\rho_{Al}}\omega_{AL}}} \tag{5.13}$$

For some systems encountered in this work, equation (5.13) can be simplified by making the assumption that the liquid phase has a constant mass density with the final result:

$$D_{AB} = \frac{n_A^m L_d}{\rho} \frac{1}{\ln \frac{1+\omega_{Ao}}{1+\omega_{AL}}} \tag{5.14}$$

5.8 Treatment of Data for Diffusivity Measurements at Atmospheric Pressure

The rate of the gas-saturated solvent bead travelling down the capillary tube, denoted by (ROB), is determined by the slope of the straight line obtained from plotting the bead position against the corresponding time. The volumetric rate of shrinkage of gas and associated vapor (V_s) can be determined by the following equation:

$$V_s = (ROB)\frac{A_u}{A_l} \tag{5.15}$$

In the above equation, A_u, and A_l, are the cross-sectional areas of the upper, and lower capillary tubes, respectively.

Usually, the solubility data are reported at 101.3 kPa partial pressure of solute gas, so they have to be corrected to the experimental pressure. Assuming Henry's

law is valid, then

$$x_p = \frac{x_1 p_p}{101.3} \tag{5.16}$$

In the above equation, x_p, and x_1, are mole fractions of solute in solution at experimental pressure, and at 101.3 kPa partial pressure of solute gas, respectively, and p_p is the partial pressure of the solute gas in kPa at the experimental pressure. The partial pressure can be obtained by Raoult's law:

$$p_p = p_A = P_t - p_B^s(1 - x_p) \tag{5.17}$$

In the equation, P_t is the total pressure in the system, and p_B^s is the vapor pressure of the solvent. By substituting equation (5.17) into equation (5.16) and by rearranging, the following expression is obtained:

$$x_p = \frac{x_1(P_t - p_B^s)}{(101.3 - x_1 p_B^s)} \tag{5.18}$$

The Ostwald coefficient (OST) can be determined from the mole fraction by the following equation:

$$(OST) = \frac{x_p(MV_A)}{(MV_B)(1 - x_p)} \tag{5.19}$$

In the above equation, MV_A, and MV_B, are molar volumes of solute, and solvent, respectively.

Since the quantity of solute gas in the solution is small, the solution density can be considered to be simply the solvent density. Based on the solubility data, the mass fraction of the solute at the gas-liquid interface can be calculated by:

$$\omega_{Ao} = \frac{(OST)p_A(M_A/MV_A)}{\rho_B + (OST)p_A(M_A/MV_A)} \tag{5.20}$$

In the above expression, ρ_B is the density of solvent, and M_A is the molecular weight of solute.

Assuming that $\omega_{AL} = 0$, and utilizing equation (5.13), the diffusivitiy can be calculated:

$$D_{AB} = \frac{V_s p_A M_A}{M V_A \rho_{Al}} \frac{L_d}{\ln \frac{1+\frac{\rho}{\rho_{Al}}\omega_{Ao}}{1+\frac{\rho}{\rho_{Al}}\omega_{AL}}} \tag{5.21}$$

The value of ρ_{Al} can be estimated by means of Hankinson-Brobst- Thomson technique [89]. Theoretically, the actual concentration in the bulk of the cell can be estimated by an equation given by Crank [108]. For relatively long period of time for diffusion:

$$\omega_{AL} = \frac{A_l L_d \omega_{Ao}}{(VC)} \left(\frac{D_{AB} t}{L_d^2} - \frac{1}{6} \right) \tag{5.22}$$

In the equation above, (VC) is the volume of solution contained in the cell reservoir, and t is the time for development of the steady-state concentration profile. The initial estimated diffusivity is used in equation (5.22). After ω_{AL} is calculated, the final value of diffusivity is re-calculated by equation (5.21).

5.9 Density Measurements of Pure Solvents at Elevated Pressures

The Anton Paar densitometer with a high-pressure measuring cell was utilized for the measurements of solvent densities at elevated pressures. This densitometer was similar to the one described in section 5.1; it also consisted of two components. One was the high peressure sensing unit DMA512, which contained a stainless steel sample tube connecting to a measuring oscillator. The capacity of the sample tube

was approximately $2.5 \times 10^{-6}\ m^3$, and the sample tube was enclosed by a jacket for circulating constant temperature fluid to control the temperature of sample to within ± 0.01 K. Both ends of the sample tube were equipped with Swagelok connectors. The unit, DMA512, was suitable for dynamic measurements, and it could be used for pressures up to 40 MPa and temperatures to 423.15 K. The other component was DMA60 which was a frequency counter and digital display component as described in section 5.1. The period of oscillation of the liquid or gas in the sample tube of the DMA512 was determined and displayed by means of this component.

A schematic diagram of the apparatus used for density measurements of solvents at elevated pressures is shown in Figure 5.5. The solvent was degassed by means of helium gas bubbled inside the solvent holding tank. After the degassing was completed, the solvent was delivered to the system by means of a Milton Roy Co., model 396 high pressure metering pump. A pulse damper (SSI model LP-21 LO-Pulse) was installed at the discharge of the pump to reduce pressure pulsations from the reciprocating action of the pump. The degassed solvent was pumped through the sample tube of the DMA512 and then through a Hoke adjustable relief valve for controlling the system pressure. A pressure transducer was installed upstream of the densitometer to measure the system pressure. The pressure transducer was calibrated by means of a dead weight gauge.

Prior to the density measurements of solvents, the densitometer was calibrated. Calibrations were carried out at the same temperatures as those used for the density

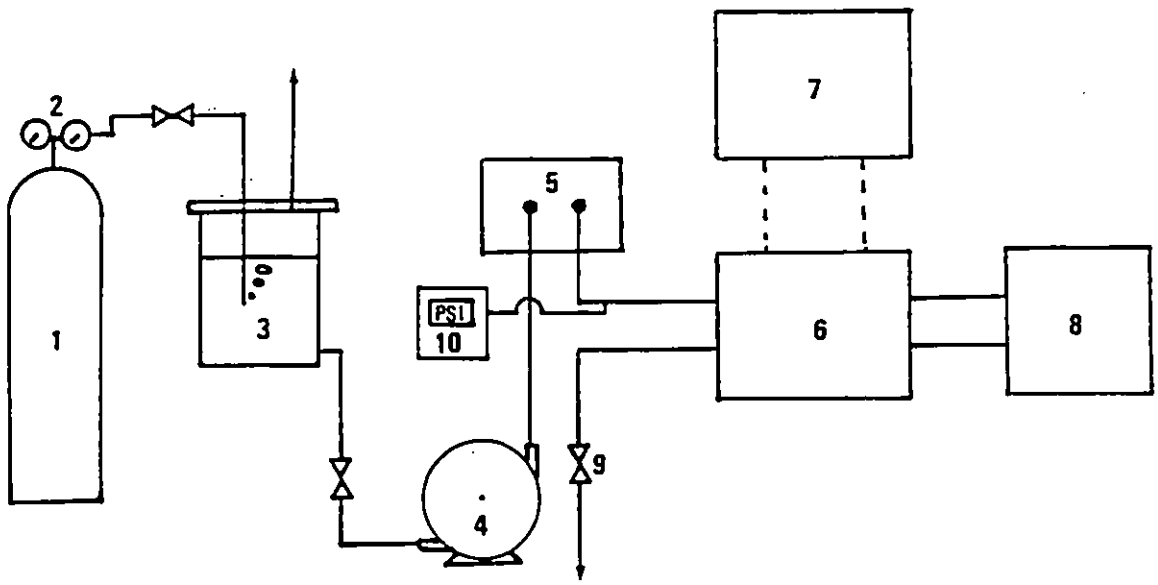

(1) helium gas cylinder, (2) regulator, (3) solvent holding tank, (4) metering pump, (5) pulse damper, (6) DMA 512 densitometer, (7) DMA 60 display unit, (8) temperature bath, (9) relief valve, (10) pressure transducer

Figure 5.5: A schematic diagram of the apparatus used for density measurements of solvents at elevated pressures

measurements. Two reference substances which densities for different pressures were known, were required for the calibrations. In this work, distilled water and nitrogen were used.

The densities of distilled water at the calibration temperatures and elevated pressures were taken from Haar, Gallagher & Kell [109]. It was found that the molar volumes of nitrogen were very accurately reproduced by utilizing the Pitzer-Curl method [110] to predict the second virial coefficients [106]. Thus the Pitzer-Curl method was used to estimate the second virial coefficients, then the molar volumes of the nitrogen were determined by equation (4.3). The densities of nitrogen were calculated by:

$$\rho = \frac{M}{MV} \tag{5.23}$$

In the equation above, MV is the molar volume and M is the molecular weight.

The calibration constant (A_p) for ..gh-pressure density measurements is expressed by the following equation:

$$A_p = \frac{\Omega_1^2 - \Omega_2^2}{\rho_1 - \rho_2} \tag{5.24}$$

In this equation, ρ_1 and ρ_2 are the densities of the reference substances, and Ω_1 and Ω_2 are the periods of oscillation read from the DMA60 unit for the reference substances. In this work, '1' represents distilled water, and '2' represents nitrogen gas. At a constant temperature, the value of the calibration constant (A_p) has been found to be pressure independent [106]. Therefore, the density of the sample, ρ, whose period of oscillation is read as Ω from the DMA60, is expressed by the

following equation:

$$\rho = \frac{1}{A_p}(\Omega^2 - \Omega_2^2) + \rho_2 \tag{5.25}$$

In the above equation, the period of oscillation for nitrogen, Ω_2, was found to be linearly correlated with the absolute pressure at any particular temperature:

$$\Omega_2 = k_1 + k_2 P \tag{5.26}$$

In this equation, k_1 and k_2 are temperature dependent constants which were estimated by a linear regression for each temperature.

Thus by substituting equation (5.26) into equation (5.25), the density of a sample is expressed as a function of pressure P and the period of the oscillation Ω as:

$$\rho = \frac{1}{A_p}[\Omega^2 - (k_1 + k_2 P)^2] + \frac{M_2}{MV_2} \tag{5.27}$$

The values for the calibration constants, A_p, k_1, k_2 and the second virial coefficient B of nitrogen are reported for the calibration temperatures of 298.15, 323.15 and 348.15 K in Appendex D.

5.10 Diffusivity Measurements at Elevated Pressures

The diffusivities of propene gas were measured in n-butanol, chlorobenzene, ethylene glycol and n-octane at different temperatures and at elevated pressures by an apparatus which was based on the phenomenon of Taylor dispersion. The technique essentially consisted of injecting a pulse of dilute solution into a stream of solvent in laminar flow and allowing it to pass through a long capillary tube.

According to Taylor's analysis of dispersion in liquids [17,18], the concentration profile at the end of the tube is gaussian, and the variance is related to the diffusion coefficient of the solute in the solvent.

A schematic diagram of the Taylor dispersion apparatus constructed for this study is shown in Figure 5.6. The solvent was degassed by means of bubbling with helium gas inside the solvent holding tank. Then the degassed solvent was delivered at room temperature and at a low and steady flowrate by a metering pump to the capillary tube. The metering pump was a Milton Roy Co., model 396 pump, and it was specified to give a constant pumping rate to within $\pm 0.3\%$. A pulse damper (SSI model LP-21 LO-Pulse) was installed downstream of the pump to reduce any pressure pulsations from the pump. Two on-line filters (15 micron and 2 micron) were used to ensure that there were no small dust particles in the system. The solvent could be divided into two streams by means of a SSI three-way valve. One portion was directed into the reference cell of a differential refractometer, and the other portion was directed through an injection valve, thence to a dispersion column consisting of a long capillary, a restricted passage and then finally into the sample cell of the differential refractometer. The injection valve was a Reodyne valve and was suitable for injecting small quantities, $2.0 \times 10^{-8}\ m^3$ of gas saturated solvent, into the system. The solvent was essentially saturated by bubbling the solute gas through the solvent at room temperature for at least one hour. The column was made of 68 m long, $1.59 \times 10^{-3}\ m$ outside diameter and $7.60 \times 10^{-4}\ m$ inside diameter stainless steel capillary tube wound into a coil of 0.105 m radius. It was

submerged in a constant temperature bath (Tamson bath) that could maintain at constant temperature to within ±0.01 K. After several hours, the fluid, containing the injected pulse of solute, passed through a restricted passage which consisted of a fine metering valve and a short section of small diameter capillary tube; this restricted passage provided a resistance to flow and hence controlled the pressure inside the capillary to 6900 kPa by viscous friction. A pressure transducer was installed upstream of the injection valve to measure the system pressure, and the system pressure was recorded by means of a recorder for checking the constancy of the pressure. The pressure transducer was calibrated by means of a dead weight gauge. The analyzer utilied was a Waters R401 differential refractometer, which was utilized to monitor the axial solute concentration profile within the capillary. The concentration profile was recorded by a linear Instructment Corp. recorder. Prior to the diffusivity measurements, the linearity of the differential refractometer was checked by following the procedure in the operation instruction manual. Usually a series of solute pulses were injected in sequence so that several response curves were obtained after the peaks eventually reached the detector. This resulted in a more rapid rate of accumulation of the diffusion coefficient data.

5.11 Theory for the Taylor Dispersion Method

Consider a δ-function pulse of a dilute solution introduced in a stream which is flowing in a straight tube in laminar flow. In an isothermal laminar flow system, with no chemical reaction and with a concentration distribution being axial symmetical,

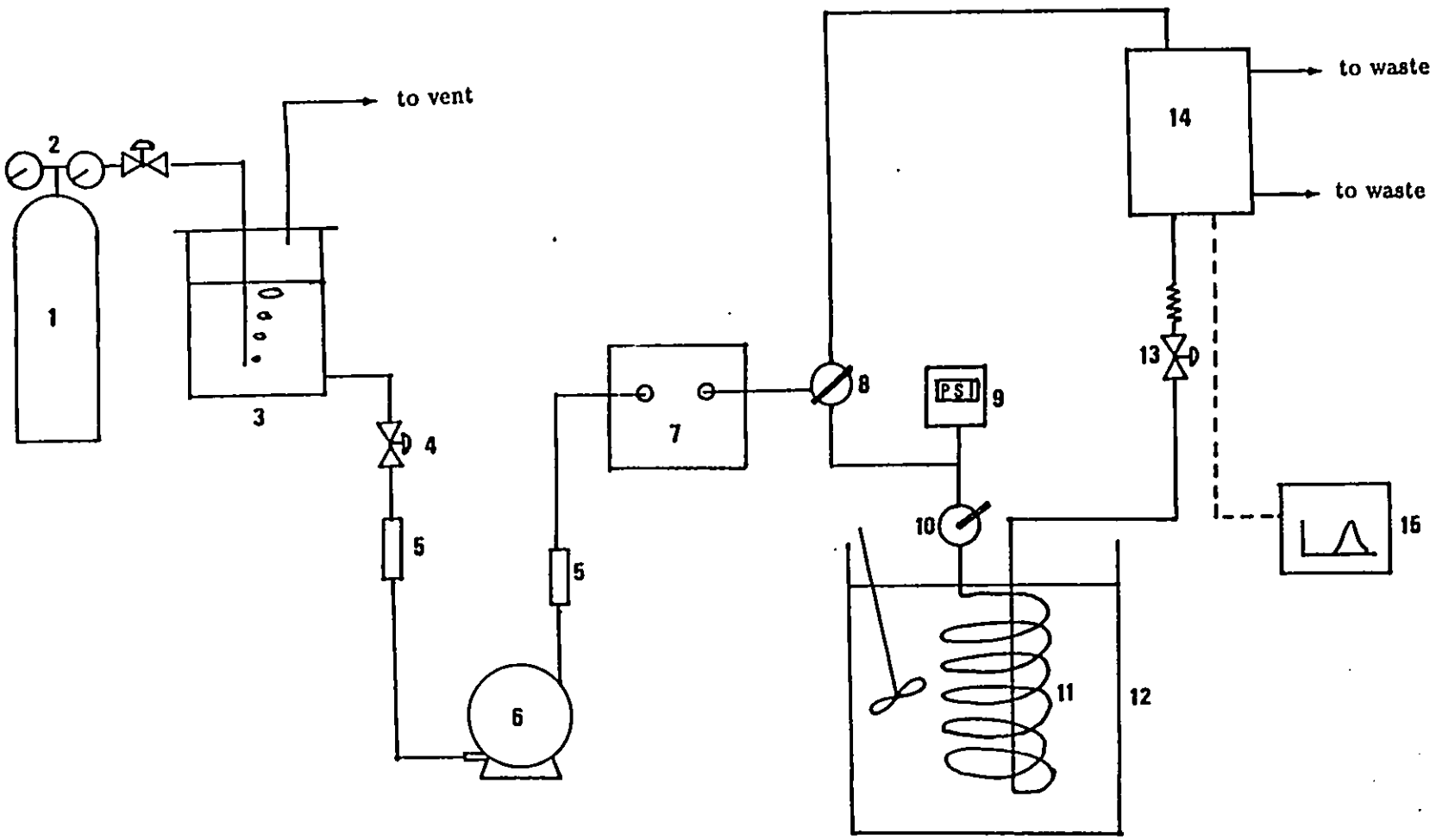

(1) helium gas cylinder, (2) regulator, (3) solvent holding tank, (4) shut-off valve, (5) filters, (6) metering pump, (7) pulse damper, (8) 3-way valve, (9) pressure transducer, (10) injection valve, (11) dispersion column, $L = 68.0m$, $i.d. = 0.76 \times 10^{-3}m$, $R_c = 0.105m$, (12) temperature bath, (13) restricted passage, (14) differential refractometer, (15) recorder

Figure 5.6: A schematic diagram of the Taylor dispersion apparatus

the mass balance for fully developed flow is given by:

$$\frac{\delta C_A}{\delta t} + 2v_m\left[1 - \frac{r^2}{R^2}\right]\frac{\delta C_A}{\delta x} = D_{AB}\left[\frac{1}{r}\frac{\delta}{\delta r}\left(r\frac{\delta C_A}{\delta r}\right) + \frac{\delta^2 C_A}{\delta x^2}\right] \tag{5.28}$$

In the above equation, C_A is the concentration in mass units per unit volume, t is the time, r is the radial distance measured perpendicular to the axis of the tube which has a radius, R, D_{AB} is the diffusion coefficient which is assumed to be independent of concentration, x is the axial coordinate, and v_m is the average velocity which is equal to half of the maximum velocity. If the ratio r/R is written as z, then:

$$v_x = 2v_m(1 - z^2) \tag{5.29}$$

It is convenient to measure the concentration distribution relative to an axial coordinate x_m, which moves with the average fluid velocity v_m. The flow velocity relative to this new frame of reference, u_x, is:

$$u_x = v_x - v_m = v_m(1 - 2z^2) \tag{5.30}$$

Then equation (5.28) becomes:

$$\frac{\delta^2 C_A}{\delta z^2} + \frac{1}{z}\frac{\delta C_A}{\delta z} + R^2\frac{\delta^2 C_A}{\delta x_m^2} = \frac{R^2}{D_{AB}}\frac{\delta C_A}{\delta t} + \frac{R^2 v_m}{D_{AB}}(1 - 2z^2)\frac{\delta C_A}{\delta x_m} \tag{5.31}$$

In the equation, the operator $\delta/\delta t$ is taken at constant x_m, that is, at planes fixed with repect to a reference frame moving with velocity v_m. The term $\delta^2 C_A/\delta x_m^2$ represents axial transport by diffusion, and Taylor [17,18] has shown that this can be neglected when the solute concentration is examined after passing through a tube of length L if:

$$\frac{4L}{R} \gg \frac{Rv_m}{D_{AB}} \gg 6.9 \tag{5.32}$$

Thus, for those conditions, equation (5.31) can be reduced to:

$$\frac{\delta^2 C_A}{\delta z^2} + \frac{1}{z}\frac{\delta C_A}{\delta z} = \frac{R^2}{D_{AB}}\frac{\delta C_A}{\delta t} + \frac{R^2 v_m}{D_{AB}}(1 - 2z^2)\frac{\delta C_A}{\delta x_m} \tag{5.33}$$

The simplest parameter to measure experimentally, is the mean concentration of the solute C_m at any selected plane in the average velocity reference frame. This is defined by:

$$C_m = 2\int_0^1 C_A z dz \tag{5.34}$$

Taylor [17,18] and Aris [19] have shown that when the conditions for equation (5.32) are fulfilled, the mean concentration obeys the following differential equation:

$$\frac{\delta C_m}{\delta t} = K\frac{\delta^2 C_m}{\delta x_m^2} \tag{5.35}$$

Aris [19] showed that:

$$K = D_{AB} + \frac{R^2 v_m^2}{48 D_{AB}} \tag{5.36}$$

The quantity, K, is called the 'Taylor diffusion coefficient' or 'dispersion coefficient'. Equation (5.35) can be solved for the case of injection of a δ-function pulse into the flowing stream [17]. The solution is:

$$C_m = \frac{m}{\pi R^2 (2\pi)^{1/2}(2Kt)^{1/2}} \exp\left[\frac{-x_m^2}{2(2Kt)}\right] \tag{5.37}$$

In this equation, m is the mass of solute in the pulse injected. Equation (5.37) describes a gaussian curve with variance (τ^2) of $2Kt$. The above derivation is based on the assumption that the tube is straight. However, it is difficult to utilize a sufficiently long straight capillary tube in practice because of the long length required, so that it is usually necessary to coil the tube in the form of a helix.

Two additional but opposing modes of mass transport need to be considered when a helical form is used for the capillary tube. At different positions in the tube, the fluid traverses different path lengths in its passage through the tube, an effect which tends to increase the dispersion. In addition, the helical form sets up secondary flows which decrease the dispersion. The net effect of these additional mass transport mechanisms in a helical tube is that a correction term must be added to equation (5.36) [111].

$$K = D_{AB} + \frac{R^2 v_m^2 [1 + 192 f(\phi, Re, Sc)]}{48 D_{AB}} \tag{5.38}$$

The correction term (f) within the square bracket is a function of ϕ, the ratio of the helix radius to the tube radius, the Reynolds (Re) and Schmidt (Sc) numbers. For diffusion in liquids, the first term of equation (5.38) can be dropped, then:

$$K = \frac{R^2 v_m^2 [1 + 192 f(\phi, Re, Sc)]}{48 D_{AB}} \tag{5.39}$$

The function $f(\phi, Re, Sc)$ tends to zero at low Reynolds number. The diffusivity can be determined from the nature of the concentration distribution curve, and the flow and capillary tube parameters. Diffusivities can be measured at elevated temperatures and pressures using this technique.

5.12 Treatment of Data for Diffusivity Measurements at Elevated Pressures

The variance (τ^2) of equation (5.37) is $2Kt$. Utilizing the definition of K (equation (5.36)), the variance can be expressed as:

$$\tau^2 = 2D_{AB}t + \frac{R^2 v_m^2 t}{24 D_{AB}} \tag{5.40}$$

For liquid diffusion, the first term on the right hand side of equation (5.40) can be neglected and the term $t = L/v_m$. Thus:

$$\tau^2 = \frac{R^2 v_m L}{24 D_{AB}} \tag{5.41}$$

Utilizing the theories for chromatography which are applicable to these experiments, the plate height can be defined as [112]:

$$H = \frac{\tau^2}{L} \tag{5.42}$$

Equation (5.41) can be rearranged to give:

$$D_{AB} = \frac{R^2 v_m}{24 H} \tag{5.43}$$

The plate height is related to the peak width, the residence time in the column, and the columnn length by means of the following relationship [113]:

$$H = \frac{L W_{1/2}^2}{5.54 t_R^2} \tag{5.44}$$

In the last equation, t_R is the residence time of the solute in the column, and $W_{1/2}$ is the width at half the solute peak height. This relationship is valid for a gaussian peak only.

Combining equations (5.43) and (5.44), the following equation can be obtained:

$$D_{AB} = 0.231 \frac{R^2 t_R}{W_{1/2}^2} \tag{5.45}$$

The values of diffusivity measured were calculated by means of equation (5.45).

Chapter 6

RESULTS AND DISCUSSIONS

The presentation and discussion of the experimental results has been organized into six sections. Section one deals with the density and viscosity measurements of pure solvents at atmospheric pressure; the measured results are compared with reported data in the literature. Section two deals with the gas solubility measurements at atmospheric pressure; the effects of polarity and tendency for self-association of the solvent on the gas solubility are discussed. Section three discusses the diffusivity measurements at atmospheric pressure; the diffusivities obtained in this investigation are compared with predicted results from diffusion theories and existing correlations in the literature. Section four deals with the density measurements at elevated pressures; the experimental data are correlated by means of the Tait equation [131] and by a two-parameter linear equation. Section five deals with the diffusivity measurements at elevated pressures; the design criteria for utilizing the Taylor dispersion method are also discussed. In the last section of this chapter, the RHS theory is tested based on the experimental data for diffusivities at high pressures.

6.1 Density and Viscosity Measurements of Solvents at Atmospheric Pressure

6.1.1 Density Measurements of Solvents at Atmospheric Pressure

The densities of acetic acid, acetone, n-butanol, chlorobenzene, N,N dimethyl formamide, ethyl acetate, ethylene glycol and n-octane were measured at atmospheric pressure utilizing the Anton Paar densitometer. These data were required for precise determination of gas solubilities. The measurements were carried out at, at least four different temperatures for each solvent. The experimental error was estimated to be ±0.2%. The measured results are presented in Table 6.1 and Table 6.2 along with those available in the literature.

As indicated in Table 6.1 and Table 6.2, good agreement is obtained between the densities reported by other workers and those measured in this study. Therefore, it can be concluded that the method utilized for the density measurements at atmospheric pressure yields satisfactory density data.

6.1.2 Viscosity Measurements of Solvents at Atmospheric Pressure

The viscosities of acetic acid, acetone, n-butanol, chlorobenzene, N,N, dimethyl formamide, ethyl acetate, ethylene glycol, and n-octane were measured by the Cannon-Fenske viscometer immersed in a constant temperature bath. The measurements were conducted at three different temperatures. The viscosity is an

SOLVENT	TEMPERATURE(K)	DENSITY(kg/m^3) THIS WORK	DENSITY(kg/m^3) LITERATURE
acetic acid	293.15	1049.1	1049.1, 1049.2
			1049.3[114]
	295.15	1046.9	——
	298.15	1042.1	1040.0[115]
			1044.1[116]
	323.15	1016.2	1015.8[115]
			1016.5[116]
acetone	278.15	806.5	807.4[116]
	288.15	796.9	796.0[114]
	293.15	791.3	790.8[114]
	295.15	789.0	——
	298.15	785.1	785.0,784.6[114]
			785.4[115]
			785.3[116]
n-butanol	278.15	820.0	——
	293.15	809.6	809.6[114]
	295.15	808.3	——
	298.15	806.0	806.0[106]
			805.7[117]
			806.1[118]
	323.15	786.6	786.6[106]
			786.7[119]
chlorobenzene	278.15	1121.0	——
	293.15	1106.0	1106.1, 1106.2[114]
	295.15	1104.1	——
	298.15	1100.9	1100.8[106]
			1100.9,1101.0[114]
			1100.9[119]
	323.15	1073.3	1073.3[106]
			1074.0[114]

Table 6.1: Densities of the acetic acid, acetone, n-butanol, chlorobenzene at atmospheric pressure

SOLVENT	TEMPERATURE(K)	DENSITY(kg/m^3) THIS WORK	DENSITY(kg/m^3) LITERATURE
N,N dimethyl	278.15	961.6	969.1[116]
formamide	293.15	948.8	——
	295.15	946.9	——
	298.15	944.9	943.9[115]
			944.3[116]
	323.15	920.1	920.1[115]
			920.6[116]
ethyl acetate	278.15	920.2	918.7[114]
			920.2[116]
	288.15	906.6	906.7,905.5[114]
	293.15	900.5	900.6[114]
	295.15	898.0	——
	298.15	894.3	894.4,894.5[114]
			894.1[115]
			894.2[116]
	323.15	863.2	863.2[115]
			803.1[116]
ethylene glycol	278.15	1122.9	——
	293.15	1113.4	——
	295.15	1112.0	——
	298.15	1109.9	1109.9,1110.0[114]
	323.15	1092.1	——
n-octane	278.15	713.3	——
	293.15	702.5	702.2,702.5,
			702.7[114]
	295.15	700.9	——
	298.15	698.6	698.7[106]
			698.8,698.5[114]
			698.5[120]
	323.15	678.0	678.1[106]
			677.8,678.1[114]

Table 6.2: Densities of N,N, dimethyl formamide, ethyl acetate, ethylene glycol, n-octane at atmospheric pressure

important transport property of the liquid, and it is closely related to the diffusion process. Furthermore, the viscosity data are required for predicting the diffusivities from most of the existing correlations. The viscosities measured in this study are shown in Table 6.3 along with those reported by other workers. The experimental error was estimated to be ±1%.

As shown in Table 6.3, good agreement is generally found between the results of this work and the values reported in the literature except for the cases of acetic acid and N,N dimethyl formamide. For the case of acetic acid, the viscosity data reported in "International Critical Table" [121] are consistently higher than the data measured in this work. However, when these data are compared with the data reported by Timmerman [114] in Figure 6.1, the data from "International Critical Table" [121] are significantly higher. Thus the data from reference [121] are considered questionable. Also in Figure 6.1, the viscosities of n-butanol and n-octane as measured in this study are compared with the data from the literature; it shows good agreement for both of those solvents. It is difficult to make any conclusion for N,N dimethyl formamide because there is lack of reported experimental data. However, based on the good agreement of the results for other solvents, it can be concluded that the method utilized for viscosity measurements at atmospheric pressure in this work has produced accurate results.

SOLVENT	TEMPERATURE(K)	VISCOSITY ($\times 10^{-3} kg/m.s$) THIS WORK	VISCOSITY ($\times 10^{-3} kg/m.s$) LITERATURE
acetic acid	293.15	1.218	1.265[121]
	298.15	1.125	1.155[121]
	323.15	0.794	0.810[121]
acetone	278.15	0.375	——
	288.15	0.338	0.337[114]
	298.15	0.315	0.308[114]
			0.324[121]
n-butanol	278.15	4.355	——
	298.15	2.593	——
	323.15	1.405	——
chlorobenzene	278.15	0.973	——
	298.15	0.755	0.758[114]
	323.15	0.572	0.571[114]
N,N dimethyl	278.15	1.052	——
formamide	298.15	0.846	0.802[122]
	323.15	0.635	——
ethyl acetate	278.15	0.545	——
	288.15	0.475	0.473[114]
	298.15	0.427	0.424[114]
	323.15	0.335	——
ethylene glycol	278.15	40.829	——
	298.15	16.200	——
	323.15	6.896	——
n-octane	278.15	0.660	——
	298.15	0.510	0.508[114]
	323.15	0.392	——

Table 6.3: Viscosities of the solvents at atmospheric pressure

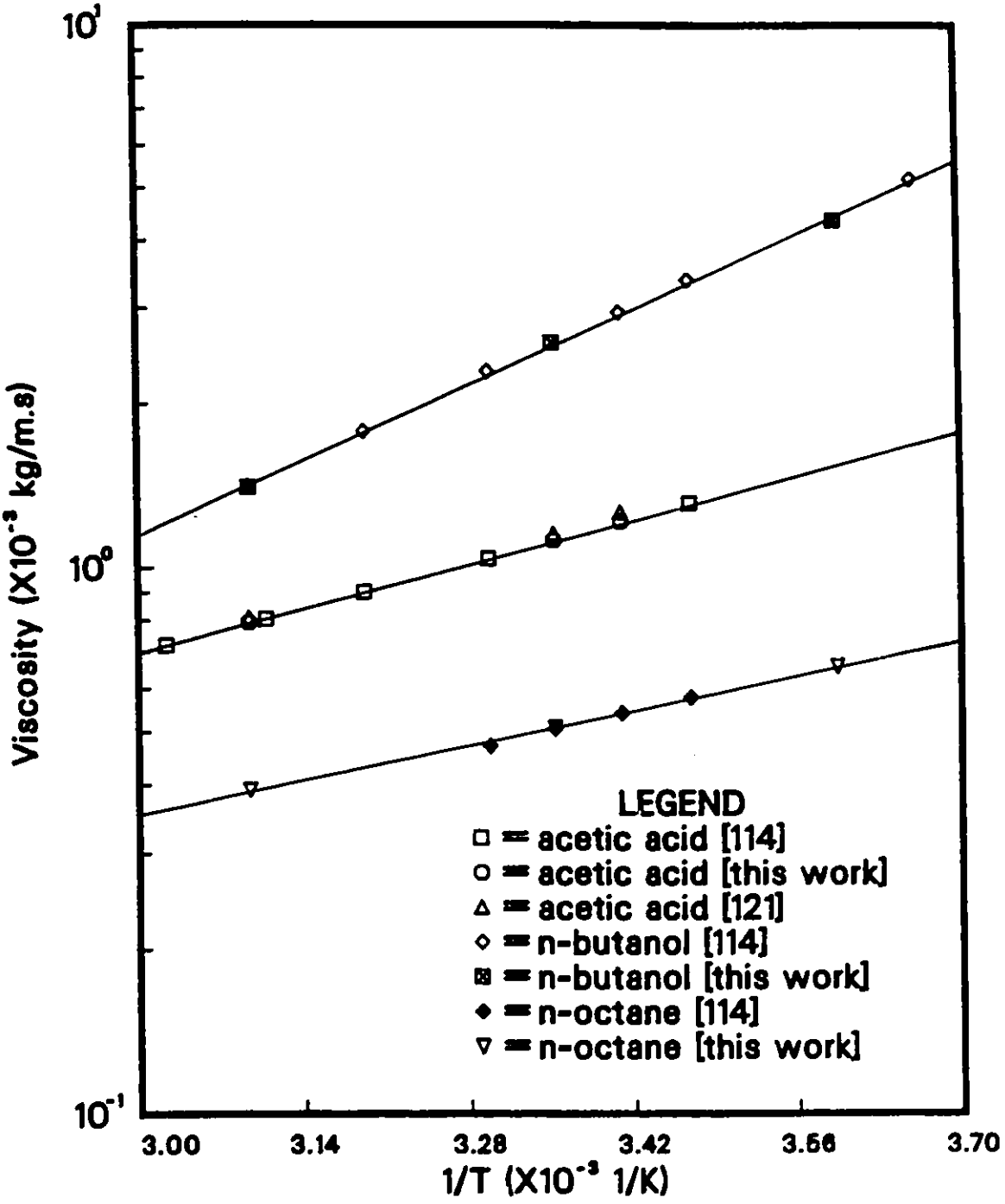

Figure 6.1: Plot of ln μ versus 1/T for acetic acid, n-butanol and n-octane

6.2 Gas Solubility Measurements at Atmospheric Pressure

In the steady-state capillary cell method for determining diffusivities of dissolved gases, a knowledge of the gas solubility is required. Therefore, the solubilities of propene were measured at atmospheric pressure in acetic acid, acetone, n-butanol, chlorobenzene, N,N dimethyl formamide, ethyl acetate, ethylene glycol and n-octane by utilizing the solubility apparatus mentioned in Chapter 5. The experiments were conducted at three different temperatures for each solvents, and the experiments were repeated at least three times for each system at the same temperature. The deviations of the multiple results were always less than $\pm 1\%$ from the average, and the experimental error was estimated to be $\pm 2\%$.

It is conventional to convert gas solubilities measured at some experimental pressures to that calculated for a solute partial pressure of 101.3 kPa. It is considered that such a conversion allows a comparison of solubilities for a common gas partial pressure. Table 6.4 shows the gas solubilities at 101.3 kPa solute partial pressure and a variation about the mean corresponding to one standard deviation of the multiple results and a comparison with solubilities available in the literature. The calculation procedure described in section 5.5 was used for the determination of gas solubility. A sample calculation is given in Appendix E.

Two potential errors can affect significantly the results in the gas solubility measurements, namely, incomplete deaeration and less than complete saturation

SOLVENT	TEMPERATURE (K)	SOLUBILITY (mole fraction)	LITERATURE VALUE
acetic acid	293.15	0.0246 ± 0.0002	
	298.15	0.0224 ± 0.0002	
	323.15	0.0133 ± 0.0001	
acetone	278.15	0.0679 ± 0.0003	
	288.15	0.0542 ± 0.0002	
	298.15	0.0453 ± 0.0004	
n-butanol	278.15	0.0652 ± 0.0001	
	298.15	0.0390 ± 0.0001	0.0389[106]
	323.15	0.0223 ± 0.0001	0.0221[106]
chlorobenzene	278.15	0.1153 ± 0.0001	
	298.15	0.0698 ± 0.0001	0.0697[106]
	323.15	0.0400 ± 0.0001	0.0400[106]
N,N dimethyl-	278.15	0.0407 ± 0.0001	
formamide	298.15	0.0278 ± 0.0001	
	323.15	0.0184 ± 0.0002	
ethyl acetate	278.15	0.1037 ± 0.0002	
	288.15	0.0826 ± 0.0001	
	298.15	0.0661 ± 0.0002	
	323.15	0.0414 ± 0.0003	
ethylene glycol	278.15	0.0035 ± 0.0001	
	298.15	0.0023 ± 0.0001	
	323.15	0.0015 ± 0.0000	
n-octane	278.15	0.1757 ± 0.0001	
	298.15	0.1062 ± 0.0001	0.1060[106]
	323.15	0.0636 ± 0.0001	0.0635[106]

Table 6.4: Gas solubilities of propene in various solvents at 101.3 kPa partial pressure of solute gas

of the solvent. To verify that the deaeration was complete, different durations of the degassing time were utilized for the multiple runs, and the deviations of the results were less than ±1%. Thus it could be concluded that all the deaerations were complete and independent of deaeration times. To verify that the solvent was saturated with the solute gas, different motor speeds of the syringe pump, that is, different infusion rates of the degassed solvent, were utilized for the multiple runs. If the measured gas solubilities were independent of the motor speed of the syringe pump as found in these experiments, then the solvent could be considered to be completely saturated with the solute gas.

Gas solubilities that were previously reported by other workers are compared with those obtained in this study in Figures 6.2 and 6.3. It is observed in these figures that generally good agreement is obtained between the data from the literature and those measured in the work. It can be concluded that the apparatus used in this study for the measurements of gas solubility at atmospheric pressure is accurate.

Figures 6.2 and 6.3 are the plots of the logarithm of the mole fraction solubility versus the logarithm of the absolute temperature. In these figures, the ideal gas solubilities are indicated as dashed lines with the ideal gas solubility calculated from the following equation:

$$x_A^{ideal} = \frac{101.3}{p_A^s} \tag{6.1}$$

In the equation above, p_A^s is the vapor pressure of the gas which is determined by the Gometz-Nieto and Thodos method [123]. Equation (6.1) indicates that the

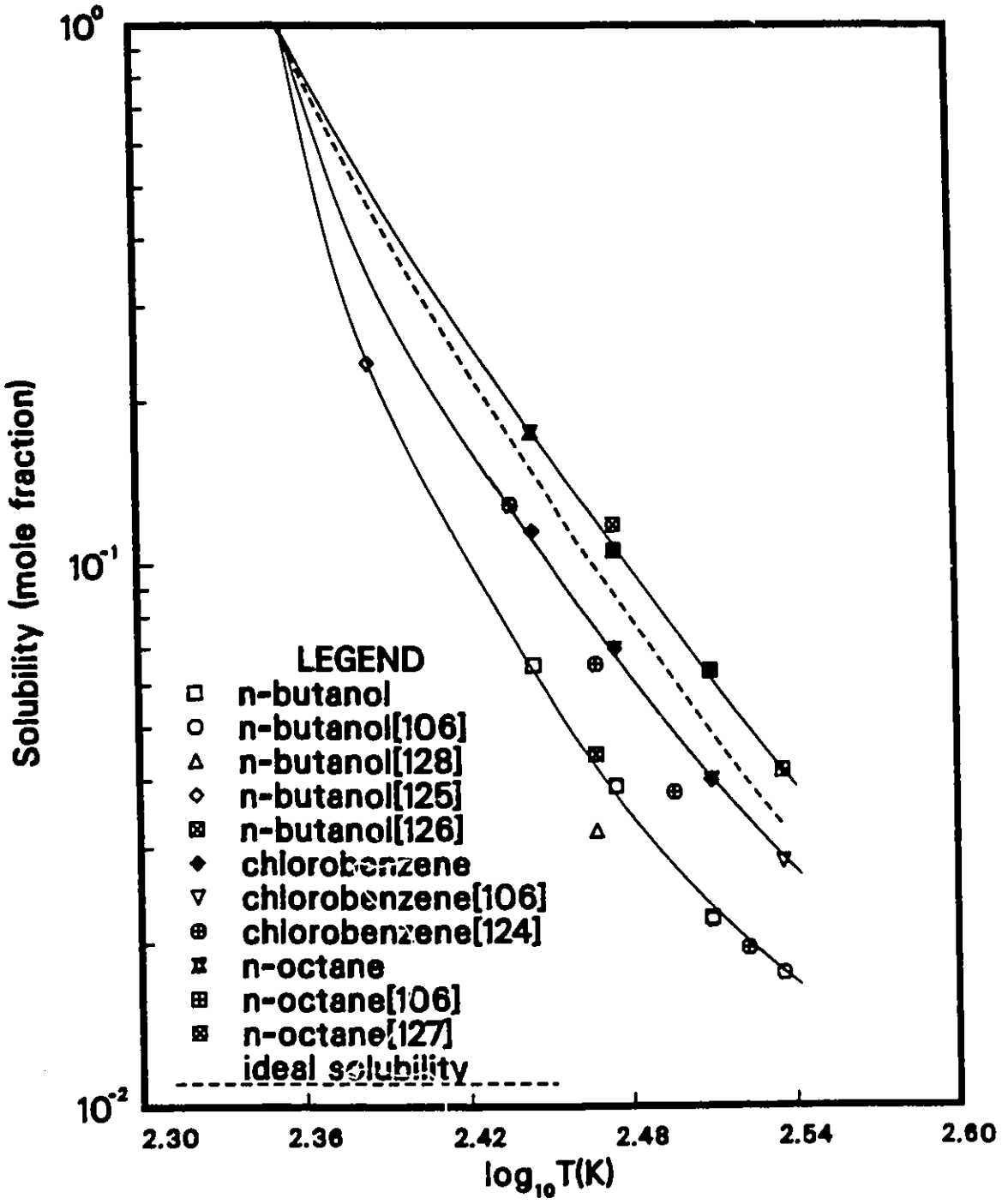

Figure 6.2: Temperature dependence of the gas solubilities of propene in n-octane, chlorobenzene and n-butanol

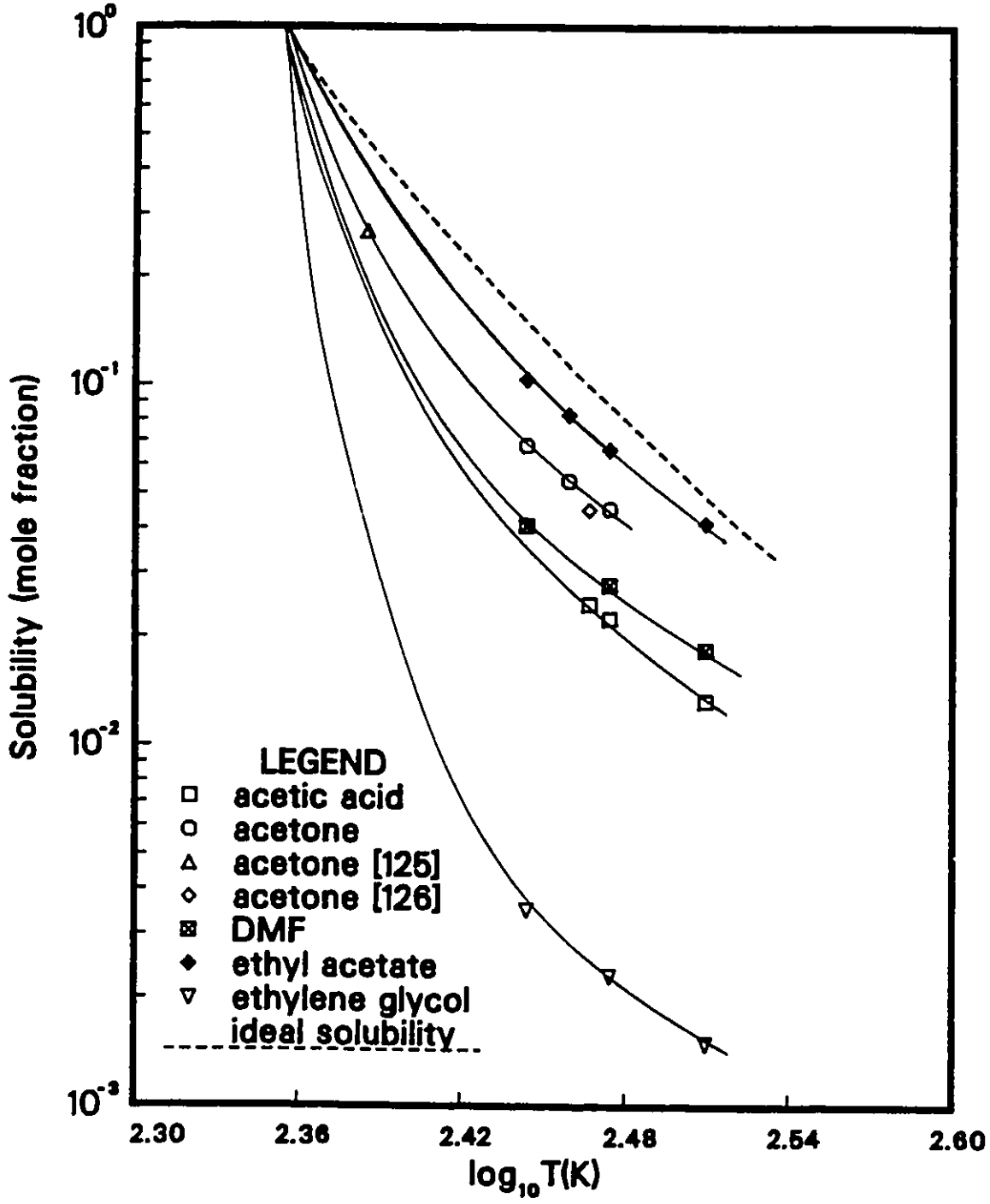

Figure 6.3: Temperature dependence of the gas solubilities of propene in acetic acid, acetone, N,N dimethyl formamide, ethyl acetate, ethylene glycol

ideal gas solubility becomes unity at the normal boiling point of the solute gas. In these figures, it can be observed that of all the solvents used, only the solubilities of propene in n-octane are higher than the ideal gas solubilities.

It appears possible that polarity of the solvent or tendency for self-association of the solvent molecules, influences the gas solubility. In Figure 6.2, gas solubilities of propene in n-octane, chlorobenzene and n-butanol are compared. It is observed that the solubilities of propene are highest in n-octane, lower in chlorobenzene and lowest in n-butanol. Since n-octane is non-polar, chlorobenzene is polar but non-associating, and n-butanol is highly polar and associating, it appears likely that the gas solubilities are reduced in polar solvents which tend to self-associate. This result agrees with the hypothesis proposed by Hayduk and Laudie [129] that large reductions in gas solubility from the ideal gas solubility were attributed to the formation of strong hydrogen-bonds in solvents.

6.3 Diffusivity Measurements at Atmospheric Pressure

The diffusivities at atmospheric pressure of propene were measured by the steady-state capillary cell method in acetic acid, acetone, n-butanol, chlorobenzene, N,N dimethyl formamide, ethyl acetate and n-octane. The experiments were conducted at three different temperatures for each system, and the experiments were repeated at least three times for each system at the same temperature. The deviations of the multiple runs were always less than 2%, and the experimental

error was estimated to be ±3%. The diffusivity of propene in ethylene glycol was not measured by the steady-state capillary cell method because the time required for development of a steady-state concentration profile was extremely long (about 20 days) due to the extremely low diffusion rate.

The average values of diffusivity and their standard deviations for the repeated measurements of propene in the seven solvents are shown in Table 6.5. The procedure described in section 5.8 was used for calculation of the diffusivities. A sample calculation is presented in Appendix F. Linear relationships were obtained for all systems when semi-logarithm plots of diffusivity versus reciprocal of absolute temperature were constructed as shown in Figure 6.4. This diagram verifies that the temperature dependence of diffusivity can be described by an equation of the Arrhenius type (3.1) at least for the temperature range studied in this investigation.

The experimental data obtained in this study are considered new because there are no data available in the literature for comparison. To verify the accuracy of the diffusivity measurement apparatus and procedure which were employed in this investigation, the diffusivity of propane gas was measured in n-butanol at 298.15K. The result obtained for this solvent is compared in Table 6.6 with reported values from the literature from two different sources. The deviations between the experimental result and the values from the literature are about 1%, which is within the experimental error. Therefore, it is concluded that the diffusivity measurement apparatus and procedure utilized in this study can produce accurate results.

A potential error in the steady-state capillary cell method is the 'Δl effect' which

SOLVENT	TEMPERATURE (K)	NO. OF RUNS	DIFFUSIVITY (MEAN) ($\times 10^{-9} m^2/s$)
acetic acid	293.15	5	1.60 ± 0.03
	298.15	5	1.77 ± 0.06
	323.15	4	2.70 ± 0.09
acetone	278.15	4	4.82 ± 0.07
	288.15	4	5.43 ± 0.09
	298.15	4	6.18 ± 0.08
n-butanol	278.15	3	0.83 ± 0.02
	298.15	5	1.34 ± 0.02
	323.15	5	2.37 ± 0.02
chlorobenzene	278.15	4	1.80 ± 0.06
	298.15	4	2.40 ± 0.09
	323.15	4	3.37 ± 0.06
N,N dimethyl-	278.15	3	1.45 ± 0.04
formamide	298.15	4	1.89 ± 0.04
	323.15	5	2.66 ± 0.06
ethyl acetate	278.15	4	3.66 ± 0.09
	288.15	4	4.26 ± 0.14
	298.15	4	4.95 ± 0.13
	323.15	4	6.86 ± 0.20
n-octane	278.15	3	2.52 ± 0.07
	298.15	4	3.40 ± 0.09
	323.15	4	4.77 ± 0.07

Table 6.5: Diffusivities of propene in various solvents at atmosphric pressure

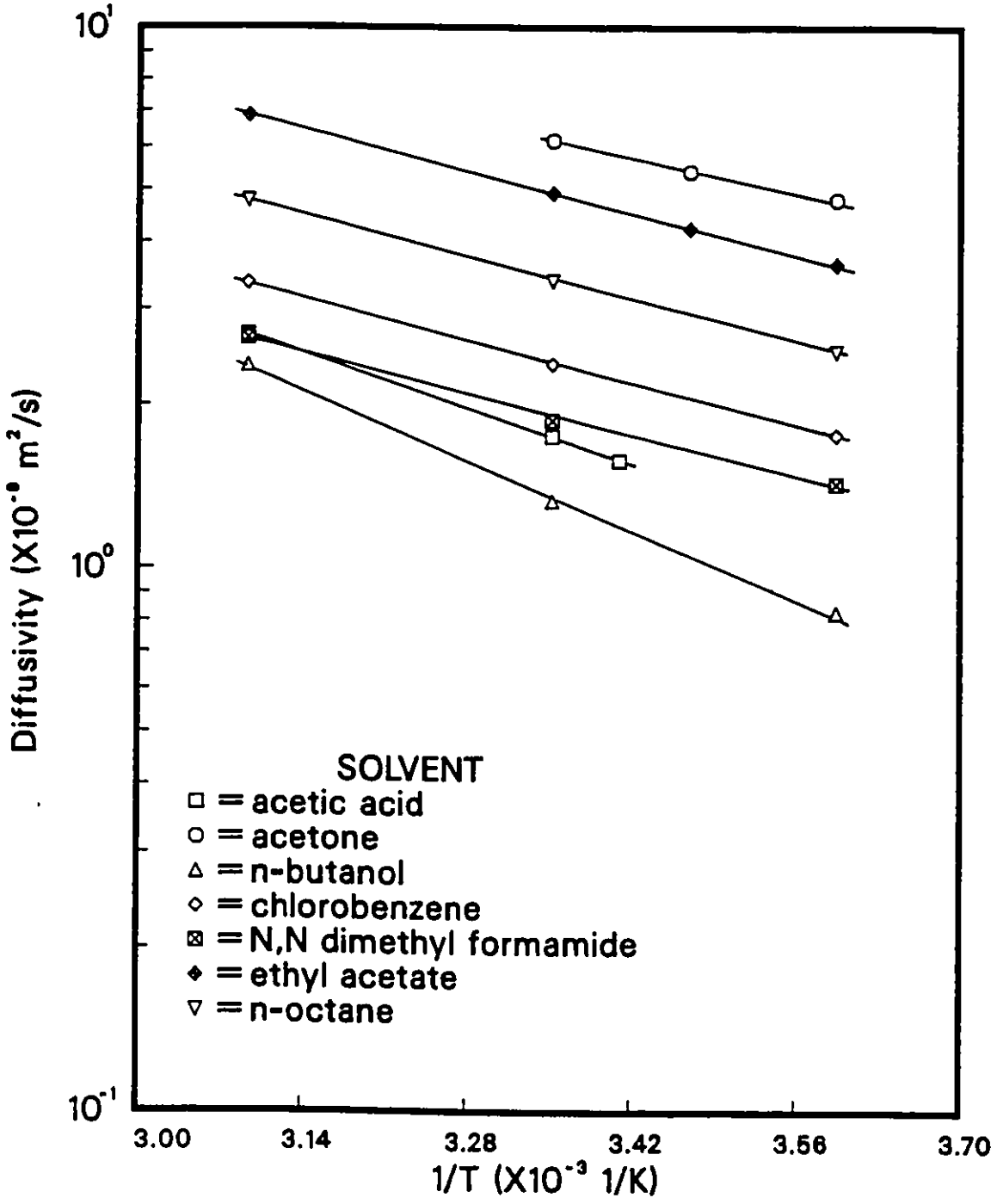

Figure 6.4: Plot of ln D^{o}_{AB} versus 1/T for propene in various solvents

SOLUTE	SOLVENT	TEMPERATURE (K)	DIFFUSIVITY ($\times 10^{-9} m^2/s$)	LITERATURE VALUE
propane	n-butanol	298.15	1.58 ± 0.01	1.57[140] 1.57 ± 0.04[58]

Table 6.6: Diffusivities of propane in n-butanol at atmospheric pressure

arises because the actual length of the diffusion path may differ from the geometric length owing to a concentration build up at the lower end of the capillary [130]. It has been found that the effect from the difference between the effective length and the apparent length of the diffusion paths becomes negligible above a certain length. It is, of course, impossible to measure the effective length of the diffusion path which includes the region of solute accumulated at the end of the capillary. The relation between diffusivity at 298.15 K and apparent diffusion path length for propene in ethyl acetate is shown in Figure 6.5. From this figure, it is evident that the length of the diffusion path beyond which 'Δl effects' become negligible, is about 0.02 m. This minimum length of 0.02 m was applied to all the experiments involving the steady-state capillary cell method to ensure that the end effects were negligible.

It has been found that the tendency for self-association of the solvent molecules by means of the formation of hydrogen-bonds reduces the rate of diffusion. The solvent N,N dimethyl formamide, acetic acid and n-butanol are known to have a

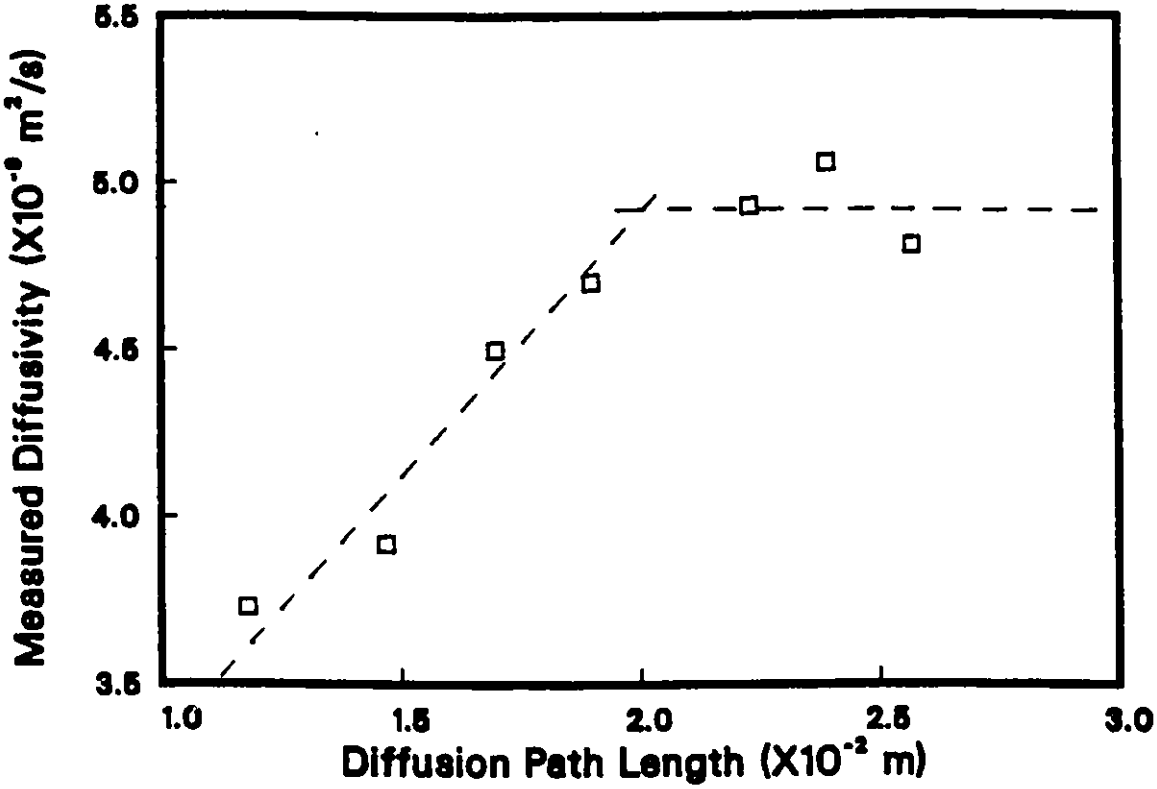

Figure 6.5: The relation between diffusivities and apparent diffusion path lengths for propene in ethyl acetate at 298.15 K and atmospheric pressure

strong tendency for forming hydrogen-bonds. Thus the diffusivities of propene in those three solvents are lower than in the other four solvents which have a much lower tendency for the formation of hydrogen-bonds, as shown in Figure 6.4. It is also evident that the diffusivity increases with decreasing viscosity of solvent based on the comparison of the data in Table 6.3 and Table 6.5 and shown in Figure 6.6.

The diffusivities of propene gas in n-butanol as measured at the three temperatures in this study are compared with the values predicted by means of several available correlating equations previously discussed in Chapter 2, in Figure 6.7. The Umesi and Danner correlation (2.35) under-predicts the propene molecular diffusivities; the reason for this is considered to result from the fact that the correlation was developed for predicting diffusivities in nonpolar solvents only. The Sridhar and Potter correlation (2.33) also seriously under-predicts the propene diffusivities. The Akgerman and Gainer equation (2.27), on the other hand, under-predicts the propene diffusivities at low temperatures and over-predicts them at high temperatures. Finally, the Sovová correlation (2.32) and the proposed correlation (3.12) for dissolved gases in liquids both over-predict the propene diffusivities at low temperatures and under-predict them at higher temperatures. However, the new correlation proposed here gives a much better prediction of the diffusivity for propene in n-butanol than those of the other correlations mentioned. Similar comparisons of the diffusivities of propene gas in each of the other six solvents measured in this study are shown in Appendix G. For most of the systems studied, the new correlation and the Akgerman and Gainer correlation give relatively good predictions of the

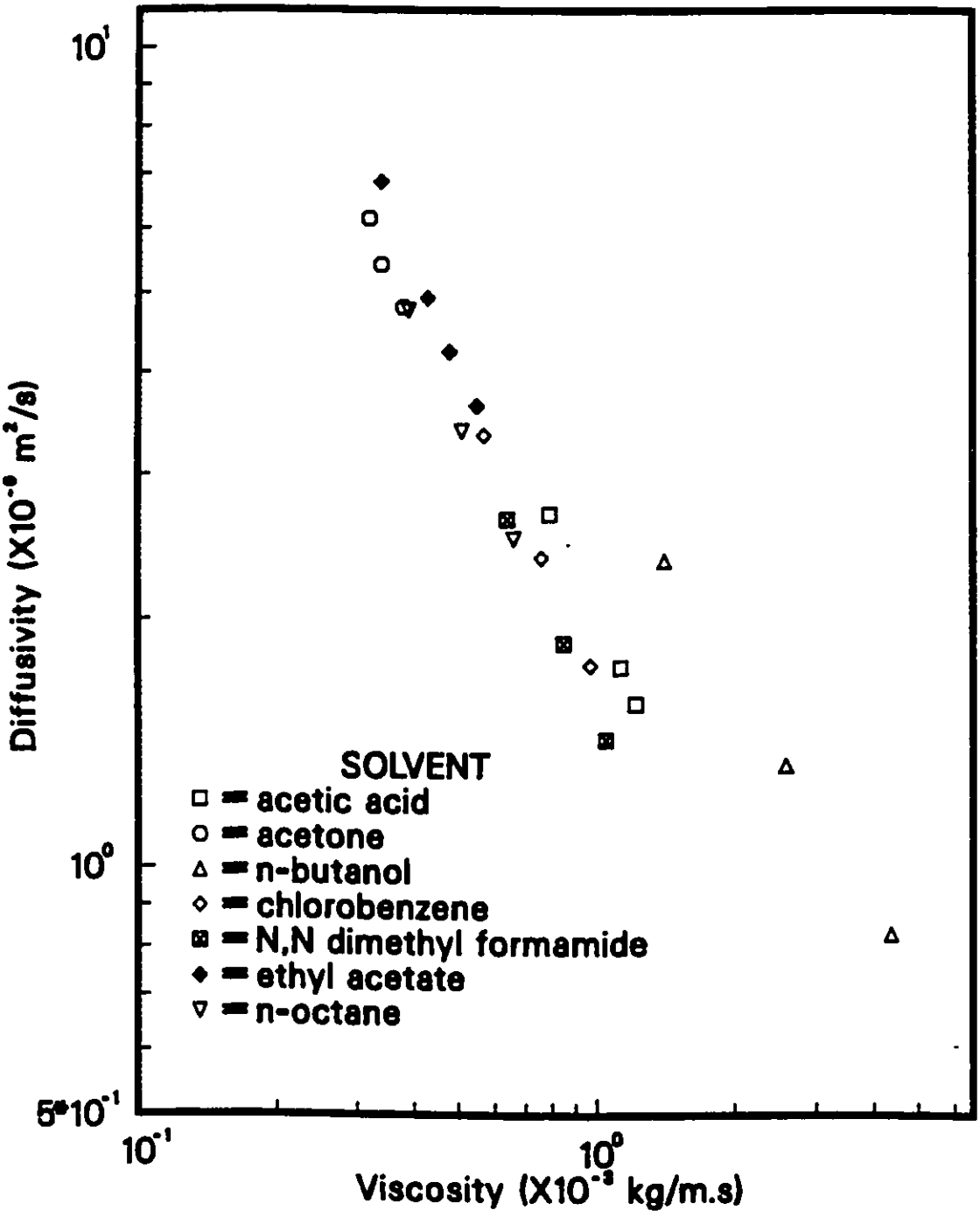

Figure 6.6: Plot of ln D°_{AB} versus ln μ for propene in various solvents at atmospheric pressure

propene diffusivities. However, the new correlation for the prediction of diffusivities for dissolved gases in liquids gives a significantly lower average error than do the other correlations tested, based on 352 data, as mentioned in Chapter 3.

The diffusivities of propene gas in n-butanol as measured at the three temperatures in this investigation are compared with values predicted by utilizing the hydrodynamic theory (equations (2.3) and (2.4)) and the rate theory of Eyring (equation (2.8)), in Figure 6.8. When required, the radius of molecules are estimated, utilizing the value of the molar volume at the normal boiling point, and assuming that the molecules are spherical. Both these diffusion theories seriously under-predict the propene diffusivities. The Stokes-Enistein equation (2.3) is usually considered applicable only for the case where the size of the solute molecules are relatively large, when compared with the size of the solvent molecules; hence it is not considered applicable for the case of diffusion of dissolved gases in liquids. Another form of the hydrodynamic theory as expressed by equation (2.4) is expected to give better predictions for systems in which molecular sizes of solute and solvent are comparable; this situation is not always true for diffusion of dissolved gases in liquids. However, as mentioned before, equation (2.8) of Eyring's only gives values of diffusivity of the proper order of magnitude only; so it is not surprising to find that the predicted results using equation (2.8) are far different from the experimental data. The same results are obtained for the other six solvents as shown in Appendix H. It can be concluded that neither the hydrodynamic theory nor the rate theory of Eyring are able to give reliable predictions of diffusivity for gas-liquid systems.

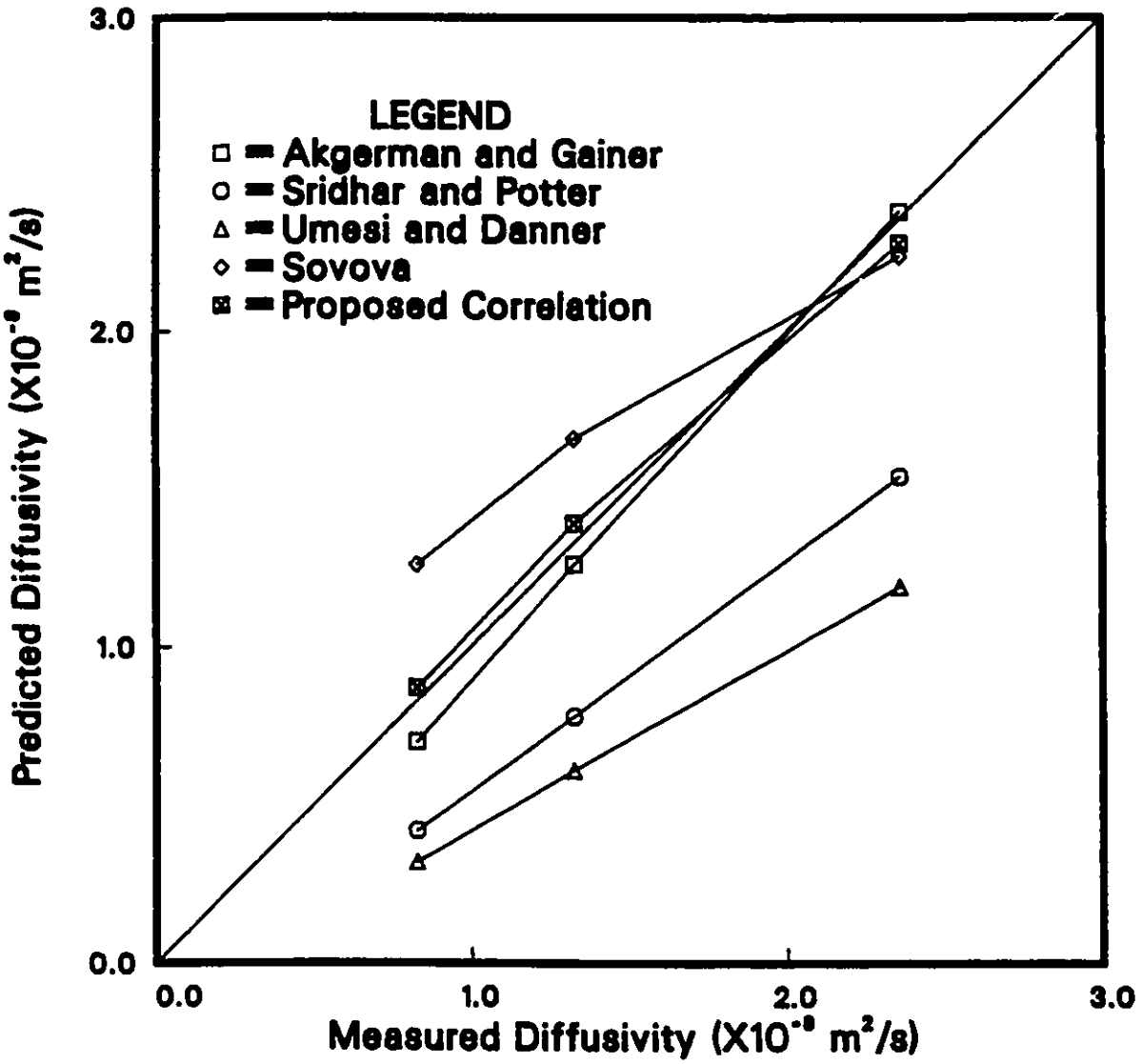

Figure 6.7: Comparsion of the experimental diffusivities with the predicted values from available correlations for propene gas in n-butanol

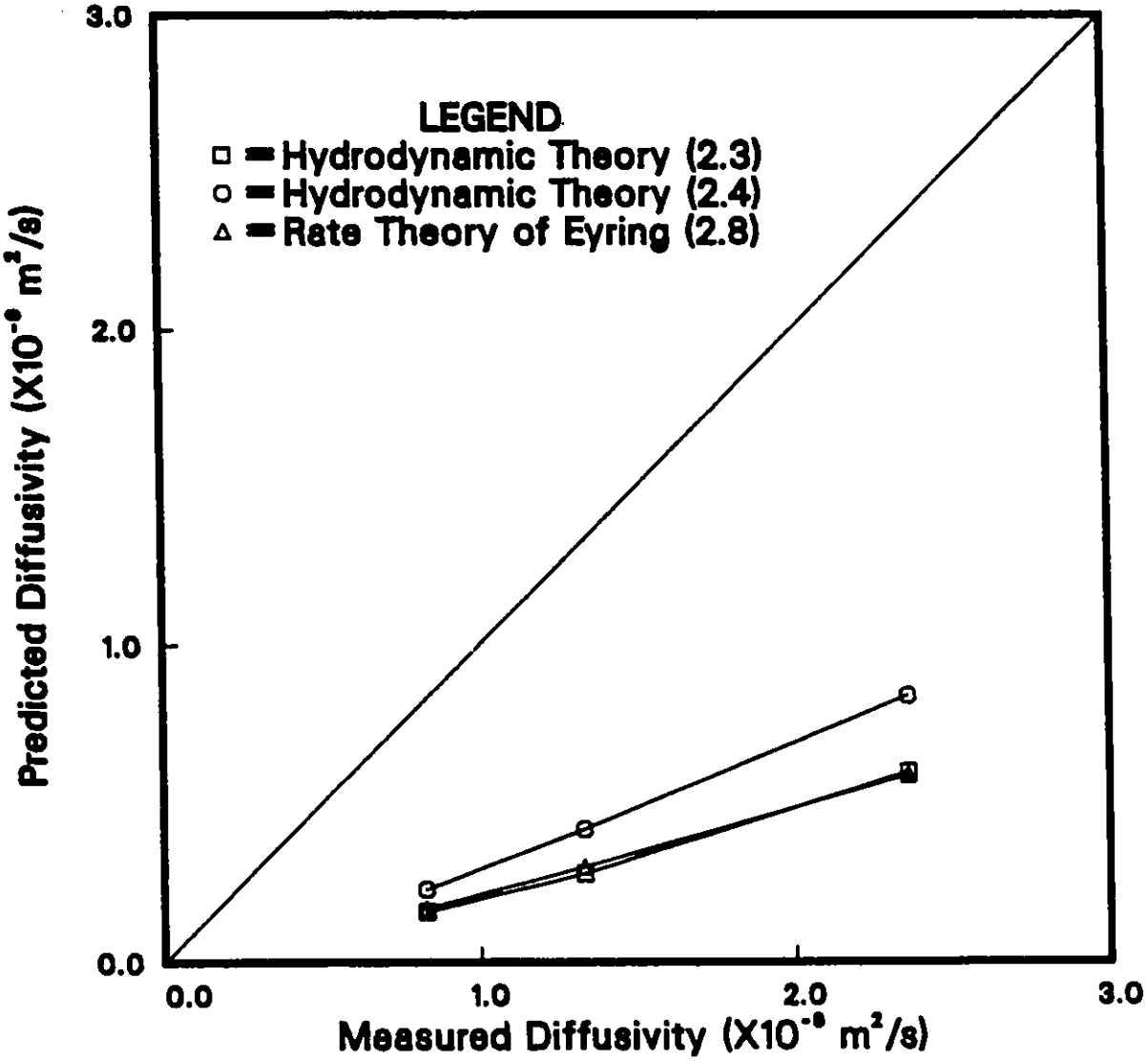

Figure 6.8: Comparsion of the experimental diffusivities with the predicted values from available diffusion theories for propene gas in n-butanol

6.4 Density Measurements of Solvents at Elevated Pressures

The densities of the solvents of n-butanol, chlorobenzene, ethylene glycol and n-octane were measured at elevated pressures utilizing the Anton Paar densitometer equipped with a high-pressure measuring cell. These data were required to determine the molar volumes of the solvents at elevated pressures. The measurements were carried out at 298.15 K, 323.15 K and 348.15 K and at pressures up to 6891.2 kPa for each solvent. The experimental results are shown in Tables 6.7 to 6.10. The experimental error was estimated to be $\pm 0.5\%$.

To verify the consistency of the high pressure Anton Paar densitometer, the densities of the four solvents at 101.3 kPa pressure as listed in Table 6.7 through Table 6.10 were compared with those obtained with the low pressure densitometer as listed in Tables 6.1 and 6.2, and good agreement was obtained in all cases. Therefore, it can be considered that the equipment and method utilized for the density measurements at elevated pressures is likely to produce reliable density data.

The classical relationship for expressing the pressure dependence of the molar volume is the Tait equation [131], usually written in terms of the coefficient of compression, κ, as:

$$\kappa = \frac{V_1 - V_p}{V_1} = G \log\left(\frac{E+P}{E+1}\right) \tag{6.2}$$

In the equation above, V_1, and V_p, are molar volumes at 101.3 kPa pressure, and

at a higher pressure P, respectively, and the pressure, P is in atmospheres. In the same equation, E and G are constants. The Tait equation (6.2) can be rewritten in terms of densities as follows:

$$\kappa = 1 - \frac{\rho_1}{\rho_p} = G \log\left(\frac{E+P}{E+1}\right) \tag{6.3}$$

The values of E and G in equation (6.3) for the four solvents which densities were measured in this work, were estimated by means of the nonlinear regression analysis; again the NLIN package in the SAS library was utilized. The estimated values of E and G and the average deviations from densities predicted by utilizing equation (6.3) are reported in Table 6.11. The average deviation is the average value of the absolute percent error defined by equation (3.10). The predicted values calculated using equation (6.3) are compared with the experimental data for n-butanol in Figure 6.9. From Figure 6.9, it is apparent that the Tait equation gives good predictive results at high temperatures (i.e. 323.15 K and 348.15 K), but gives poor predictions at low temperature (i.e. 298.15 K) probably because of the extremely large values of E and G at low temperature. Similar observation can be made for the density data for all the other solvents.

Based on a linear relationship observed from a plot of density versus pressure within the pressure range studied in this investigation, the pressure dependence of the density can be expressed by a two-parameter linear equation such as:

$$\rho = Q + S \cdot P \tag{6.4}$$

In this equation, ρ is density in kg/m^3, and P is pressure in kPa. The values

of the constants Q and S were estimated by a linear regression analysis, and the results are presented in Table 6.12. Since the values of the slope S in equation (6.4) increases with increasing temperature, it implies that the effect of pressure on density becomes more significant with increasing temperature. In Figure 6.9, the experimental data for n-butanol are compared with the results predicted by means of equation (6.4).

Based on the observation of the results obtained and calculations made as shown in this section, equation (6.3) was found to give the best predictive results for densities at high temperatures and equation (6.4) to give the best predictions for densities at low temperatures for the pressure range studied in this investigation. It was also observed that the changes of density with increasing pressure are more significant at higher temperatures.

6.5 Diffusivity Measurements at Elevated Pressures

6.5.1 Design Criteria for the Taylor Dispersion Method

Because the diffusion coefficients of dissolved gases and the solvent viscosities both vary greatly with temperature and because of the particular solute-solvent interactions for the systems being studied, it was necessary to check the design criteria for each measurement of diffusivity utilizing the Taylor dispersion technique. For each experiment, the design criteria were evaluated and compared with the operating conditions actually used for the experiment to insure that the conditions

PRESSURE (kPa)	DENSITY (kg/m^3)		
	298.15 K	323.15 K	348.15 K
101.3	806.0	786.8	760.0
344.6	806.1	786.9	760.3
689.1	806.2	787.1	760.7
1378.2	806.4	787.6	761.4
2067.3	806.7	788.1	762.1
2756.5	806.9	788.5	762.8
3445.6	807.2	788.9	763.5
4134.7	807.5	789.4	764.2
4823.8	807.8	789.8	764.9
5512.9	808.1	790.2	765.6
6202.0	808.4	790.6	766.1
6891.2	808.7	791.0	766.6

Table 6.7: Densities of n-butanol at elevated pressures

PRESSURE (kPa)	DENSITY (kg/m^3)		
	298.15 K	323.15 K	348.15 K
101.3	1100.9	1073.0	1047.0
344.6	1100.9	1073.6	1047.3
689.1	1101.0	1073.9	1047.7
1378.2	1101.3	1074.5	1048.5
2067.3	1101.7	1075.0	1049.3
2756.5	1102.1	1075.6	1050.1
3445.6	1102.6	1076.3	1051.0
4134.7	1103.2	1076.9	1051.6
4823.8	1103.6	1077.5	1052.4
5512.9	1104.1	1078.2	1053.1
6202.0	1104.6	1078.7	1053.8
6891.2	1105.2	1079.3	1054.6

Table 6.8: Densities of chlorobenzene at elevated pressures

PRESSURE (kPa)	DENSITY (kg/m^3)		
	298.15 K	323.15 K	348.15 K
101.3	1109.9	1092.3	1073.1
344.6	1109.9	1092.4	1073.3
689.1	1109.9	1092.5	1073.5
1378.2	1109.9	1092.7	1073.9
2067.3	1109.9	1092.9	1074.2
2756.5	1109.9	1093.1	1074.6
3445.6	1110.0	1093.2	1075.0
4134.7	1110.1	1093.4	1075.4
4823.8	1110.2	1093.6	1075.7
5512.9	1110.3	1093.8	1076.1
6202.0	1110.4	1094.0	1076.5
6891.2	1110.5	1094.2	1076.9

Table 6.9: Densities of ethylene glycol at elevated pressures

PRESSURE (kPa)	DENSITY (kg/m^3)		
	298.15 K	323.15 K	348.15 K
101.3	698.4	678.3	660.0
344.6	698.5	678.5	660.3
689.1	698.6	678.8	660.7
1378.2	698.9	679.4	661.8
2067.3	699.3	679.9	662.6
2756.5	699.7	680.5	663.4
3445.6	700.1	681.1	664.3
4134.7	700.5	681.6	665.1
4823.8	700.8	682.2	666.0
5512.9	701.2	682.8	666.9
6202.0	701.6	683.3	667.8
6891.2	702.0	683.9	668.6

Table 6.10: Densities of n-octane at elevated pressures

SOLVENT	TEMPERATURE (K)	E (atm.)	G	AVE. DEV. (%)
n-butanol	298.15	8.44×10^{15}	9.65×10^{11}	0.144
	323.15	550.99	0.1072	0.003
	348.15	187.29	0.0660	0.005
chlorobenzene	298.15	2.51×10^{16}	3.32×10^{12}	0.236
	323.15	152.82	0.0368	0.009
	348.15	330.88	0.0897	0.003
ethylene glycol	298.15	6.71×10^{16}	1.10×10^{12}	0.016
	323.15	562.04	0.0351	0.002
	348.15	644.91	0.0816	0.003
n-octane	298.15	7.94×10^{15}	1.39×10^{12}	0.224
	323.15	1686.09	0.4832	0.003
	348.15	727.03	0.3363	0.006

Table 6.11: Estimated values of E and G for equation (6.3)

SOLVENT	TEMPERATURE (K)	Q (kg/m^3)	S ($kg/m^3.kPa$)	AVE. DEV. (%)
n-butanol	298.15	805.90	3.973×10^{-4}	0.006
	323.15	786.73	6.285×10^{-4}	0.005
	348.15	760.02	9.890×10^{-4}	0.011
chlorobenzene	298.15	1100.50	6.456×10^{-4}	0.012
	323.15	1073.20	8.970×10^{-4}	0.007
	348.15	1047.00	1.077×10^{-3}	0.014
ethylene glycol	298.15	1109.50	1.451×10^{-4}	0.010
	323.15	1092.31	2.721×10^{-4}	0.002
	348.15	1073.10	5.488×10^{-4}	0.002
n-octane	298.15	698.30	5.369×10^{-4}	0.009
	323.15	678.23	8.228×10^{-4}	0.003
	348.15	659.91	1.267×10^{-3}	0.007

Table 6.12: Estimated values of Q and S for equation (6.4)

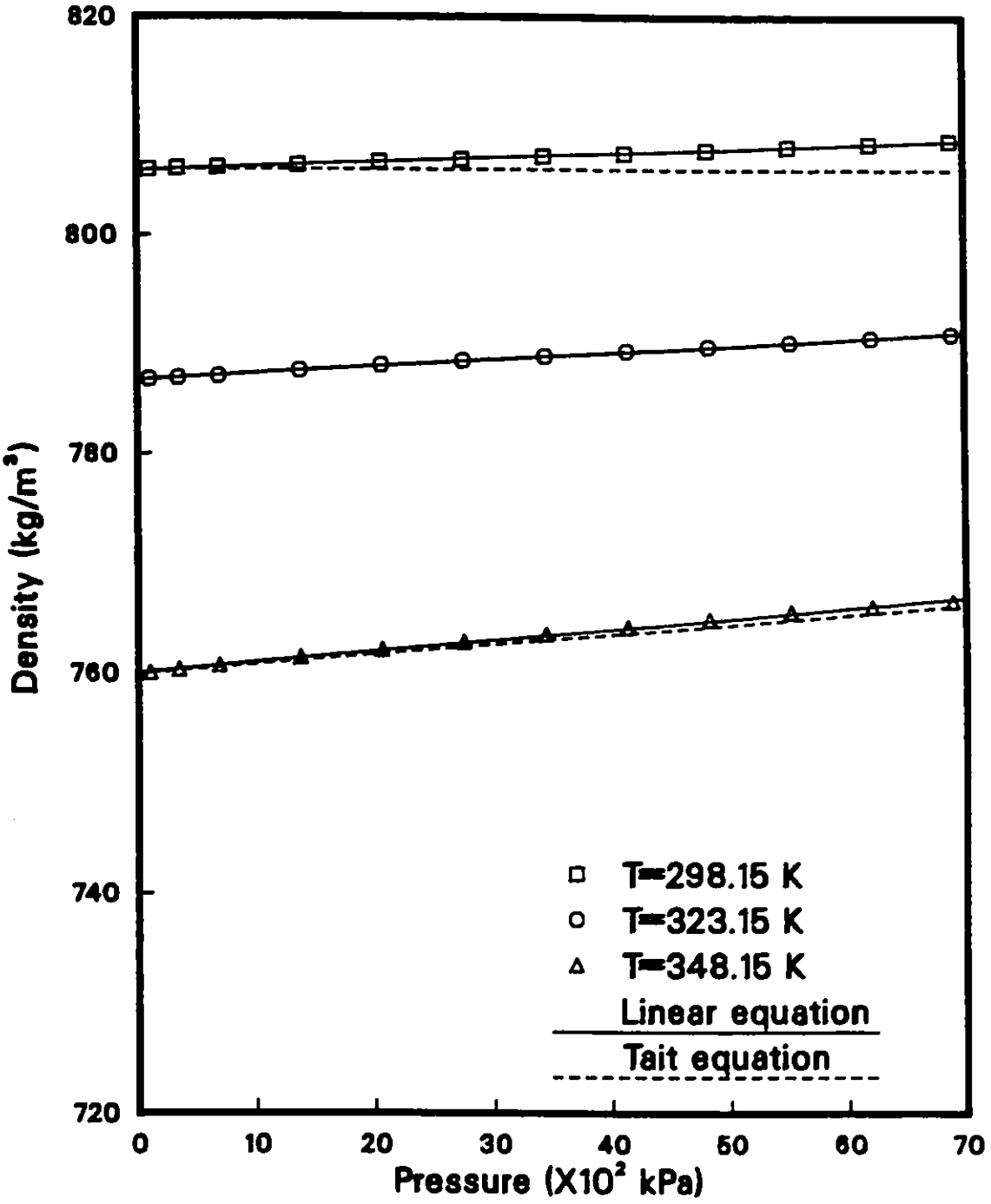

Figure 6.9: Plot of densities of n-butanol versus pressure

were kept within the necessary limits.

Based on Taylor's analysis [17,18], some dispersion of the injected pulse occurs in laminar flow. Therefore, the Reynolds number was checked for each experiment to ensure that the flow was in the laminar region. In this investigation, the highest Reynolds number used was about 6.0.

In the Taylor dispersion analysis, it was shown that the eluted solute concentration as a function of time was a gaussian curve; thus the concentration distribution was necessarily symmetrical. A test for symmetry was carried out for each experiment in this study. The distances on both sides from the center vertical line of each eluted peak were measured, and the ratio was calculated as:

$$Ratio = \frac{x_l - x_r}{(x_l + x_r)/2} \tag{6.5}$$

In the above equation, x_l, and x_r, are the distances of the left hand side, and of the right hand side, from the curve to the center line of the peak, respectively. For the worst case in this study, the ratio was 0.009. Therefore, the eluted peaks in this work were generally symmetrical. Another measurement of the peak symmetry could have been obtained by using the third statistical moment, but it required a digital analysis for the eluted concentration peak.

Experimentally, it is impossible to satisfy the Taylor dispersion condition that the injected pulse should be a true δ-function. In practice, the injection employed gives a square pulse of finite length. Levenspiel and Smith [132] showed that if the volume of injected solution was less than 1.0% of the internal volume of the column, then the error from the imperfection of the δ-function was negligible. In this study,

the volume of injected solution was always $2.0 \times 10^{-8}\ m^3$ and the internal volume of the dispersion column was $3.08 \times 10^{-5}\ m^3$. Therefore, the above criterion was satisfied for all the experiments in this work.

An important assumption made by Taylor [17,18] is that the effect of molecular diffusion in the axial direction is negligible, and this assumption can be made if the following conditions are fulfilled:

$$\frac{4L}{R} \gg \frac{v_m R}{D_{AB}} \gg 6.9 \tag{6.6}$$

In this study, the value of $4L/R$ was approximately 715800, and the value of $v_m R/D_{AB}$ was approximately 510. Therefore, the conditions of equation (6.6) were satisfied, and the effect of molecular diffusion in axial direction was considered negligible.

In this investigation, the dispersion column was wound in a coil having a 0.105 m radius because of its long length (68.0 m). It is recognized that secondary flow occurs when fluid passes through a curved tube. The secondary flow can reduce the degree of dispersion and hence, in effect, increase the measured diffusivity. However, secondary flow effect can be neglected if the ratio of the coil diameter to the tube inside diameter is large and the flow velocity is relatively low. Alizadeh et. al. [133] have recommended that if $De^2Sc \leq 20$, then the effect of secondary flow is negligible. De is the Dean number ($Re/\sqrt{R_c/R}$), and Sc is the Schmidt number ($\mu/\rho D_{AB}$). For the worst case in this study, the value of De^2Sc was about 16 which was less than 20. Therefore, the secondary flow effects were considered to be negligible in this work.

It is known that the effect of increasing the solvent flow rate beyond a certain limited value leads to erroneous results [28]. Experiments were performed at a number of different flowrates to see if there was an effect of flowrate on the measured diffusivity. In Figure 6.10, the apparent diffusion coefficients for propene in n-butanol and n-octane at 298.15 K and at atmospheric pressure are plotted as a function of the solvent velocities. It is apparent that as the velocity increases, the apparent diffusivity will increase well above the true value. The velocity limit as indicated in Figure 6.10 is used to guide the choice of the flowrates used for the experiments. In general, the range of the velocity (v_m) used in this study was between 0.2 and 0.4 $\times$ 10^{-2} m/s, well below the limit for reliable diffusivity measurements.

In this study, the temperature and pressure of the solvent were lowered to 298.15 K and atmospheric pressure before it entered the detector. Since the residence time in the cooling and pressure reducing section was very small as compared to the period for which the dispersion proceeded. The error on measured diffusivities carried by temperature and pressure reduction was expected to be negligible.

6.5.2 Experimental Data for Diffusivities by the Taylor Dispersion Method

The diffusivities of propene were measured by the Taylor dispersion method at elevated pressures in the solvents n-butanol, chlorobenzene, ethylene glycol and n-octane. The experiments were conducted at 298.15, 323.15 and 348.15 K for each

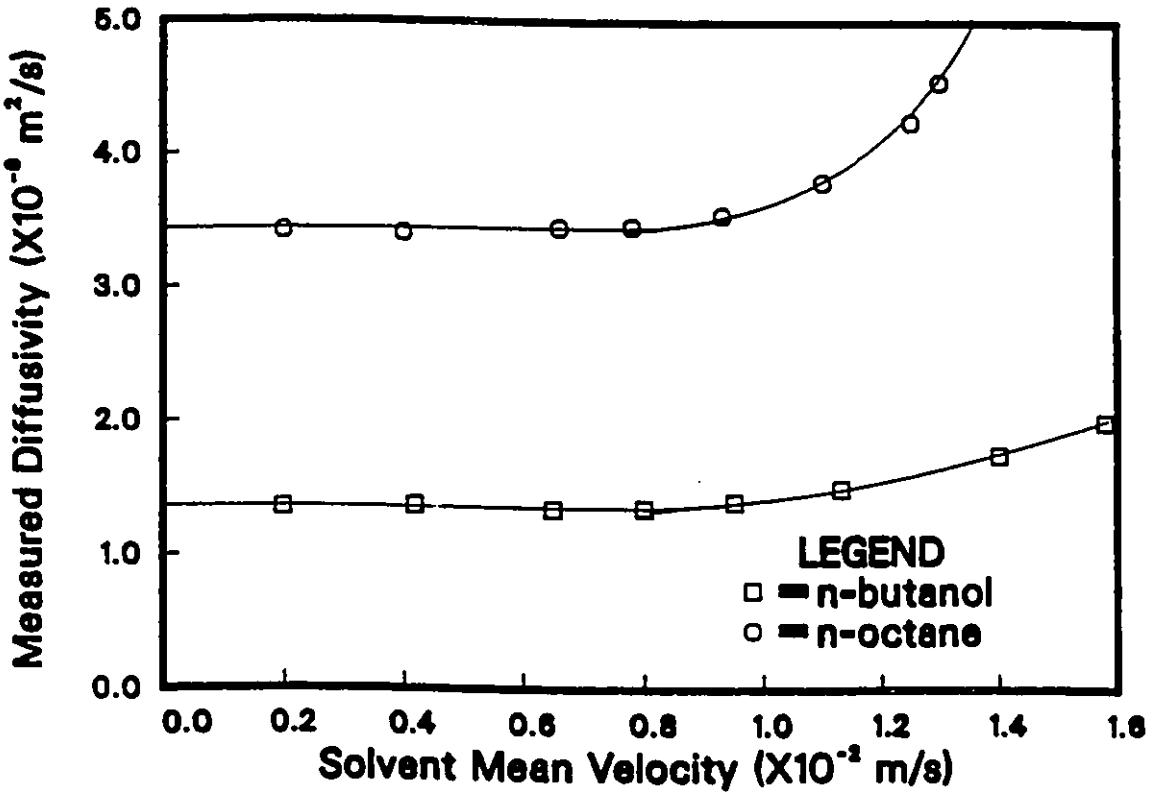

Figure 6.10: Effect of the solvent velocity on diffusivity as measured by means of the Taylor dispersion method for propene in n-butanol and n-octane at 298.15 K and at atmospheric pressure

system and for pressures from 101.3 to 6890 kPa. The experiments were repeated at least three times for each system at the same temperature and pressure, and the experimental error was estimated to be ± 3 %.

As a confirmation of the proper design of the Taylor dispersion apparatus, a comparison of some of the diffusivities measured by the Taylor dispersion method was made with values measured by the steady-state capillary cell method as shown in Table 6.13. The agreement is generally very good, the maximum difference being 2.0%. Therefore, it is considered that both measurement methods can produce reliable results since it is unlikely that similar results could be coincidentally obtained by those different experimental techniques.

The average values of the diffusivities of propene in the four solvents are shown in Tables 6.14 to 6.17. The uncertainties indicated in the tables correspond to one standard deviation. The calculation procedure described in section 5.12 was utilized for the determination of the diffusivity. A sample calculation is also presented in Appendix I.

The diffusivities of the propene in n-butanol, chlorobenzene, ethylene glycol and n-octane are given in Figures 6.11 through 6.14 as a function of temperature and pressure. The lines in those figures represent the results of linear regression analyses of the experimental data. It is evident that the diffusivity decreases with increasing pressure. However, the effect of pressure on the diffusion coefficients is relatively small for pressures from 101.3 to 6891 kPa. Based on observations of the results obtained, it may be stated that the effect of pressure on the diffusion coefficients

becomes more significant at higher temperatures. This phenomenon is similar to the effect of pressure on densities mentioned in section 6.4. Since the density increases with increasing pressure, it may be considered that the free space between the liquid molecules through which diffusion occurs, is decreased; thus it is considered that the rate of diffusion will also decrease because the space for diffusion is reduced.

It has been found that the polarity of the solvent and the tendency for self-association of the solvent molecules affect the diffusion process. In Figure 6.15, the diffusivities of propene in n-butanol, chlorobenzene, ethylene glycol and n-octane at atmospheric pressure are compared. It is shown that the diffusivities of propene in n-octane is the highest, following by chlorobenzene and n-butanol, and the diffusivities of propene in ethylene glycol is the lowest among those solvents. N-octane is nonpolar and non-associating, chlorobenzene is slightly polar but non-associating, n-butanol is highly polar and associating and ethylene glycol is even more polar and strongly associating due to its two hydroxyl groups. These solvents show a typical effect; that is, the higher the degree of molecular association in the solvent, the greater the reduction in diffusivity of dissolved gases.

6.6 Rough Hard Sphere Treatment of Diffusivity

According to the rough hard sphere (RHS) theory discussed in Chapter 2, the temperature dependence of the diffusivity should have the following form:

$$\frac{D^{\circ}_{AB}}{\sqrt{T}} = \gamma(V_B - V_D) \tag{6.7}$$

SOLVENT	TEMP.(K)	DIFFUSIVITY ($\times 10^{-9} m^2/s$)	
		STEADY-STATE CAPILLARY CELL METHOD	TAYLOR DISPERSION METHOD
n-butanol	298.15	1.34 ± 0.02	1.35 ± 0.01
	323.15	2.37 ± 0.02	2.40 ± 0.04
chlorobenzene	298.15	2.40 ± 0.09	2.44 ± 0.01
	323.15	3.37 ± 0.06	3.40 ± 0.01
n-octane	298.15	3.40 ± 0.09	3.42 ± 0.00
	323.15	4.77 ± 0.07	4.78 ± 0.05

Table 6.13: Comparison of experimental results for atmospheric pressure of two different methods for measuring diffusivities of dissolved propene gas in n-butanol, chlorobenzene and n-octane

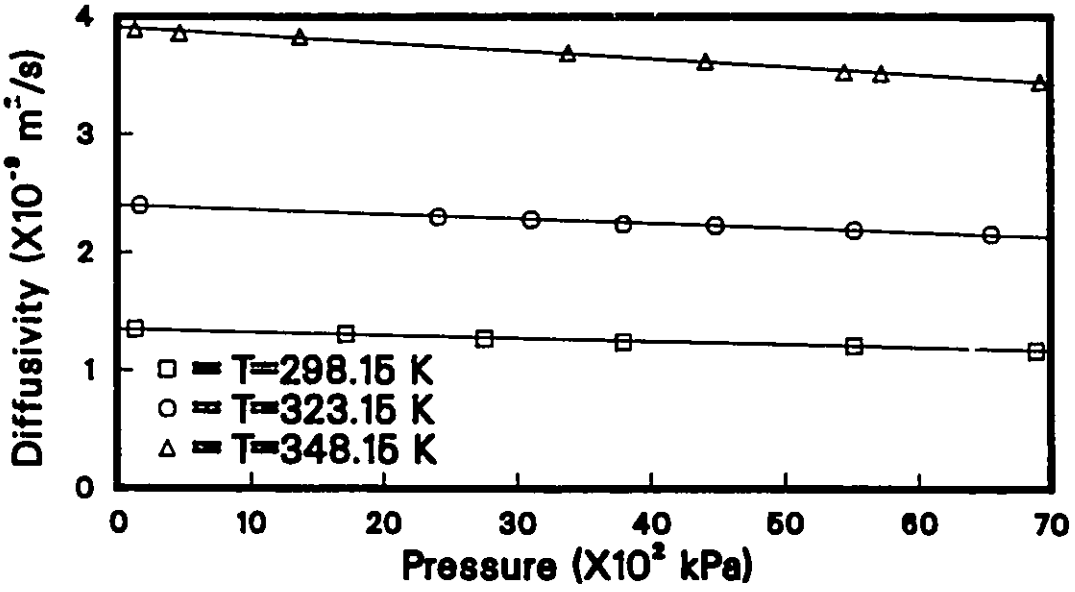

Figure 6.11: Plot of diffusivities of propene in n-butanol as a function of temperature and pressure

PRESSURE (kPa)	DIFFUSIVITY ($\times 10^{-9} m^2/s$)		
	298.15 K	323.15 K	348.15 K
137.8	1.35 ± 0.01	—	3.89 ± 0.03
172.3	—	2.40 ± 0.04	—
468.6	—	—	3.86 ± 0.07
1378.2	—	—	3.83 ± 0.00
1722.8	1.31 ± 0.01	—	—
2411.9	—	2.30 ± 0.04	—
2756.5	1.27 ± 0.01	—	—
3101.0	—	2.28 ± 0.02	—
3376.7	—	—	3.69 ± 0.04
3790.1	1.24 ± 0.03	2.24 ± 0.05	—
4410.3	—	—	3.62 ± 0.03
4479.3	—	2.23 ± 0.04	—
5444.0	—	—	3.53 ± 0.05
5512.9	1.21 ± 0.02	2.19 ± 0.02	—
5719.7	—	—	3.52 ± 0.00
6546.6	—	2.16 ± 0.02	—
6822.2	—	—	3.45 ± 0.04
6891.2	1.17 ± 0.03	—	—

Table 6.14: Diffusivities of propene in n-butanol at elevated pressures

PRESSURE (kPa)	DIFFUSIVITY ($\times 10^{-9} m^2/s$)		
	298.15 K	323.15 K	348.15 K
117.2	—	3.40 ± 0.01	4.35 ± 0.05
124.0	2.44 ± 0.01	—	—
206.7	—	3.40 ± 0.02	—
241.2	—	—	4.35 ± 0.05
1033.7	2.42 ± 0.01	—	—
1378.2	—	—	4.29 ± 0.07
1585.0	—	3.33 ± 0.03	—
2136.3	2.42 ± 0.03	—	—
2480.8	—	—	4.19 ± 0.03
2549.7	—	3.27 ± 0.03	—
3445.6	2.40 ± 0.01	—	—
4272.5	—	3.24 ± 0.02	—
4582.6	—	—	4.09 ± 0.04
5099.5	2.37 ± 0.05	—	—
5237.3	—	3.22 ± 0.06	—
5857.5	—	3.19 ± 0.02	—
6202.0	2.33 ± 0.02	—	—
6271.0	—	—	4.03 ± 0.02

Table 6.15: Diffusivities of propene in chlorobenzene at elevated pressures

PRESSURE (kPa)	DIFFUSIVITY ($\times 10^{-9} m^2/s$)		
	298.15 K	323.15 K	348.15 K
344.6	—	—	0.756 ± 0.003
379.0	—	0.437 ± 0.003	—
447.9	0.200 ± 0.001	—	—
1378.2	—	0.433 ± 0.002	0.750 ± 0.002
1791.7	0.211 ± 0.003	—	—
2239.6	—	0.431 ± 0.004	—
2687.6	—	0.431 ± 0.002	—
2894.3	—	—	0.740 ± 0.008
3424.9	0.202 ± 0.001	—	—
3721.2	0.189 ± 0.001	—	—
4134.7	—	0.426 ± 0.005	0.721 ± 0.008
4892.7	—	0.425 ± 0.002	—
5375.1	0.192 ± 0.001	—	—
5512.9	—	—	0.710 ± 0.001
6753.3	0.188 ± 0.001	—	0.692 ± 0.001
6891.2	—	0.419 ± 0.002	—

Table 6.16: Diffusivities of propene in ethylene glycol at elevated pressures

PRESSURE (kPa)	DIFFUSIVITY ($\times 10^{-9} m^2/s$)		
	298.15 K	323.15 K	348.15 K
103.4	3.42 ± 0.00	4.78 ± 0.05	—
137.8	—	—	6.41 ± 0.06
826.9	3.30 ± 0.02	—	—
1378.2	3.25 ± 0.02	—	—
1447.1	—	—	6.26 ± 0.08
1722.8	—	4.67 ± 0.01	—
2274.1	3.21 ± 0.03	4.67 ± 0.05	6.16 ± 0.02
2756.5	3.17 ± 0.03	—	—
3101.0	3.18 ± 0.02	4.60 ± 0.04	—
3514.5	—	—	6.01 ± 0.06
4134.7	—	—	5.95 ± 0.01
4444.8	—	4.52 ± 0.04	—
5099.5	3.07 ± 0.03	—	—
5685.2	—	4.43 ± 0.04	—
5995.3	—	—	5.71 ± 0.04
6202.0	3.01 ± 0.03	—	—
6753.3	—	—	5.63 ± 0.05
6856.7	—	4.32 ± 0.01	—

Table 6.17: Diffusivities of propene in n-octane at elevated pressures

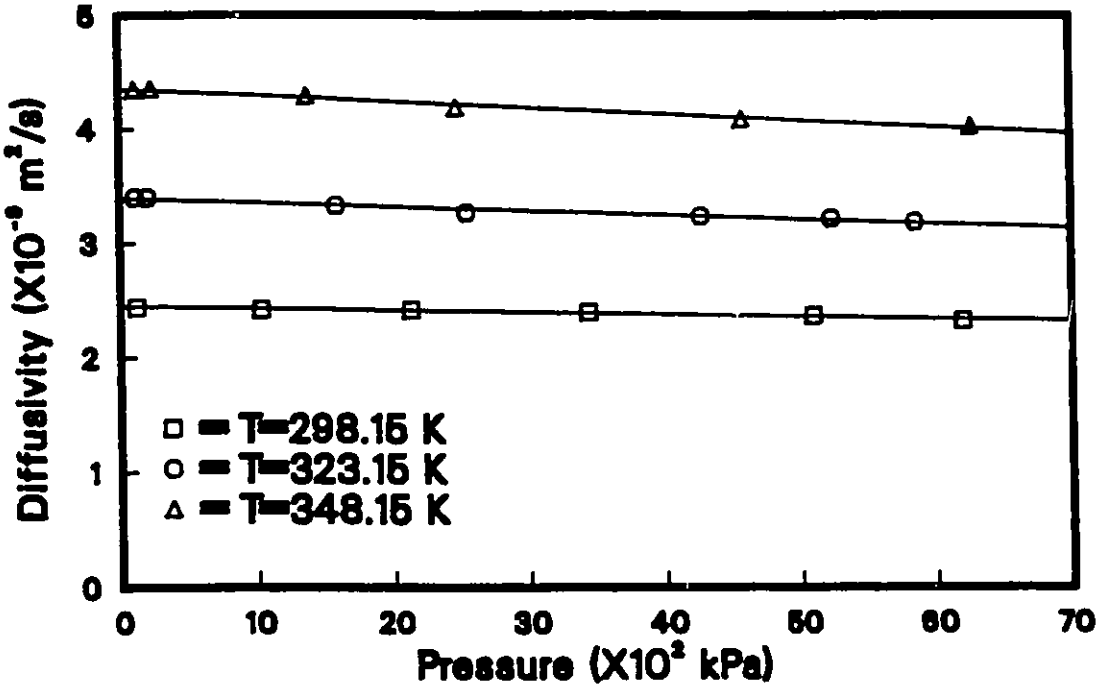

Figure 6.12: Plot of diffusivities of propene in chlorobenzene as a function of temperature and pressure

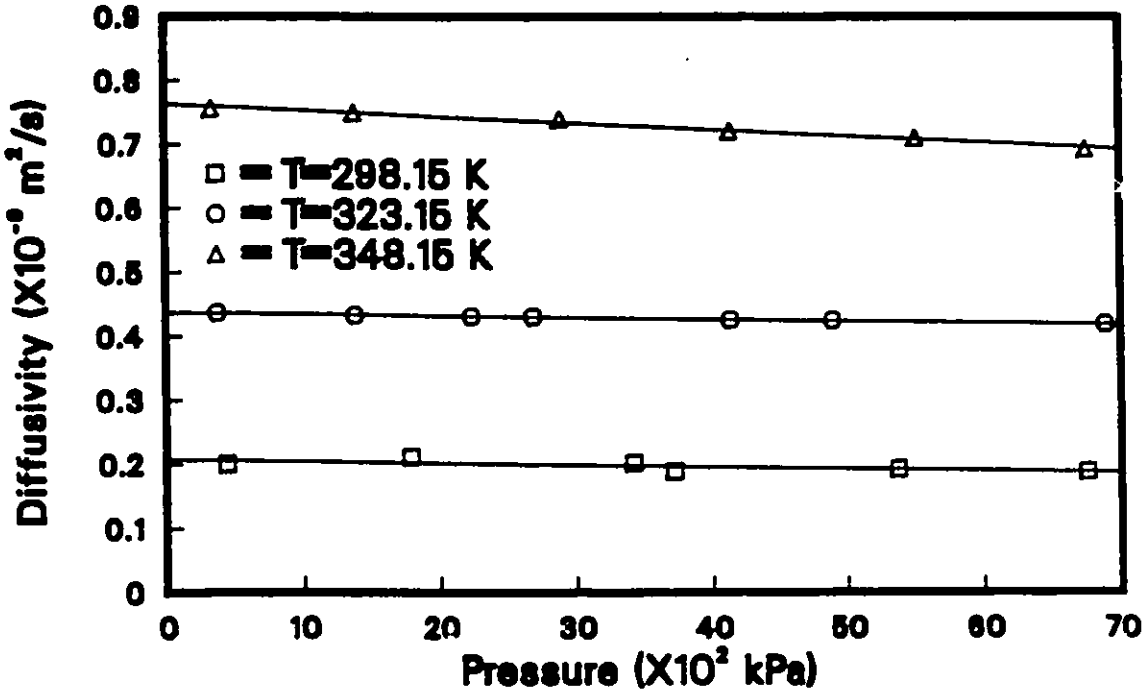

Figure 6.13: Plot of diffusivities of propene in ethylene glycol as a function of temperature and pressure

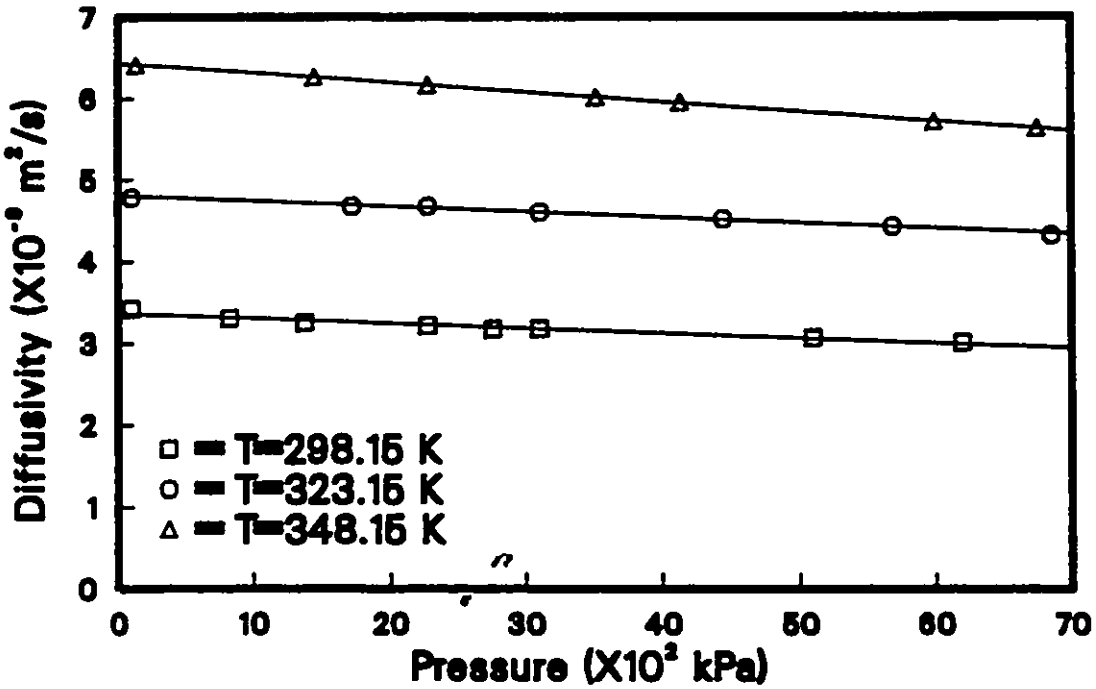

Figure 6.14: Plot of diffusivities of propene in n-octane as a function of temperature and pressure

If this relationship is valid, then it would be possible to predict the diffusivity for a given solute-solvent system by using one physical property (the solvent molar volume, V_B) and two parameters, γ and V_D. Because the form of equation (6.7) is relatively simple, it is easy to use.

Figures 6.16 to 6.19 are plots of $D^{\circ}_{AB}/\sqrt{T}$ versus the solvent molar volume, V_B, for propene in n-butanol, chlorobenzene, ethylene glycol and n-octane at different temperatures and pressures. In Figure 6.20, $D^{\circ}_{AB}/\sqrt{T}$ is plotted against the solvent molar volume, V_B, for propene in acetic acid, acetone, N,N dimethyl formamide and ethyl acetate at different temperatures and atmospheric pressure. All the figures show linear relationships between $D^{\circ}_{AB}/\sqrt{T}$ and V_B. Thus equation (6.7) can be successfully used to describe the diffusivities measured in the ranges of temperature and pressure utilized in this study.

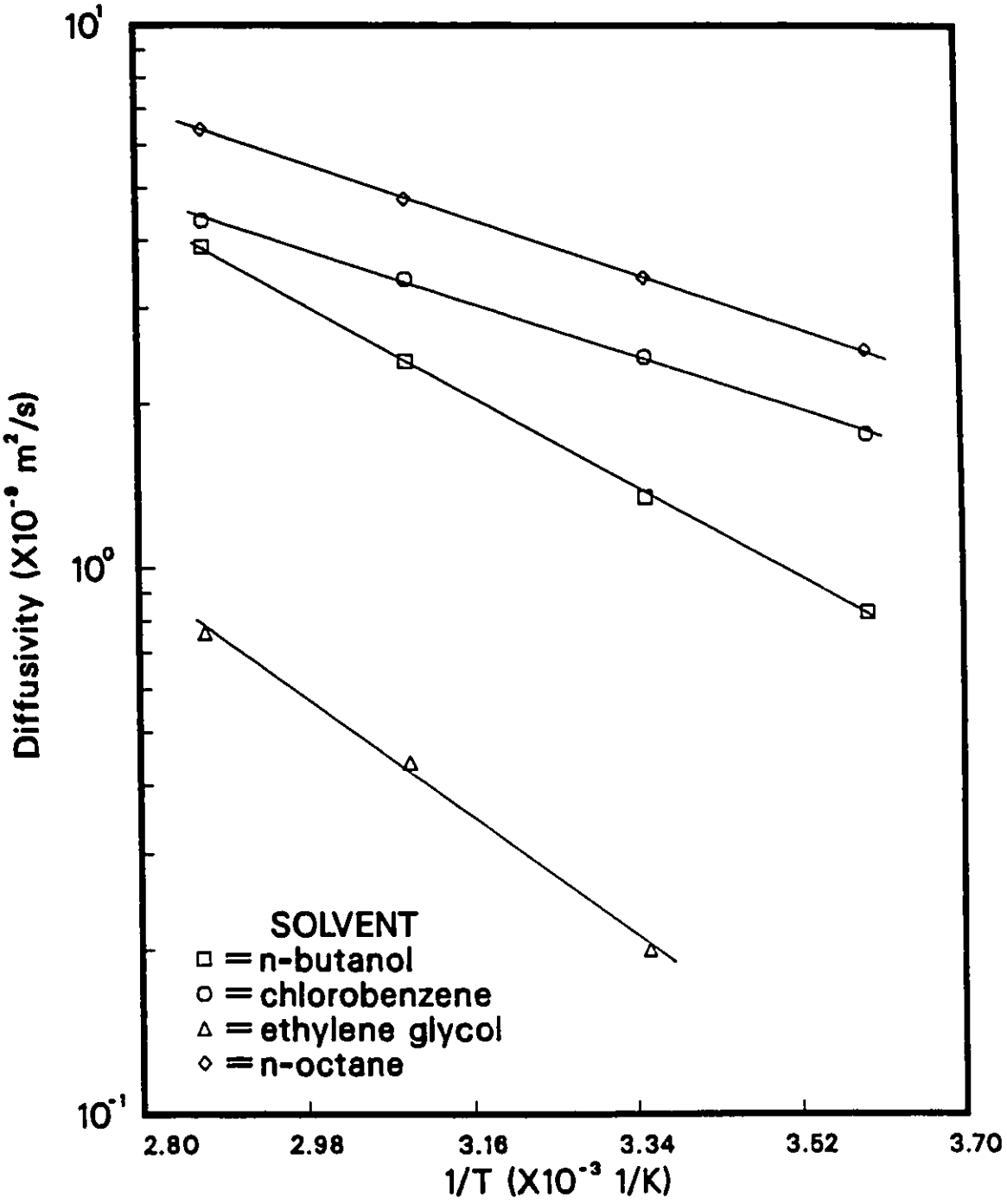

Figure 6.15: Plot of ln D°_{AB} versus $1/T$ for propene in n-butanol, chlorobenzene, ethylene glycol and n-octane at atmospheric pressure

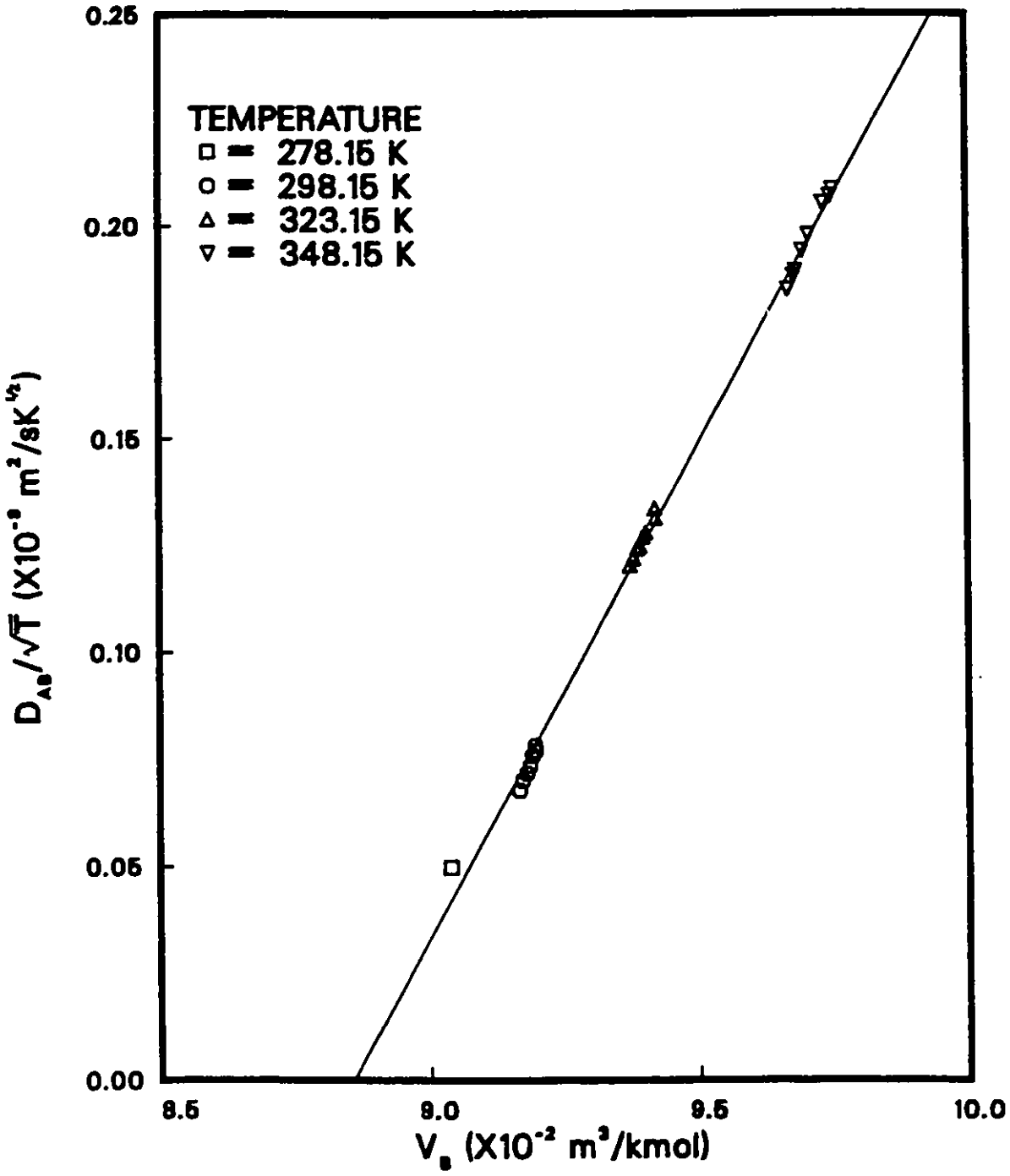

Figure 6.16: Plot of $D^{o}_{AB}/\sqrt{T}$ versus V_B for propene in n-butanol at different pressures

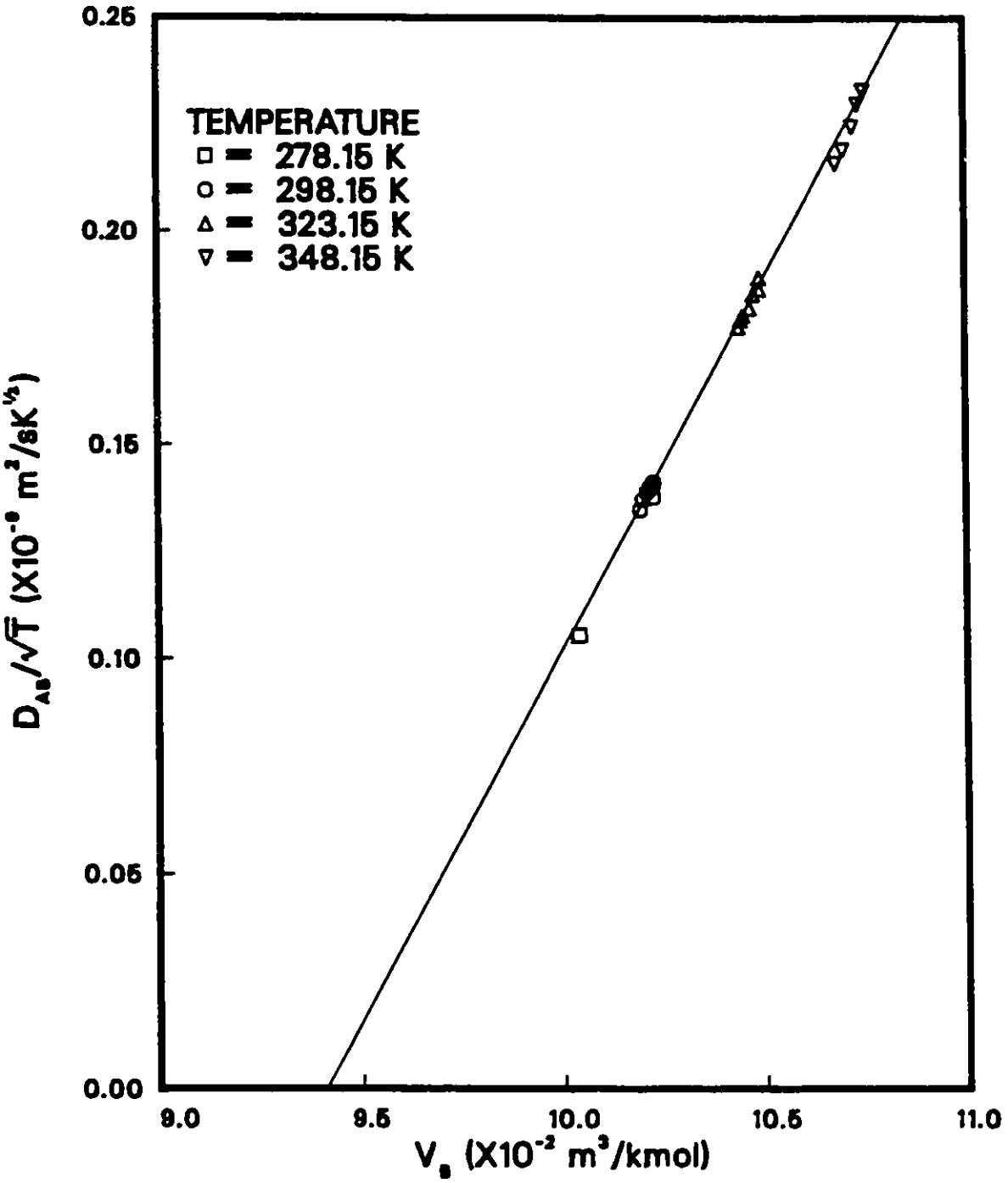

Figure 6.17: Plot of $D^{\circ}_{AB}/\sqrt{T}$ versus V_B for propene in chlorobenzene at different pressures

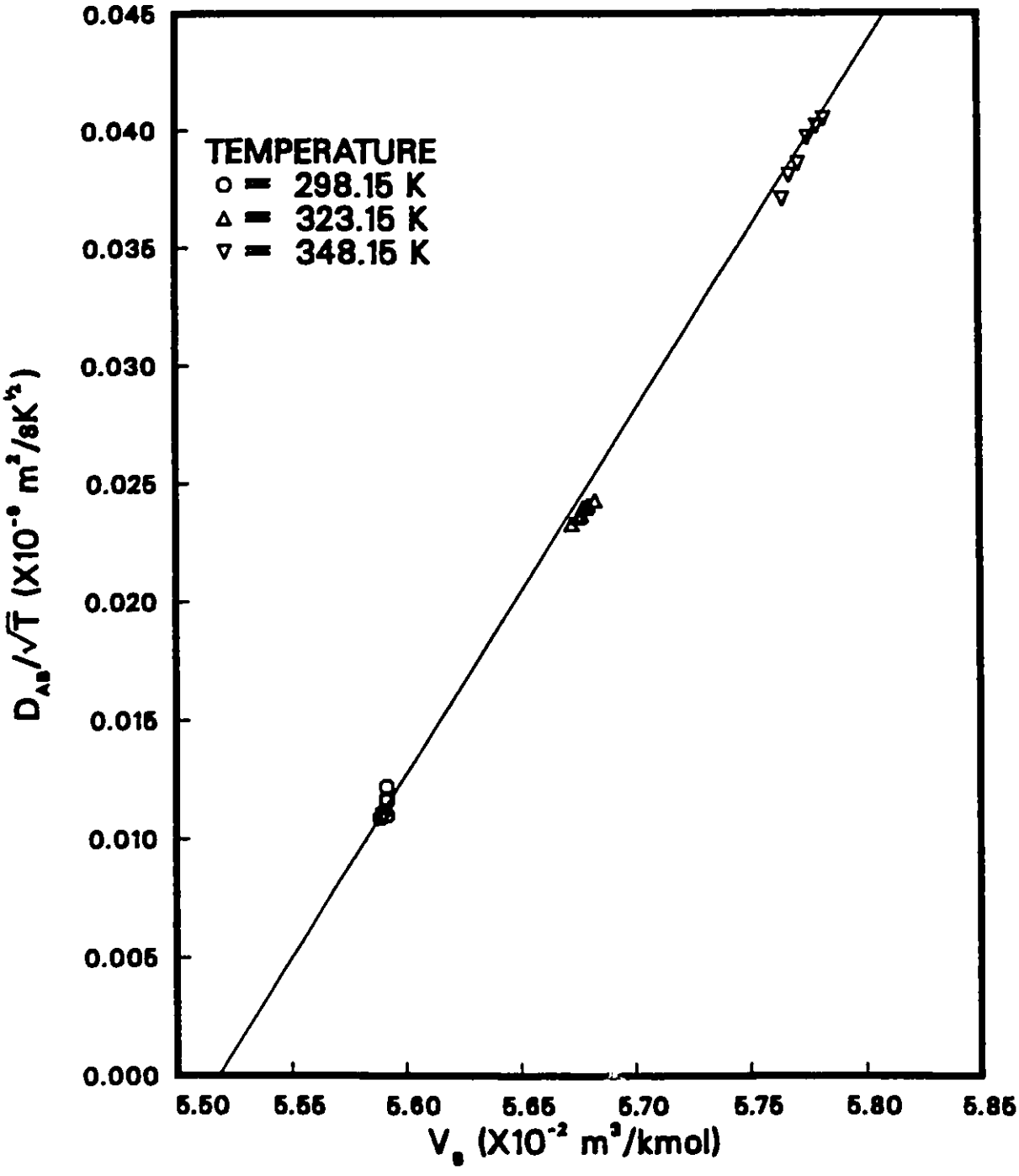

Figure 6.18: Plot of $D^{\circ}_{AB}/\sqrt{T}$ versus V_B for propene in ethylene glycol at different pressures

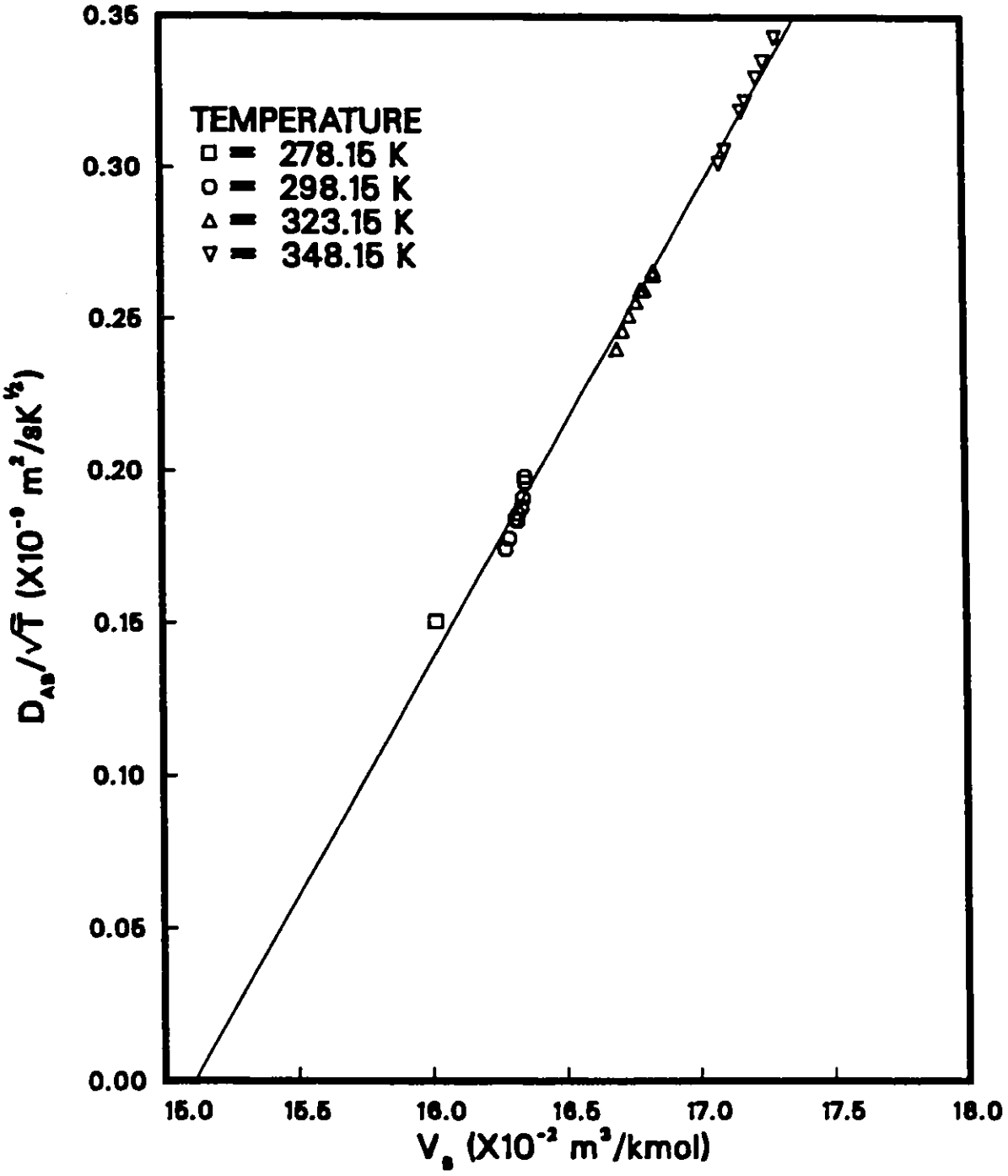

Figure 6.19: Plot of $D^{o}_{AB}/\sqrt{\mathrm{T}}$ versus V_B for propene in n-octane at different pressures

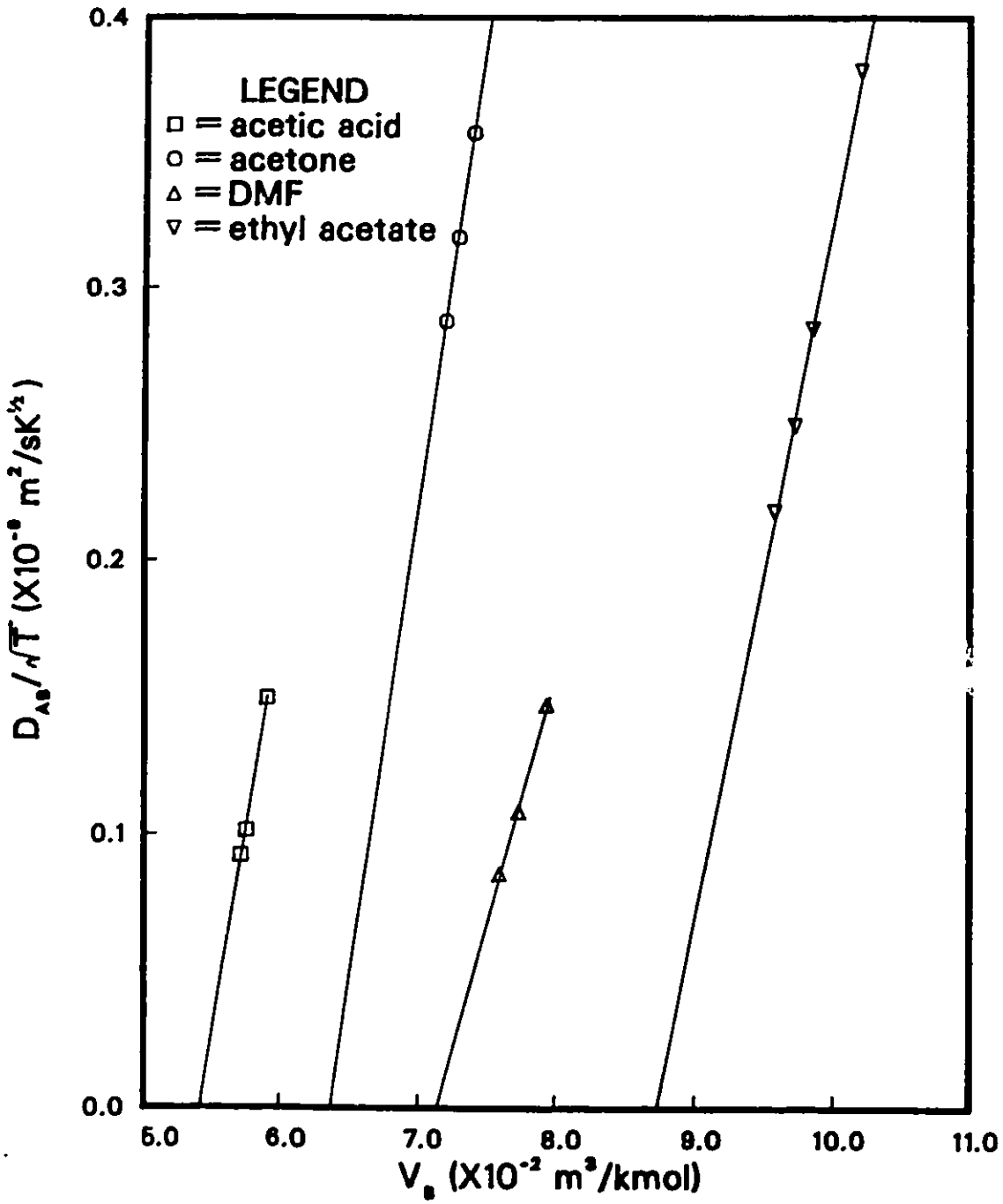

Figure 6.20: Plot of $D^{\circ}_{AB}/\sqrt{\mathrm{T}}$ versus V_B for propene in acetic acid, acetone, N,N dimethyl formamide and ethyl acetate at atmospheric pressure

The parameters, γ and V_D, were determined by a linear regression of the experimental results for each system and the estimated values are given in Table 6.18. The values of the solvent critical volumes are also given in Table 6.18. It was found that the values of V_D increased in a regular way with increasing solvent critical volumes. This relation, based on the eight systems investigated in this study, is expressed as follows:

$$V_D = 0.306 V_{CB} \tag{6.8}$$

The maximum error of the above equation was found to be 7.6%. The above relationship is slightly different from the result reported by Matthews [28] that $V_D = 0.302\ V_{CB}$ for the gaseous solutes. Since the parameter V_D can be estimated from the critical volume of the solvent, it is consistent with the discussion in Chapter 2 that V_D is dependent on the properties of the solvent only.

Physically, V_D can be considered to be the hypothetical solvent molar volume at which the diffusion coefficient goes to zero. The physical meaning of V_D can be checked by calculating the hard sphere diameter, σ_B, based on the values of V_D calculated from the experimental data using the following expression:

$$V_D = bV_o = \frac{bN\sigma_B^3}{\sqrt{2}} \tag{6.9}$$

In the equation above, N is Avogado's number, and the constant b has been found to be 1.358 [75]. The calculated values of the diameter, σ_B, are compared with the predicted values of diameter, σ_{VDW}, based on the van der Waals volumes in Table 6.19. The van der Waals volumes are calculated from the group contribution

SOLVENT	V_{CB} $(m^3/kmol)$	γ $(\times 10^{-9} kmol/msK^{0.5})$	V_D $(m^3/kmol)$
acetic acid	0.171	30.70	0.054
acetone	0.209	34.76	0.064
n-butanol	0.274	23.14	0.090
chlorobenzene	0.308	17.30	0.094
N,N dimethyl formamide	0.249	18.24	0.071
ethyl acetate	0.286	25.66	0.087
ethylene glycol	0.186	15.14	0.055
n-octane	0.492	15.47	0.151

Table 6.18: Values of V_{CB}, γ and V_D for propene in the eight solvents

method of Bondi [134]. From Table 6.19, it is shown that there is relatively good agreement between the two diameter values. The ratio of σ_B to σ_{VDW} is found on the average to be:

$$\frac{\sigma_B}{\sigma_{VDW}} = 0.960 \tag{6.10}$$

This provides another method to calculate V_D if V_{CB} is not known. The van der Waals volumes can be calculated by means of the Bondi method [134] and V_D by means of equations (6.9) and (6.10). The above finding is consistent with the result reported by Matthews [28] for n-alkane systems for which it was reported that $\sigma_B = 0.974\sigma_{VDW}$.

Equation (6.7) would appear to have a sound theoretical basis which is supported by the experimental data as discussed in the above section, and it is relatively simple for use for predictive proposes. Thus an attempt was made to correlate the values of V_D and γ with the physical properties of solute and solvent, and then to use equation (6.7) to predict the diffusivities.

Matthews [28] suggested that diffusivities of gases in liquids and of liquids in liquids might not be correlated in a single equation due to the large differences in molecular weight, size and shape of the solute molecules. Therefore, only the diffusivities for gaseous solutes in liquids were used for this correlation. Data for forty six gas-liquid systems were collected from the literature and were added to data from this study. In total, 329 diffusivity data, at different temperatures and pressures, were involved. A listing of the solute-solvent systems involved is shown in Appendix J. The temperature range for the data was from 273.15 to 567.15 K,

SOLVENT	σ_B $(\times 10^{-10} m)$	σ_{VDW} $(\times 10^{-10} m)$
acetic acid	4.54	4.68
acetone	4.79	4.98
n-butanol	5.35	5.46
chlorobenzene	5.46	5.66
N,N dimethyl formamide	4.98	5.48
ethyl acetate	5.36	5.52
ethylene glycol	4.57	4.78
n-octane	6.39	6.56

Table 6.19: Comparison of the calculated diameters of RHS and VDW for the eight solvents

and the pressure range was from 101.3 to 6981 kPa. For each system, the values of γ and V_D were estimated by means of a linear regression analysis.

Since the value of V_D was found to increase with increasing solvent critical volume, V_{CB}, a simple relation was assumed to exist between the two variables; thus the value of V_D was calculated by the following equation:

$$V_D = \varpi V_{CB} \tag{6.11}$$

The average value of ϖ was found to be 0.308 ± 0.011 based on 54 systems. The value of V_D could also be calculated by means of equations (6.9) and (6.10) as mentioned before.

Based on the RHS theory, the parameter, γ, is considered to contain all the information on the interactions between the solute and solvent. It is known that the parameter, γ, is related to the solute and solvent molecular masses and molecular diameters.

After a number of forms for the correlation of γ were examined , a correlation was found, that gave the best predictive results for γ based on the 54 systems and which had only a few parameters. This proposed correlation for γ is:

$$\gamma = \delta_1 M_A^{\delta_2} M_B^{\delta_3} \left(\frac{V_{bA}}{V_{bB}}\right)^{\delta_4} \tag{6.12}$$

The parameters in the above equation were estimated by means of the nonlinear regression analysis; again the NLIN package in the SAS library was used. The estimated values of the parameters in equation (6.12) are: δ_1 = 11973 ± 8902, δ_2 = -0.2754 ± 0.0542, δ_3 = -1.2314 ± 0.2106 and δ_4 = - 0.3565 ± 0.1826. In the above

equation, M_A, and M_B, are the molecular weights of solute, and solvent in $kg/kmol$, respectively, V_{bA}, and V_{bB}, are the molar volumes of solute, and solvent at normal boiling point in $m^3/kmol$, respectively. The plots of residuals were examined and all residuals were randomly distributed in those plots. Thus there was no evidence for lack of fit of equation (6.12).

Therefore, the diffusivities of dissolved gases in liquids can be predicted based on the RHS theory by the following correlation and related equation:

$$\frac{D^o_{AB} \times 10^9}{\sqrt{T}} = 11973 M_A^{-0.2754} M_B^{-1.2314} \left(\frac{V_{bA}}{V_{bB}}\right)^{-0.3565} (V_B - V_D) \qquad (6.13)$$

$$V_D = 0.308 V_{CB} \qquad (6.14)$$

In these equations, D^o_{AB} is in m^2/s, T is in K, and molar volume of solvent, V_B, and solvent critical volume, V_{CB}, are in $m^3/kmol$. It is important to note that these equations are intended to describe the diffusivity not only as a function of temperature and molecular sizes but indirectly, of pressure as well.

Equation (6.13) suggests the following physical interpretations. (1) The diffusivity is strongly influenced by the molar volume of the solvent. (2) The diffusivity decreases with increasing molecular weights of solute and solvent, and the effect of changes in solvent molecular weight are more significant than those of the solute. (3) The diffusivity is influenced by the ratio of molecular sizes of solute and solvent.

Diffusivities were predicted using equation (6.13), and the resulting average absolute percent deviation from the experimental data was found to be 41.8% based on 329 data; this average percentage deviation is considered very high. There are

several reasons for the high percentage deviation from equation (6.13). The values of ϖ in equation (6.11) for several systems are far from the average value of 0.308. For example, the values of ϖ for different solutes in n-butanol and in cyclohexane are about 0.321; thus, the predicted diffusivities for these systems are, consequently, higher than expected, and the average error is forced up. Therefore, the calculation method for V_D based on equation (6.11) is not considered entirely successful. The estimation procedure for V_D needs further study based on more experimental data for high pressure, for example. Although equation (6.13) does not appear to be able to give acceptable predictive results for all gas-liquid systems, it has been shown by Matthews [28] that an equation of similar form can be used for diffusivity predictions for chemically similar system such as for n-alkane systems.

It is concluded that the RHS theory, summarized by equation (6.7), is a promising method for correlating diffusion coefficients in chemically similar solute-solvent systems. Further experiments are required, however, to investigate the application of the RHS theory to a generalized correlation for diffusivities, applicable a wide range of temperatures and pressures.

Chapter 7

CONCLUSIONS

The effect of temperature on diffusivity in liquids was investigated in this study based on the available experimental data. In total, diffusivities for 296 solute-solvent pairs (2325 data) involving both gas and liquid solutes in liquid solvents, obtained from the literature were used. The temperature for the data ranged from 194.65 K to 561.65 K. It was found that the equations, as the form of equations (3.1) and (3.2), could describe the effect of temperature on diffusivity adequately for the moderate temperature range of the data utilized.

Three new correlations have been proposed for prediction of diffusivities for specified solute-solvent systems. The first is for the n-alkane systems, the second correlation is for dissolved gases in organic solvents, and the last one is for dissolved gases in water.

The proposed correlation for diffusivities in n-alkane systems, equation (3.9), was compared with three available correlations for n-alkane systems in the literature and was found to give the lowest average absolute error of 2.8% based on 104 data. In addition to better representing the diffusivity data for n-alkanes, the proposed

correlation is easier to use than existing correlations because only the temperature and the molecular weights of solute and solvent are required.

The proposed correlation for diffusivities for dissolved gases in organic solvents, equation (3.12), was compared with four correlations for gas-liquid systems from the literature and was found to give the lowest average absolute error of 15.8% based on 352 experimental data. The average absolute error was approximately half the comparable errors obtained with the other existing correlations. It is concluded that the proposed correlation, equation (3.12), successfully describes the data on which it is based and may be used for the prediction of diffusivities of dissolved gases in organic solvents with confidence.

A simple correlation, equation (3.13), has been proposed for the prediction of diffusivities of dissolved gases in water. The proposed correlation was compared with seven available correlations for gas-liquid systems in the literature and was found to give the lowest average absolute error of 13.5% based on 309 data. However, the correlations of Othmer and Thaker and Sovová were all considered equally successful, based on a comparison of the average absolute errors. Therefore, it is concluded that those two correlations as well as the new, proposed correlation, equation (3.13), can be used for predicting the diffusivities of dissolved gases in water equally well.

All three proposed correlations are purely empirical correlations; thus there is no theoretical basis for them. Caution must be taken when they are used for prediction outside the limits of the conditions and properties for which they were developed.

The diffusion coefficients of propene gas were measured by the steady-state capillary cell method at atmospheric pressure in the solvents acetic acid, acetone, n-butanol, chlorobenzene, N,N dimethyl formamide, ethyl acetate and n-octane. These data were not previously available in the literature. When these diffusivity data were compared with predicted diffusivities obtained by utilizing the hydrodynamic theory and the rate theory of Eyring, it was shown that the two diffusion theories for the diffusion of dissolved gases in liquids had serious drawbacks in describing observed behavior.

The diffusivities of propene were measured by the Taylor dispersion method at elevated pressures of up to 6891 kPa in the solvents n-butanol, chlorobenzene, ethylene glycol and n-octane. These data were considered new in the literature. An experimental apparatus based on Taylor dispersion phenomenon was constructed for operation at high pressures and temperatures. It was confirmed that this apparatus could produce reliable diffusivity data. It was generally found that the diffusivity tended to decrease with increasing pressure. However, the effect of pressure on the diffusivity was relatively small from 101.3 to 6891 kPa, and the effect became more significant at higher temperatures. The above behavior was consistent with expected behavior.

The solvents used in this investigation have different polarities and tendencies for molecular association. The diffusivities of propene in n-butanol (highly polar and associating), chlorobenzene (slightly polar but not associating) and n-octane (nonpolar and not associating) at atmospheric pressure were compared. It was

found that the diffusivities were reduced to some extent in polar solvents and were reduced even more in associating solvents.

The rough hard sphere (RHS) theory which predicts a linear relationship between $D^{\circ}_{AB}/\sqrt{T}$ and molar volume, V_B, has been investigated for dissolved gases in organic solvents over moderate ranges of temperature and pressure. In addition to demonstrating that the form of equation (6.7) correctly describes the relationship between $D^{\circ}_{AB}/\sqrt{T}$ and molar volume, V_B, methods for predicting the parameters γ and V_D in equation (6.7) have been proposed. The physical meaning of these parameters has been discussed and shown to be consistent with the RHS theory. The RHS approach is considered to be a promising method of correlating diffusion coefficients for chemically similar solute-solvents systems.

In addition to the molecular diffusivities, the gas solubilities, densities and viscosities of all the solvents used in this study, were measured by different techniques. The solubilities of propene were measured at atmospheric pressure in the eight solvents. The gas solubilities of propene in n-butanol, chlorobenzene and n-octane were chosen for comparison; it was shown that the gas solubilities were reduced in polar solvents which tend to self associate. The densities of n-butanol, chlorobenzene, ethylene glycol and n-octane were measured at elevated pressures of up to 6891 kPa. It was found that the density increased with increasing pressure, and that the changes of density with increasing pressure was most significant at higher temperatures.

Bibliography

[1] Himmelblau, D. M., *Chem. Rev.*, **64**, 527-550, (1964).

[2] Onda, K., Okamoto, T., Yamaji, Y., *Chem. Eng., Tokyo (Kagaku Kogaku)*, **24**, 918-925, (1960).

[3] Baird, M.H., Davidson, J.F., *Chem. Eng. Sci.*, **17**, 473-480, (1962).

[4] Unver, A.A., Himmelblau, D.M., *J. Chem. Eng. Data*, **9**, 428-431, (1964).

[5] Tang, Y.P., Himmelblau, D.M., *A. I. Ch. E. J.*, **11**, 54-58, (1965).

[6] Tang, Y.P., Himmelblau, D.M., *Chem. Eng. Sci.*, **20**, 7-14, (1965).

[7] Huq, A., Wood, T., *J. Chem. Eng. Data*, **13**, 256-259, (1968).

[8] Duda, J.L., Vrentas, J.S., *A. I. Ch. E. J.*, **14**, 286-294, (1968).

[9] Zandi, I., Turner, C.D., *Chem. Eng. Sci.*, **25**, 517-528, (1970).

[10] Dim, A., Gardner, G.R., Ponter, A.B., Wood, T., *J. Chem. Eng. (Japan)*, **4**, 92-95, (1971).

[11] Halmour, N., Sandall, O.C., *J. Chem. Eng. Data*, **29**, 20-22, (1984).

[12] Kramers, H., Douglas, R.A., Ulmann, R.M., *Chem. Eng. Sci.*, **10**, 190-191, (1959).

[13] Davies, G.A., Ponter, A.B., Craine, K., *Can. J. Chem. Eng.*, **45**, 372-376, (1967).

[14] Hikita, H., Asai, S., Azuma, Y., *Can. J. Chem. Eng.*, **56**, 371-374, (1978).

[15] Mazarei, A.F., Sandall, O.C., *A. I. Ch. E. J.*, **26**, 154-157, (1980).

[16] Davidson, J.F., Cullien, E.J., *Trans. Instn. Chem. Engrs.*, **35**, 51-60, (1957).

[17] Taylor, G., *Proc. R. Soc. Lond.*, **A219**, 186-203, (1953).

[18] Taylor, G., *Proc. R. Soc. Lond.*, **A225**, 473-477, (1954).

[19] Aris, R., *Proc. R. Soc. Lond.*, **A235**, 67-77, (1956).

[20] Giddings, J.C., Seager, S.L., *Ind. Eng. Chem. Fundam.*, 1, 277-283, (1962).

[21] Ferrell, R.T., Himmelblau, D.M., *A. I. Ch. E. J.*, 13, 702-708, (1967).

[22] Ferrell, R.T., Himmelblau, D.M., *J. Chem. Eng. Data*, 12, 111-115, (1967).

[23] Pratt, K.C., Slater, D.H., Wakeham, W.A., *Chem. Eng. Sci.*, 28, 1901-1903, (1973).

[24] Evans, D.F., Tominaga, T., Chan, C., *J. Solu. Chem.*, 8, 461-478, (1979).

[25] Chen, S.H., Davis, H.T., Evans, D.F., *J. Chem. Phys.*, 75, 1422-1426, (1981).

[26] Chen, S.H., Davis, H.T., Evans, D.F., *J. Chem. Phys.*, 77, 2540-2544, (1982).

[27] Chen, S.H., Evans, D.F., Davis, H.T., *A. I. Ch. E. J.*, 29, 640-644, (1983).

[28] Matthews, M.A., "Diffusion Coefficients at Infinite Dilution in n-Alkane Solvents at Temperatures to 573 K and Pressures to 3.5 MPa.", Ph. D. Dissertation, Texas A & M University, (1986).

[29] Jacob Sun, C.K., Chen, S.H., *A. I. Ch. E. J.*, 31, 1904-1910, (1985).

[30] Jacob Sun, C.K., Chen, S.H., *Chem. Eng. Sci.*, 40, 2217-2224, (1985).

[31] Jacob Sun, C.K., Chen, S.H., *Ind. Eng. Chem. Res.*, 26, 815-819, (1987).

[32] Matthews, M.A., Akgerman, A., *A. I. Ch. E. J.*, 33, 881-885, (1987).

[33] Vivian, J.E., King, C.J., *A. I. Ch. E. J.*, 10, 220-221, (1964).

[34] Tham, M.J., Bhatia, K.K., Gubbins, K.E., *Chem. Eng. Sci.*, 22, 309-311, (1967).

[35] Clegg, G.T., Tehrani, M.A., *J. Chem. Eng. Data*, 18, 59-60, (1973).

[36] Tham, M.K., Walker Jr., R.D., Modell, J.H., *J. Chem. Eng. Data*, 18, 411-412, (1973).

[37] Onda, K., Takeuchi, H., Fujine, M., *J. Chem. Eng. (Japan)*, 8, 25-29, (1975).

[38] Takahashi, M., Kobayashi, Y., Takeuchi, H., *J. Chem. Eng. Data*, 27, 328-331, (1982).

[39] Collings, A.F., Hall, D.C., McCool, M.A., Woolf, L.A., *J. of Phys. E: Sci. Instr.*, 4, 1019-1024, (1971).

[40] McCool, M.A., Collings, A.F., Woolf, L.A., *J. Chem. Soc. Fara. Trans. I*, 68, 1489-1497, (1972).

[41] McCool, M.A., Woolf, L.A., *High Temp. High Press.*, 4, 85-95, (1972).

[42] Houghton, G., Kesten, A.S., Funk, J.E., Coull, J., *J. Phys. Chem.*, **65**, 649-654, (1961).

[43] Bennett, L., Ng, W.Y., Walkley, J., *J. Phys. Chem.*, **72**, 4699-4700, (1968).

[44] Reamer, H.H., Opfell, J.B., Sage, B.H., *Ind. Eng. Chem.*, **48**, 275-282, (1956).

[45] Reamer, H.H., Duffy, C.H., Sage, B.H., *Ind. Eng. Chem.*, **48**, 282-284, (1956).

[46] Reamer, H.H., Sage, B.H., *A. I. Ch. E. J.*, **3**, 449-453, (1957).

[47] Reamer, H.H., Sage, B.H., *J. Chem. Eng. Data*, **4**, 15-21, 296-300, (1959).

[48] Reamer, H.H., Sage, B.H., *J. Chem. Eng. Data*, **6**, 481-484, (1961).

[49] Reamer, H.H., Lower, J.H., Sage, B.H., *J. Chem. Eng. Data*, **9**, 54-59, 602-606, (1964).

[50] Ross, M., Hildebrand, J.H., *J. Chem. Phys.*, **40**, 2397-2399, (1964).

[51] Nakanishi, K., Voigt, E.M., Hildebrand, J.H., *J. Chem. Phys.*, **42**, 1860-1863, (1965).

[52] Combs, R.J., Field, P.E., *J. Phys. Chem.*, **91**, 1663-1668, (1987).

[53] Combs, R.J., "Gases Diffusion in Liquids", Ph. D. Dissertation, Virginia Polytechnic Institute and State University, (1986).

[54] Malik, V.K., Hayduk, W., *Can. J. Chem. Eng.*, **46**, 462-466, (1968)

[55] Hayduk, W., Malik, V.K., *J. Chem. Eng. Data*, **16**, 143-146, (1971).

[56] Hayduk, W., Cheng, S.C., *Chem. Eng. Sci.*, **26**, 635-646, (1971).

[57] Hayduk, W., Buckley, W.D., *Chem. Eng. Sci.*, **27**, 1997-2003, (1972).

[58] Hayduk, W., Castaneda, R., Bromfield, H., Perras, R.R., *A. I. Ch. E. J.*, **19**, S59-861, (1973).

[59] Hayduk, W., Laudie, H., *A. I. Ch. E. J.*, **20**, 611-615, (1974).

[60] Sahgal, A, Hayduk, W., *J. Chem. Eng. Data*, **24**, 222-227, (1979).

[61] Hayduk, W., Minhas, B.S., *J. Chem. Eng. Data*, **32**, 285-290, (1987).

[62] Haycock, E.W., Alder, B.J., Hildebrand, J.H., *J. Chem. Phys.*, **21**, 1601-1604, (1953).

[63] Watts, H., Alder, B.J., Hildebrand, J.H., *J. Chem. Phys.*, **23**, 659-661, (1955).

[64] Naghizadeh, J., Rice, S.A., *J. Chem. Phys.*, **36**, 2710-2720, (1962).

[65] Houghton, G., Ritchie, P.D., Thomson, J.A., *Chem. Eng. Sci.*, **17**, 221-227, (1962).

[66] Wise, D.L., Houghton, G., *Chem. Eng. Sci.*, **21**, 999-1010, (1966).

[67] Krieger, I.M., Mulholland, G.W., Dickey, C.S., *J. Phys. Chem.*, **71**, 1123-1129, (1967).

[68] Wise, D.L., Houghton, G., *Chem. Eng. Sci.*, **23**, 1211-1216, (1968).

[69] Sporka, K., Hanika, J., Ružička, V., *Coll. Czech. Chem. Com.*, **34**, 3145-3148, (1969).

[70] Hanika, J., Sporka, K., Ružička, V., *Coll. Czech. Chem. Com.*, **36**, 1338-1346, 2130-2136, (1971).

[71] Pfeiffer, W.F., Krieger, I.M., *J. Phys. Chem* , **78**, 2516-2521, (1974).

[72] Sada, E., Kito, S., Oda, T., Ito, Y., *Chem. Eng. J.*, **10**, 155-159, (1975).

[73] De Blok, W.J., Fortuin, J.M.H., *Chem. Eng. Sci.*, **36**, 1687-1694, (1981).

[74] Simons, J., Ponter, A.B., *Can. J. Chem. Eng.*, **53**, 541-550, (1975).

[75] Tyrrell H.J.V., Harris K.R., "Diffusion in Liquids, A theoretical and experimental Study", Butterworths Monographs in Chemistry, London (1984).

[76] Eyring, H., *J. Chem. Phys.*, **4**, 283-291, (1936).

[77] Glasstone, S., Laidler, K., Eyring, H., "The Theory of Rate Processes", McGraw Hill, New York, (1941).

[78] Olander, D.R., *A. I. Ch. E. J.*, **9**, 207-210, (1963).

[79] Akgerman, A., Gainer, J.L., *Ind. Eng. Chem. Fund.*, **11**, 373-379, (1972).

[80] Akgerman, A., Gainer, J.L., *J. Chem. Eng. Data*, **17**, 372-377, (1972).

[81] Alder, B.J., Hildebrand, J.H., *Ind. Eng. Chem. Fund.*, **12**, 387-388, (1973).

[82] Chapman, S., Cowling, T.G., "The Mathematical theory of Non-Uniform Gases", 3rd Edition, Cambridge University Press, London, (1970).

[83] Evan, D.F., Tominaga, T., Davis, H.T., *J. Chem. Phys.*, **74**, 1298-1305, (1981).

[84] Chandler, D., *J. Chem. Phys.*, **62**, 1358-1363, (1975).

[85] Dymond, J.H., *J. Chem. Phys.*, **60**, 969-973, (1974).

[86] Ghai, R.K., Ertl, H., Dullien, F.A.L., *A. I. Ch. E. J.*, **19**, 881-900, (1973).

[87] Ertl, H., Ghai, R.K., Dullien, F.A.L., *A. I. Ch. E. J.*, **20**, 1-20, (1974).

[88] Reid, R.C., Prausnitz, J.M., Sherwood, T.K., "The Properties of Gases and Liquids", 3rd Edition, McGraw-Hill, New York, (1977).

[89] Reid, R.C., Prausnitz, J.M., Poling, B.E., "The Properties of Gases and Liquids", 4th Edition, McGraw-Hill, New York, (1987).

[90] Hayduk, W., "Encyclopedia of Fluid Mechanics", Chapter 3, Gulf Publishing Company, Houston, (1986).

[91] Wilke, C.R., Chang, P., *A. I. Ch. E. J.*, **1**, 264-270, (1955).

[92] King, C.J., Hsueh, L., Mao, K.W., *J. Chem. Eng. Data*, **10**, 348-350, (1965).

[93] Tyn, M.T., Calus, W.F., *J. Chem. Eng. Data*, **20**, 106-109, (1975).

[94] Hayduk, W., Minhas, B.S., *Can. J. Chem. Eng.*, **60**, 295-299, (1982).

[95] Siddiqi, M.A., Lucas, K., *Can. J. Chem. Eng*, **64**, 839-843, (1986).

[96] Sovová, H., *Coll. Czech. Chem. Com.*, **41**, 3715-3723, (1976).

[97] Sridhar, T., Potter, O.E., *A. I. Ch. E. J.*, **23**, 590-592, 946-948, (1977).

[98] Umesi, N.O., Danner, R.P., *Ind. Eng. Chem. Proc. Des. Dev.*, **20**, 662-665, (1981).

[99] Lo, H.Y., *J. Chem. Eng. Data*, **19**, 236-241, (1974).

[100] Chen, H.C., Chen, S.H., *Ind. Eng. Chem. Fund.*, **24**, 187-192, (1985).

[101] Othmer, D.F., Thakar, M.S., *Ind. Eng. Chem.*, **45**, 589-593, (1953).

[102] Wong, C.F., "Development of a Correlation for Binary Diffusion Coefficients of n-Paraffins at Infinite Dilution", Report for 'Modelling of Steady-State Processes' course, University of Ottawa, (1985).

[103] Minhas, B.S., Asatani, H., Hayduk, W., "A Simple Correlation for the Second Virial Coefficients of Gases and Vapors", Internal report, Department of Chemical Engineering, University of Ottawa, (1983).

[104] Smith, J.M., Van Ness, H.C., "Introduction to Chemical Engineering Thermodynamics", 3rd Edition, McGraw-Hill Book Company, New York, (1975).

[105] Henley, E.J., Seader, J.D., "Equilibruim-Stage Separation Operations in Chemical Engineering", John Wiley & Sons, New York, (1981).

[106] Asatani, H., "Solubility of Gases in Liquids", Ph. D. Thesis, University of Ottawa, (1986).

[107] Weast, R.C. (editor), "Handbook of chemistry and Physics", CRC press, 56 th Edition, (1976).

[108] Crank, J., "The Mathematics of Diffusion", Clarendon Press, London, (1956).

[109] Haar, L., Gallagher, J.S., Kell, G.S., "Steam Tables", Hemisphere Publication Co., New York, (1984).

[110] Pitzer, K.S., Curl Jr., R.F., *J. Am. Chem. Soc.*, **79**, 2369-2370, (1957).

[111] Nunge, R.J., Liu, R.S., Gill, N.N., *J. Fluid Mech.*, **51**, 363-383, (1972).

[112] Grushka, E., Kikta, E.J. Jr., *J. Phys Chem.*, **78**, 2297-2301, (1974).

[113] Cloeta, C.E., Smuts, T.W., DeClerk, K., *J. Chromatography*, **120**, 1-15, (1976).

[114] Timmermans, J., "Physico-Chemical Constants of Pure Organic Compounds", Elsevier Publishing Company, Inc., New York, (1950).

[115] Asatani, H., Hayduk, W., *Can. J. Chem. Eng.*, **61**, 227-232, (1983).

[116] Zhang, G., Hayduk, W., *Can. J. Chem. Eng*, **62**, 713-718, (1984).

[117] Miyano, Y., Hayduk, W., *J. Chem. Eng. Data*, **31**, 81-83, (1986).

[118] Sahgal, A., "Ethylene Solubility and Diffusivity in Polar and Nonpolar Solvents and Solutions", Master Thesis, University of Ottawa, (1977).

[119] Wilhoit, R.C., Zwolinski, B.J., "Physical and Thermodynamic Properties of Aliphotic Alcohols", ACS, AIP, NBS, New York, (1973).

[120] Cheng, J. S-C, "Diffusivities and Solubilities of Ethane in Normal Parallinic Liquids", Master Thesis, University of Ottawa, (1969).

[121] "International Critical Tables", McGraw-Hill Book Co., Inc., (1926).

[122] Dreisback, R.R., "Properties of Chemical Compounds, Vol. II", Advances in Chemistry Series, No. 22, American Chemical Society, (1959).

[123] Gometz-Nieto, M., Thodos, G., *Ind. Eng. Chem. Fund.*, **17**, 45-51, (1978).

[124] Marshtupa, V.P., Babin, E.P., Kolpakchi, A.A., Beginina, M.S., *Khim. Prom.*, **42**, 513-514, (1966).

[125] Hakuta, T., Suda, S., Hirata, M., *Mem. Fac. Technol. Tokyo Metrop. Univ.*, **20**, 1819-1826, (1970).

[126] Nagahama, K., Suda, S., Hakuta, T., Hirata, M., *J. Japan Petro. Inst.*, **14**, 252-256, (1971).

[127] Jadot, R., *J. Chim. Phys. Physicochim Biol.*, **69**, 1036-1040, (1972).

[128] Narasimhan, S., Natarajan, G.S., Nageshwar, G.D., *Indian J. Technol.*, **19**, 298-299, (1981).

[129] Hayduk, W., Laudie, H., *A. I. Ch. E. J.*, **19**, 1233- 1238, (1973).

[130] Malik, V.K., "Measurement of Gas-Liquid Diffusion Coefficients by Steady-State Capillary Cell Method", Master Thesis, University of Ottawa, (1968).

[131] Schornack, L.G., Eckert, C.A., *J. Phys. Chem.*, **74**, 3014-3020, (1970).

[132] Levenspiel, O., Smith, W.K., *Chem. Eng. Sci.*, **6**, 227-233, (1957).

[133] Alizadeh, A., Nieto de Castro, C.A., Wakeham, W.A., *Intern. J. of Thermophys.*, **1**, 243-284, (1980).

[134] Bondi, A., *J. Phys. Chem.*, **68**, 441-451, (1964).

[135] Douglass, D.C., McCall, D.W., *J. Phys. Chem.*, **62**, 1102-1107, (1958).

[136] Birkett, J.D., Lyons, P.A., *J. Phys. Chem.*, **69**, 2782-2783, (1965).

[137] Fishman, E., *J. Phys. Chem.*, **59**, 469-472, (1955).

[138] Bidlack, D.L., Kett, T.K., Kelly, C.M., Anderson, D.K., *J. Chem. Eng. Data*, **14**, 342-343, (1969).

[139] Shieh, J.C., Lyons, P.A., *J. Phys. Chem.*, **73**, 3258-3264, (1969).

[140] Bidlack, D.L., Anderson, D.K., *J. Phys. Chem.*, **68**, 3790-3794, (1964).

[141] Bidlack, D.L., Anderson, D.K., *J. Phys. Chem.*, **68**, 206-208, (1964).

[142] Moore, J.W., Wellek, R.M., *J. Chem. Eng. Data*, **19**, 136-140, (1974).

[143] Van Geet, A.L., Adamson, A.W., *J. Phys. Chem.*, **68**, 238-246, (1964).

[144] McCall, D.M., Douglass, D.C., *Physik Chem.*, **67**, 336-340, (1963).

[145] Hayduk, W., Ioakimidis, S., *J. Chem. Eng. Data*, **21**, 255-259, (1976).

[146] Ertl, H., Ghai, R.K., Dullien, F.A.L., *A. I. Ch. E. J.*, **20**, 1-20 (supplement), (1974).

[147] Vadovic, C.J., Colver, C.P., *A. I. Ch. E. J.*, **19**, 546-551, (1973).

[148] Takenihi, H., Fujine, M., Sato, T., Onda, K., *J. Chem. Eng. (Japan)*, **8**, 252-253, (1975).

[149] Norman, W.S., Sammak, F.Y.Y., *Trans. Inst. Chem. Engrs.*, **41**, 109-116, (1963).

[150] Fujinava, K., Tsukagoski, T., Abe, H., *Chem. Eng., Tokyo (Kagaku Kogaku)*, **31**, 590-593, (1967).

[151] Sherwood, T.K., Pigford, R.L., Wilke, C.K., "Mass Transfer", Chapter 2, McGraw Hill, New York, (1975).

[152] McManamey, W.J., Woollen, J.M., *A. I. Ch. E. J.*, **19**, 667-669, (1973).

[153] Sovová, H., Procházka, J., *Chem. Eng. Sci.*, **31**, 1091-1097, (1976).

[154] Sovová, H., "Research Report No. 29/75", Institute of Chemical Process Fundementals, Czechoslovak Academy of Science, Praque, (1975).

[155] Choudhari, R.V., Doraiswamy, L.K., *J. Chem. Eng. Data*, **17**, 428-432, (1972).

[156] Houghton, G., *J. Chem. Phys.*, **40**, 1628-1631, (1964).

[157] Calderbank, P.H., *Trans. Inst. Chem. Eng.*, **37**, 173-185, (1959).

[158] Groothuis, H., Kramers, H., *Chem. Eng. Sci.*, **4**, 17-25, (1955).

[159] Stearn, A.E., Irish, E.M., Eyring, H., *J. Phys. Chem.*, **44**, 981-995, (1940).

[160] Pollack, G.L., Enyeart, J.J., *Phys. Rev. A*, **31**, 980-984, (1985).

[161] Tammann, V.G., Jessen, V., *Z. Anorg. Allg. Chem.*, **179**, 125-131, (1929).

[162] Witherspoon, P.A., Bonoli, L., *Ind. Eng. Chem. Fund.*, **8**, 589-591, (1969).

[163] Witherspoon, P.A., Saraf, D.N., *J. Phys. Chem.*, **69**, 3752-3755, (1965).

[164] Maharajh, D.M., Walkley, J., *Can. J. Chem.*, **51**, 994-952, (1973).

[165] Kramers H., Blind, M.P.P., Snoeck, E., *Chem. Eng. Sci*, **14**, 115-123, (1961).

[166] Boerboom, A.J.H., Kleyn, G., *J. Chem. Phys.*, **50**, 1086-1088, (1969).

Appendix A

Listing of the Solute-Solvent Systems Used for Development of Correlation (3.9)

SOLUTE	SOLVENT	TEMPERATURE(K)	REFERENCE
n-pentane	n-pentane	273.15 - 308.65	[135], [136], [137]
	n-hexane	298.15	[138]
n-hexane	n-hexane	273.15 - 353.15	[135], [139]
	dodecane	298.15	[139], [140]
	hexadecane	298.15	[138], [141]
n-heptane	n-hexane	298.15	[138]
	n-heptane	273.15 - 373.15	[135], [137], [142]
	n-octane	293.15 - 298.15	[142]
	n-nonane	293.15 - 298.15	[142]
	n-decane	293.15 - 298.15	[142]
	hexadecane	298.15	[138], [140]
n-octane	n-hexane	298.15	[138]
	n-octane	273.15 - 373.15	[143], [144]
	dodecane	298.15	[139], [143]
	hexadecane	298.15	[139]
n-nonane	n-nonane	298.15	[144]
n-decane	n-hexane	298.15	[138]
	n-decane	293.15 - 298.15	[144]
dodecane	n-hexane	298.15 - 308.15	[138], [139], [140], [145]
	n-octane	298.15	[139], [143]
	dodecane	298.15	[139], [143]
	hexadecane	298.15	[145]
hexadecane	n-hexane	298.15	[138], [139], [141]
	n-heptane	298.15	[140]
	n-octane	298.15	[139]
	n-decane	298.15	[146]
	dodecane	298.15	[145]
	hexadecane	298.15	[147]
octadecane	n-hexane	298.15	[138]
	n-octane	298.15	[143]
	dodecane	298.15	[143]
	octadecane	323.15	[135]
tetracosane	n-hexane	298.15	[145]
	n-octane	298.15	[145]
	dodecane	298.15	[145]
dotriacontane	n-hexane	298.15	[145]
	n-octane	298.15	[145]

Table A.1: Experimental data used for development of correlation (3.9)

Appendix B

Listing of the Solute-Solvent systems Used for Development of Correlation (3.12)

SOLUTE	SOLVENT	TEMPERATURE(K)	REFERENCE
argon	benzene	298.15	[83]
	n-butanol	298.15 - 433.15	[24], [27], [83]
	carbon tetrachloride	273.15 - 298.15	[43], [50] [83]
	cyclohexane	298.15 - 415.85	[25], [83]
	cyclohexanol	303.15	[71]
	decane	298.15 - 373.15	[26], [83]
	hexane	298.15	[83]
	methanol	298.15 - 383.15	[27]
	n-octane	298.15 - 403.15	[26]
	n-octanol	298.15 - 430.15	[27], [83]
	tetradecane	298.15 - 430.15	[26], [83]
carbon dioxide	acetone	298.15	[148]
	n-amyl alcohol	293.15 - 298.15	[13], [148], [149]
	aniline	293.15	[150]
	benzene	293.15 - 303.15	[5], [148]
	i-butanol	293.15 - 298.15	[13], [38], [148], [149]
	n-butanol	298.15	[10], [148]
	carbon tetrachloride	293.15 - 298.15	[5], [38], [148]
	chlorobenzene	293.15	[150]
	diethyl ketone	298.15	[148]
	ethanol	279.55 - 303.15	[2], [5], [10], [71], [54]
	ethylene glycol	298.15	[55]
	formamide	298.15	[38]
	n-heptane	293.15 - 298.15	[13], [148], [149], [151]
	n-heptanol	298.15	[10], [148]
	hexadecane	298.15 - 323.15	[56]
	n-hexane	298.15	[148]
	methanol	293.15 - 298.15	[38], [148]
	methyl ethyl ketone	298.15	[148]
	4-methyl-2-pentanone	298.15 - 323.15	[152]
	nitrobenzene	293.15	[150]
	n-octanol	298.15	[10], [38], [148], [152]
	n-propanol	298.15 - 303.15	[38], [148]
	tetradecane	298.15 - 323.15	[152]
	toluene	298.15 - 323.15	[5], [148], [152], [153], [154]
	xylene	298.15	[148]

SOLUTE	SOLVENT	TEMPERATURE(K)	REFERENCE
ethane	carbon tetrachloride	298.15 - 303.15	[98]
	n-dodecane	298.15	[56]
	n-heptane	298.15 - 313.15	[54], [56]
	n-hexadecane	298.15	[56]
	n-hexane	298.15 - 303.15	[54], [56]
	n-octane	298.15	[56]
ethylene	n-butanol	298.15	[60]
	dodecane	298.15	[60]
	ethylene dichloride	288.15 - 303.15	[155]
	ethylene glycol	298.15	[60]
	hexane	298.15	[60]
	nitrobenzene	303.15 - 333.15	[155]
krypton	acetone	298.15	[83]
	benzene	298.15	[83]
	n-butanol	298.15 - 433.15	[27], [83]
	carbon tetrachloride	298.15	[83]
	cyclohexane	298.15 - 415.85	[25], [83]
	decane	298.15 - 433.15	[26], [11]
	n-hexane	298.15	[83]
	methanol	298.15 - 383.15	[27], [83]
	n-octane	298.15 - 403.15	[26]
	n-octanol	298.15 - 430.15	[27], [83]
	i-propanol	298.15	[83]
	tetradecane	298.15 - 374.15	[26], [83]
methane	acetone	298.15	[83]
	benzene	298.15	[83]
	n-butanol	298.15 - '33.15	[27], [83]
	carbon tetrachloride	273.15 - 298.15	[43], [50], [54], [98], [83]
	cyclohexane	298.15 - 415.15	[25], [83]
	decane	298.15 - 433.15	[27], [83]
	dodecane	273.15 - 323.15	[57]
	n- heptane	277.15 - 311.15	[57], [98]
	n-hexadecane	298.15	[57]
	n-hexane	298.15 - 303.15	[24], [57], [98], [83]
	methanol	298.15 - 383.15	[27], [83]
	n-octane	298.15 - 403.15	[26], [57]

SOLUTE	SOLVENT	TEMPERATURE(K)	REFERENCE
methane	n-octanol	298.15 - 430.15	[27], [83]
	i-propanol	298.15	[83]
	tetradecane	298.15 - 430.15	[26], [83]
neon	carbon tetrachloride	298.15	[51]
neopentane	decane	298.15	[83]
	neopentane	298.15	[156]
	tetradecane	298.15	[83]
nitrogen	benzene	298.15	[43], [52]
	carbon tetrachloride	273.15 - 298.15	[43], [50], [52]
	cyclohexanol	303.15	[71]
	cyclohexane	303.15	[71]
	ethanol	293.15	[72]
	ethylene glycol	303.15	[71]
	methanol	293.15	[72]
oxygen	benzene	298.15	[52]
	carbon tetrachloride	298.15	[51], [52]
	cyclohexane	302.75	[67]
	ethanol	293.15 - 302.75	[67], [72]
	ethylene glycol	293.15	[157]
	methanol	293.15	[72]
	i-propanol	293.15	[72]
	n-propanol	293.15	[72]
propane	n-butanol	273.15 - 323.15	[58], [140]
	chlorobenzene	273.15 - 323.15	[58]
	n-heptane	298.15	[58]
	hexadecane	298.15	[58]
	n-hexane	298.15	[58]
	heptanol	298.15	[10]
	n-octane	298.15	[58]
	octanol	298.15	[10]
propene	acetic acid	293.15 - 323.15	this work
	acetone	278.15 - 323.15	this work
	n-butanol	278.15 - 323.15	this work
	chlorobenzene	278.15 - 323.15	this work
	N,N dimethylformamide	278.15 - 323.15	this work
	ethyl acetate	278.15 - 323.15	this work
	n-octane	278.15 - 323.15	this work

SOLUTE	SOLVENT	TEMPERATURE(K)	REFERENCE
sulfur dioxide	n-decane	293.15	[158]
	n-dodecane	293.15	[1]
	n-heptane	293.15	[158]
	n-hexadecane	293.15	[1]
	n-nonane	293.15	[158]
vinyl chloride	benzene	281.15	[159]
xenon	acetone	298.15	[83]
	benzene	298.15	[83]
	n-butanol	298.15 - 433.15	[27], [83]
	carbon tetrachloride	298.15	[83]
	cyclohexane	298.15 - 415.85	[25], [83]
	decane	293.15 - 433.15	[26], [83]
	dodecane	293.15	[160]
	n-heptane	293.15	[160]
	hexadecane	293.15	[160]
	hexane	293.15 - 298.15	[83], [160]
	methanol	298.15 - 383.15	[27], [83]
	nonane	293.15	[160]
	n-octane	293.15 - 403.15	[26], [160]
	n-octanol	298.15 - 430.15	[27], [83]
	pentadecane	293.15	[160]
	n-pentane	293.15	[160]
	i-propanol	298.15	[83]
	tetradecane	293.15 - 430.15	[26], [83]
	tridecane	293.15	[160]
chlorine	carbon tetrachloride	298.15 - 318.15	[35]

Table B.1: Experimental data used for development of correlation (3.12)

Appendix C

Listing of the Solute-Water Systems Used for Development of Correlation (3.13)

SOLUTE	TEMPERATURE(K)	REFERENCE
acetylene	273.15 - 303.15	[161]
argon	288.15 - 298.15	[3], [151]
n-butane	277.15 - 333.15	[4], [66], [151], [162], [163]
n-butene	280.15 - 333.15	[4]
carbon dioxide	273.15 - 348.15	[1], [4], [27], [164]
carbon monoxide	283.15 - 333.15	[68], [151]
ethane	288.15 - 315.75	[3], [66], [162], [163]
ethylene	279.85 - 338.15	[4]
hydrogen sulfide	288.15 - 308.15	[1], [11]
krypton	283.15 - 333.15	[68]
mathene	277.15 - 338.15	[66], [162], [163], [164]
methyl chloride	295.25 - 298.15	[1], [164]
neon	283.15 - 333.15	[68]
nitric oxide	283.15 - 333.15	[68]
nitrogen	274.15 - 328.15	[1], [3], [22], [66], [72], [59], [151]
nitrogen dioxide	293.15 - 303.15	[165]
nitrous oxide	288.15 - 313.15	[1], [16]
oxygen	274.15 - 328.15	[1], [3], [9], [22], [66]
propane	277.15 - 333.15	[66], [151], [162]
propene	280.15 - 338.15	[4]
sulfur dioxide	293.55 - 313.15	[1]
vinyl chloride	298.15 - 348.15	[59]
xenon	273.15 - 323.15	[68], [166]
ammonia	281.15 - 293.15	[1]
chlorine	283.15 - 308.15	[1], [12], [16]

Table C.1: Experimental data used for development of correlation (3.13)

Appendix D

Calibration Constants for Density Measurements at Elevated Pressures

TEMPERATURE (K)	A_p	k_1	k_2	B $(cm^3/mole)$
298.15	1.89×10^{10}	377100.1	2.069	-4.353
323.15	1.92×10^{10}	378691.4	1.890	0.187
348.15	1.93×10^{10}	3.80648.1	1.706	3.982

Table D.1: Calibration constants for density measurements at elevated pressures and the second virial coefficients of nitrogen at the calibration temperatures

Appendix E

Sample Calculation for the Determination of Gas Solubility Measured at Atmospheric Pressure

A sample calculation to determine the solubility of propene in n-butanol at 278.15 K and 100.3 kPa (751.9 mm Hg) is illustrated as following:

- solute: propene (A)
- solvent: n-butanol (B)
- experimental temperature: 278.15 K
- experimental pressure: 100.3 kPa
- volumetric flow rate of the solvent: 0.00882 cm^3/min
- molar volume of the solute: 22392.70 $cm^3/gmol$
- molar volume of the solvent: 92.05 $cm^3/gmol$
- vapor pressure of the solvent: 0.15 KPa (1.16 mm Hg)

The volume of propene dissolved and the volume of n-butanol supplied at 5 minutes intervals measured in this experiment is shown in Table E.1 and is plotted in Figure E.1. The slope of the volume of propene dissolved to that of n-butanol supplied (SLP) is calculated by means of a linear regression analysis and the result is:

$$(SLP) = 16.74$$

The gas solubility of propene in n-butanol at 278.15 K and at 100.3 kPa is calculated from equations (5.4) and (5.5) as:

$$x_A(100.3, 278.15) = 0.0644$$

The gas solubility of propene in n-butanol for propene partial pressure of 101.3 kPa is calculated by equation (5.6) as:

$$x_A(101.3, 278.15) = 0.0652$$

TIME (min)	VOLUME OF N-BUTANOL (cm^3)	VOLUME OF PROPENE (cm^3)
0	0.0000	0.00
5	0.0441	0.74
10	0.0882	1.47
15	0.1323	2.21
20	0.1764	2.95
25	0.2205	3.69
30	0.2646	4.43
35	0.3087	5.16
40	0.3528	5.91
45	0.3969	6.65
50	0.4410	7.38
55	0.4851	8.12
60	0.5292	8.85

Table E.1: Data of volume of propene dissolved and volume of n-butanol supplied at 5 minutes intervals for measurement of gas solubility at 278.15 K and at 100.3 kPa

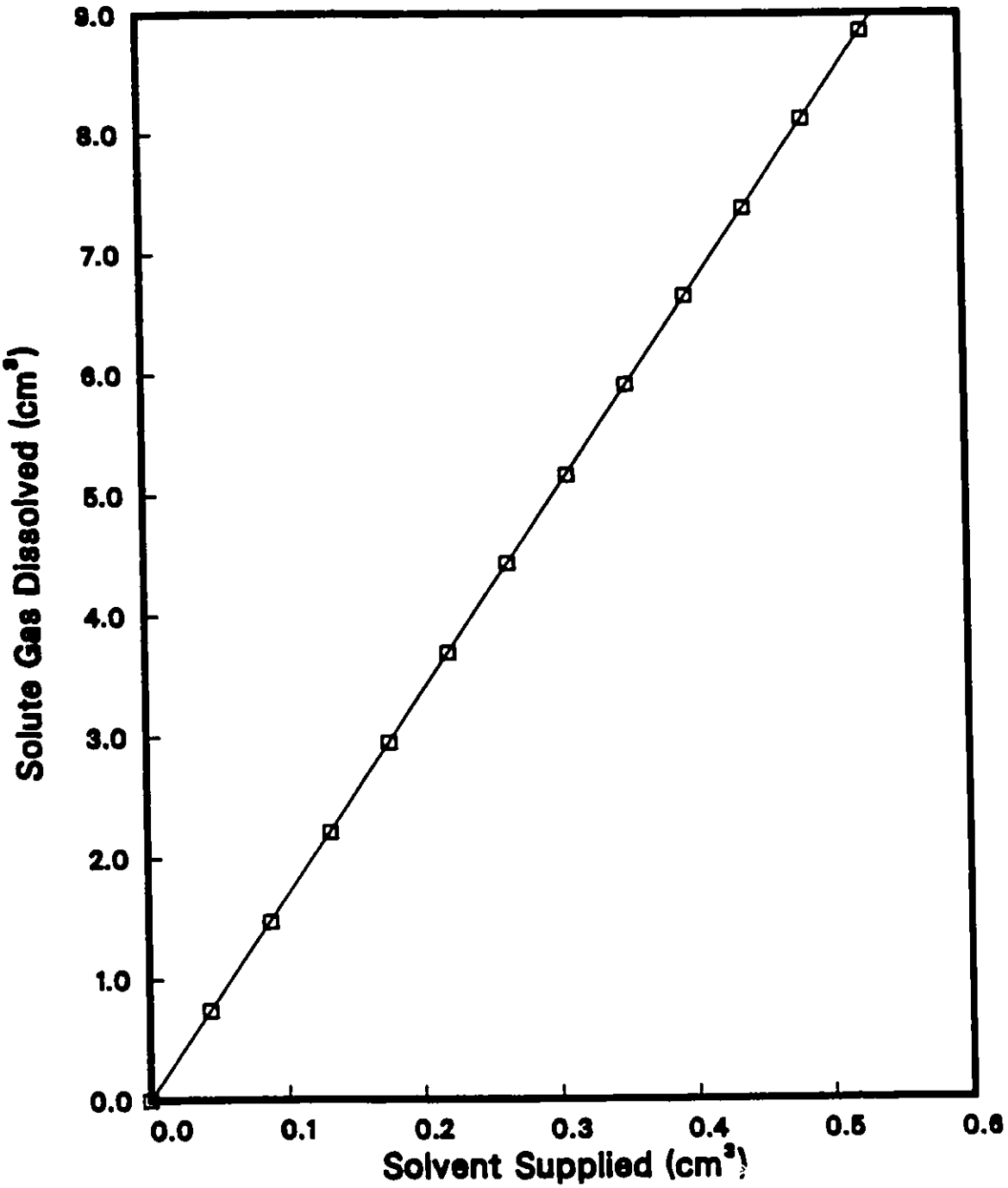

Figure E.1: Plot of the volume of propene dissolved versus the volume of n-butanol supplied for measurement of gas solubility at 278.15 K and at 100.3 kPa

Appendix F

Sample Calculation for the Determination of Diffusivity Measured at Atmospheric Pressure

A sample calculation to determine the diffusivity of propene in n-butanol at 298.15 K and 102.9 kPa (771.6 mm Hg) is illustrated as following:

- solute: propene (A)
- solvent: n-butanol (B)
- experimental temperature: 298.15 K
- experimental pressure: 102.9 kPa
- upper capillary tube diameter: 0.0613 cm
- lower capillary tube diameter: 0.1016 cm
- volume of capillary cell: 17.60 cm^3
- diffusion path length: 2.325 cm
- time for development of steady-state concentration profile: 114.0 hours
- gas solubility of propene in n-butanol at 298.15 K and 101.3 kPa partial pressure of prepene (mole fraction): 0.0373
- molecular weight of the solute: 42.081 gm/mol
- molar volume of the solute: 24109.12 cm^3/mol
- molecular weight of the solvent: 74.123 gm/mol
- density of the solvent at 298.15 K: 0.8060 gm/cm^3
- molar volume of the solvent: 91.96 cm^3/mol
- vapor pressure of the solvent at 298.15 K: 0.84 kPa (6.31 mm Hg)
- density of propene in liquid phase at 298.15 K: 0.5064 gm/cm^3

The position of the gas-saturated solvent bead and the corresponding time measured in this experiment is shown in Table F.1 and is plotted in Figure F.1. The rate of the gas-saturated bead travelling down the capillary tube, (ROB), is determined by the slope of the straight line obtained from Figure F.1. The (ROB) is determined by means of a linear regression analysis and the result is:

$$(ROB) = 0.0094 \ \ cm/min$$

The volumetric rate (V_s) of skrinkage of gas and associated vapor is calculated by equation (5.15) as:

$$V_s = 5.7 \times 10^{-5} \ \ cm^3/(cm^2 s)$$

The Ostwald coefficient of propene in n-butanol at 278.15 K and at 102.9 kPa is calculated from equations (5.18) and (5.19) as:

$$OST = 10.32 cm^3/cm^3$$

The diffusivity of propene in n-butanol before correction is calculated by means of equation (5.21) as:

$$D^o_{AB} = 1.34 \times 10^{-5} cm^2/s$$

The diffusivity of propene in n-butanol after corrected by equation (5.22) is:

$$D^o_{AB} = 1.34 \times 10^{-5} cm^2/s$$

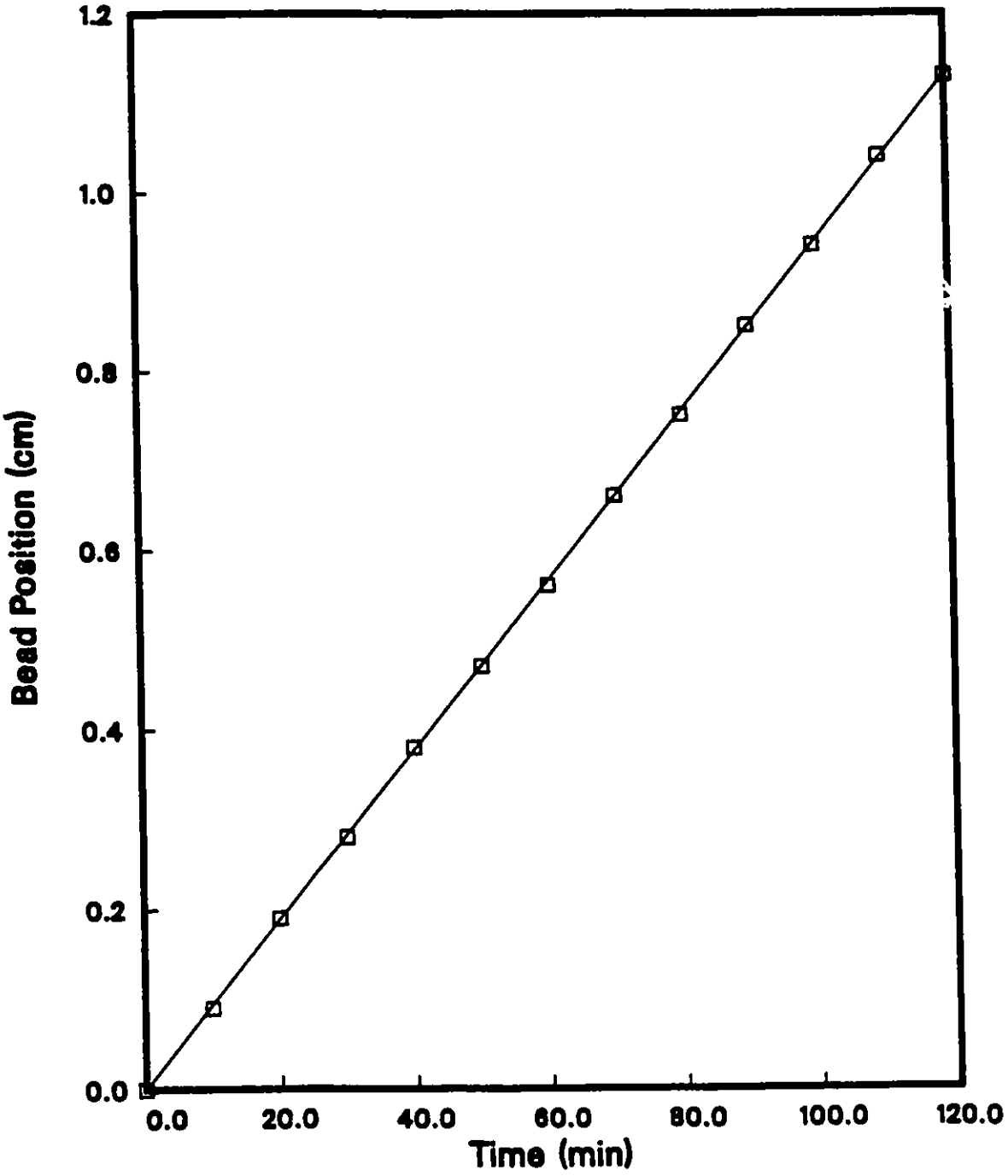

Figure F.1: Plot of the gas-saturated solvent bead position versus the corresponding time for diffusivity measurement of propene in n-butanol at 298.15 K and at 102.9 kPa

TIME(min)	BEAD POSITION (cm)
0	0.00
10	0.09
20	0.19
30	0.28
40	0.38
50	0.47
60	0.56
70	0.66
80	0.75
90	0.85
100	0.94
110	1.04
120	1.13

Table F.1: Data of the bead position and the corresponding time for diffusivity measurement of propene in n-butanol at 298.15 K and at 102.9 kPa

Appendix G

Comparisons of Experimental Diffusivities in this Study with Predicted Values from Available Correlations

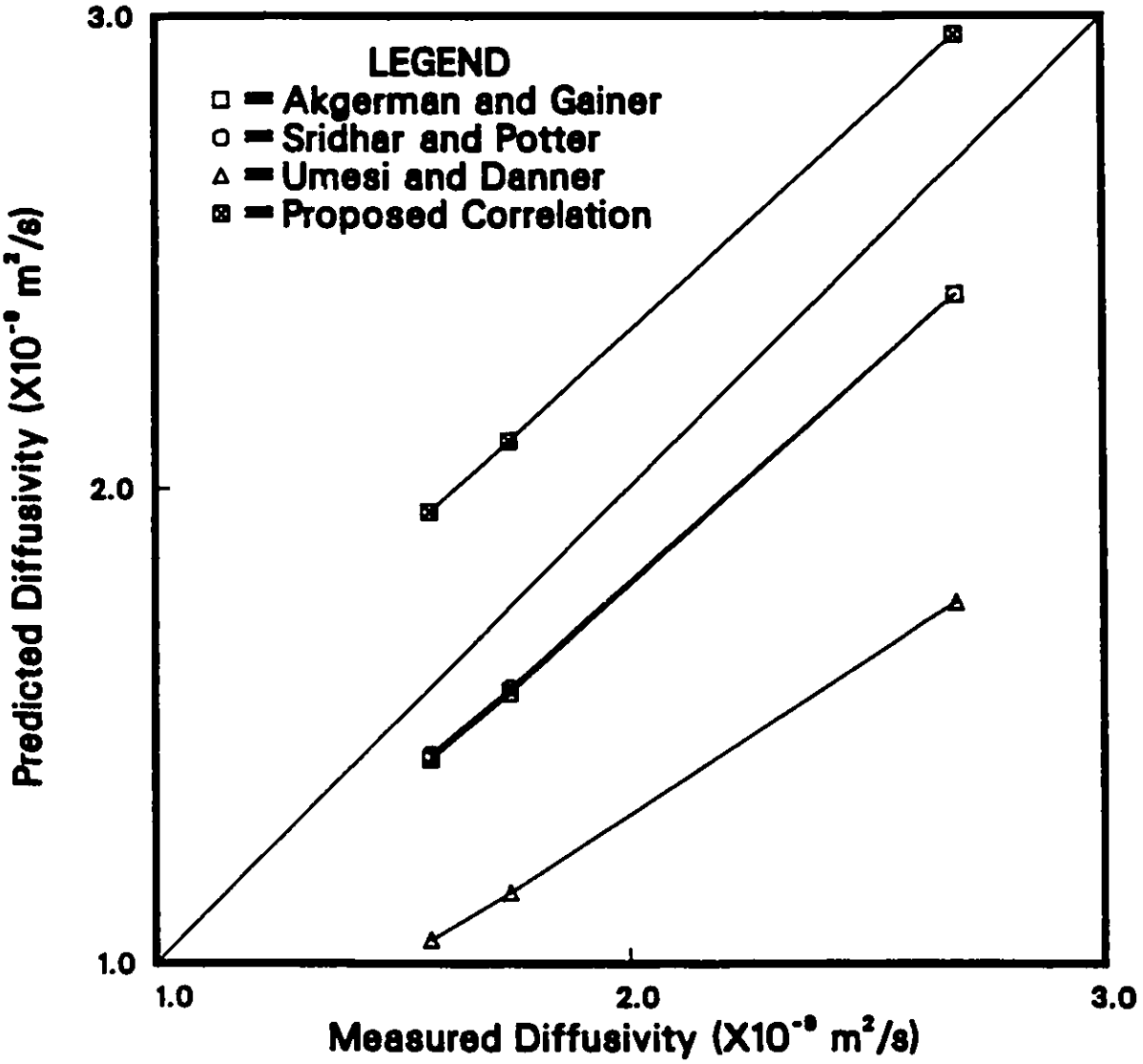

Figure G.1: Comparison of experimental diffusivity data with predicted results from the available correlations for propene in acetic acid

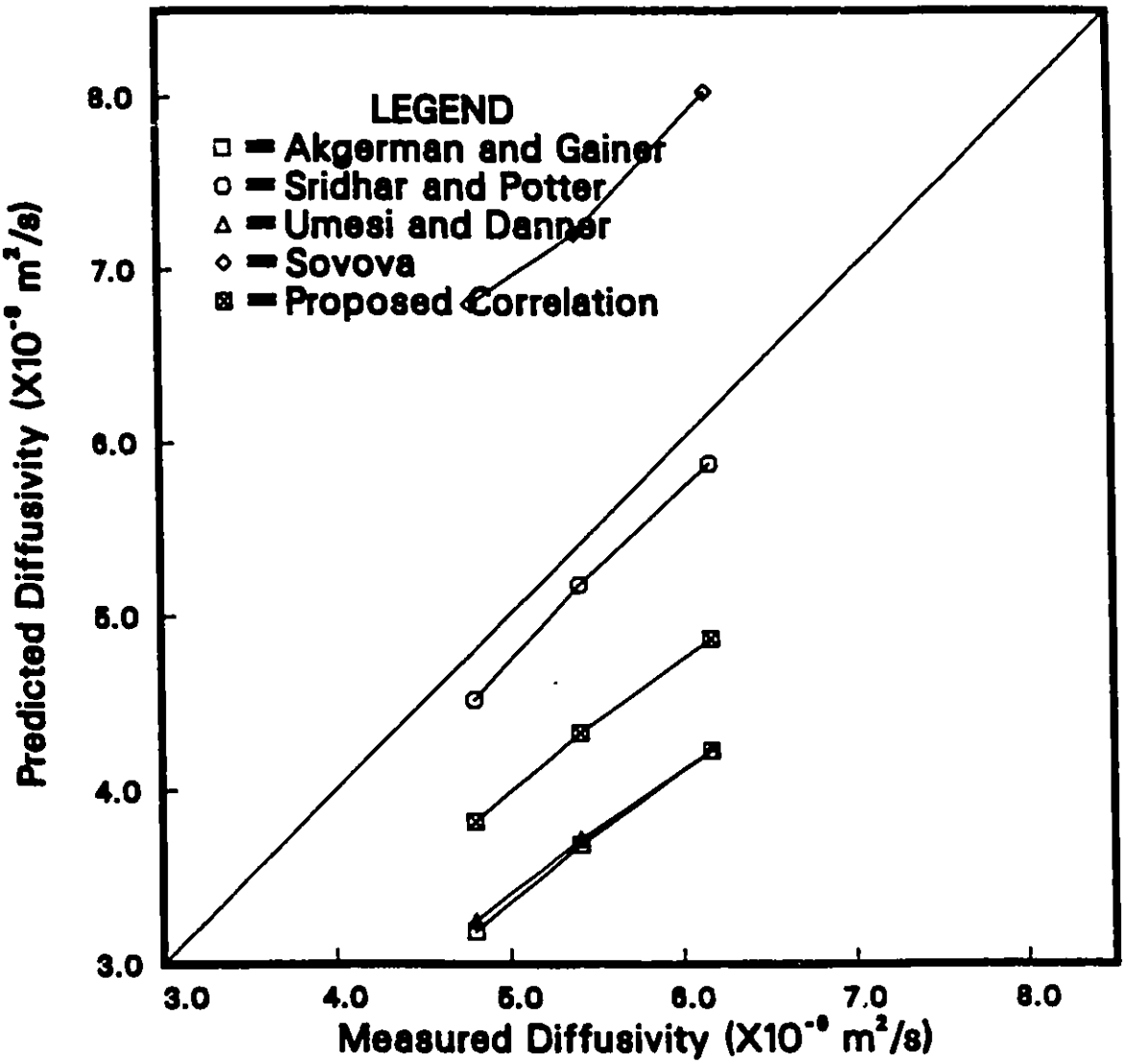

Figure G.2: Comparison of experimental diffusivity data with predicted results from the available correlations for propene in acetone

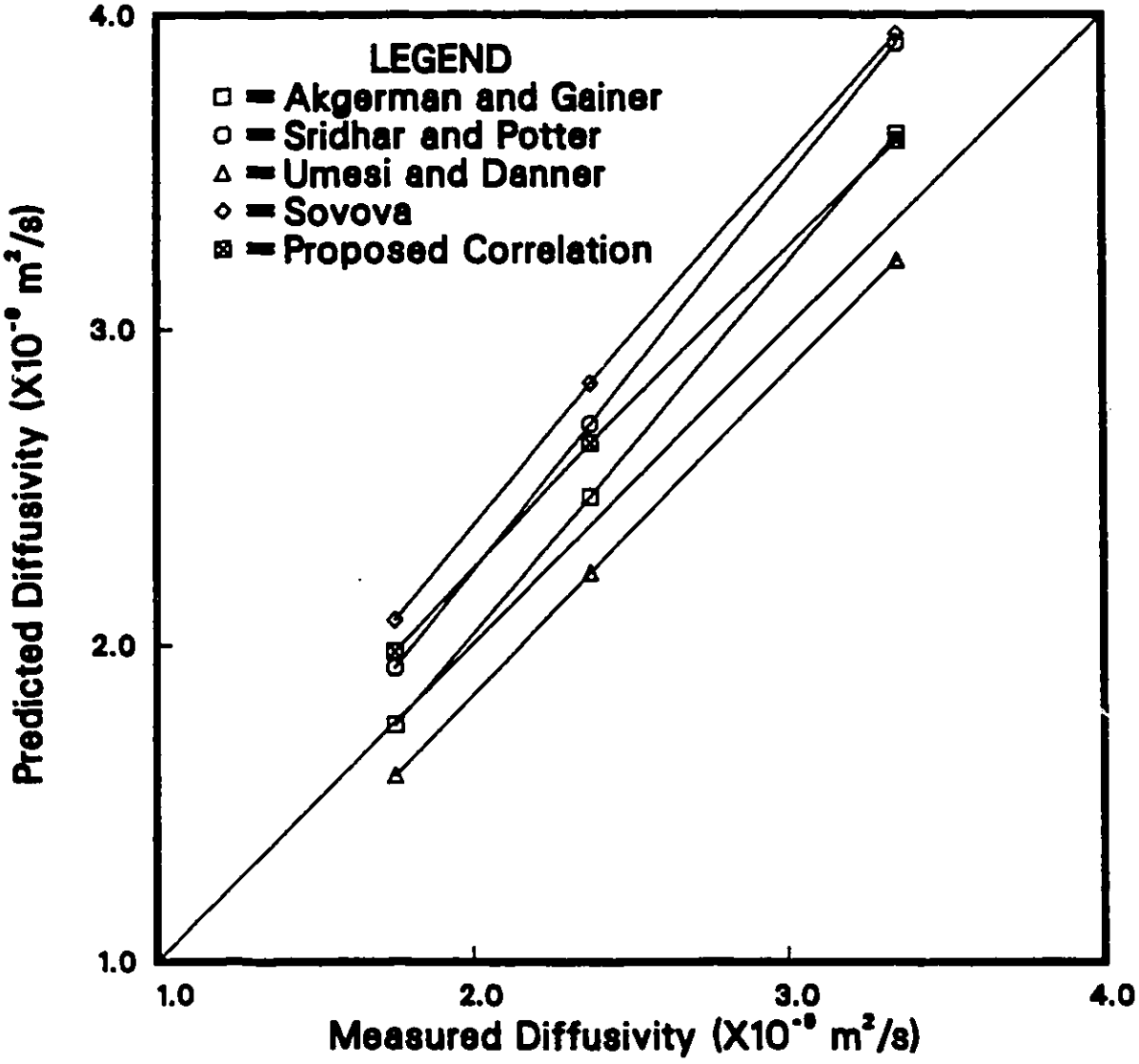

Figure G.3: Comparison of experimental diffusivity data with predicted results from the available correlations for propene in chlorobenzene

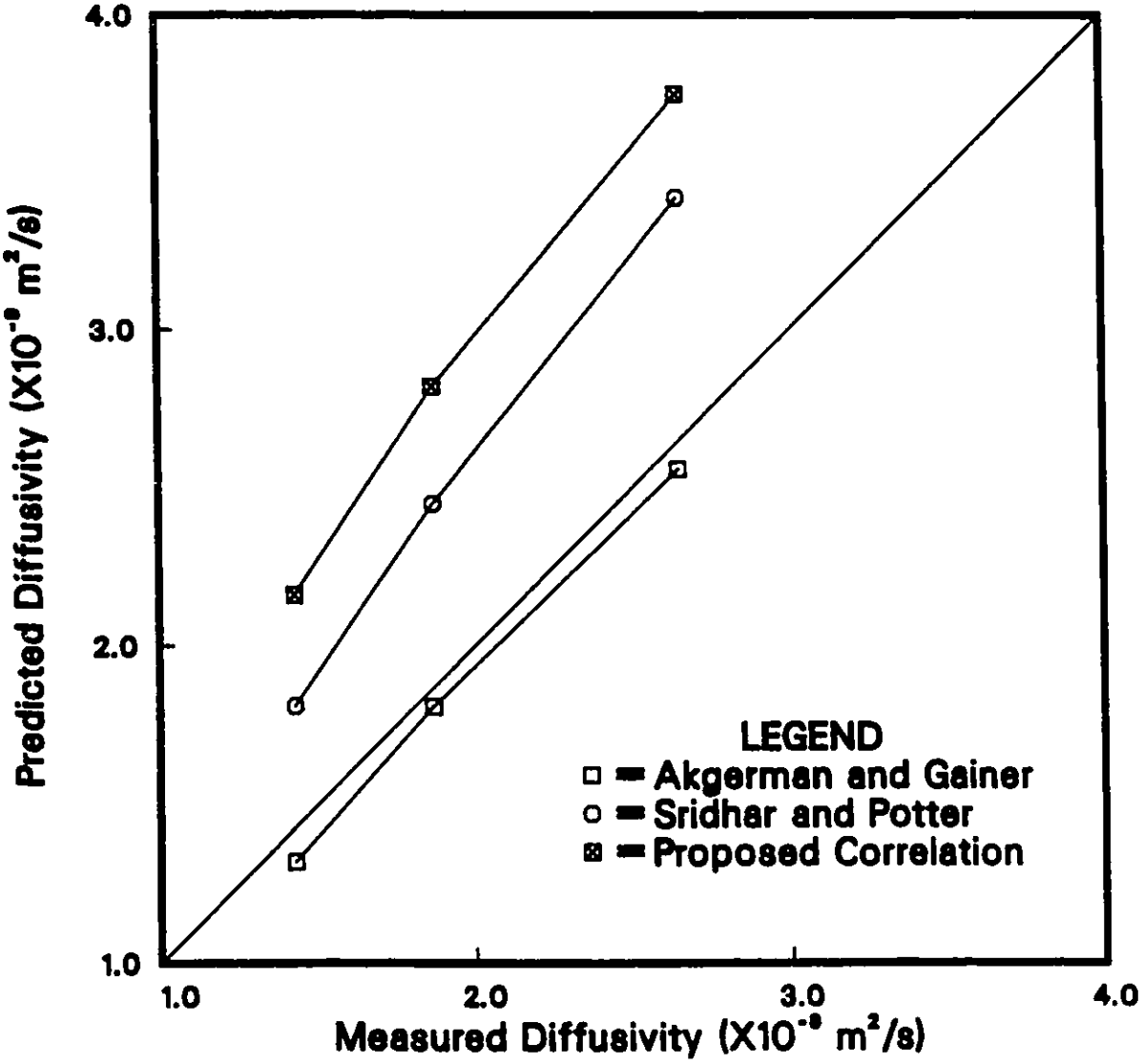

Figure G.4: Comparison of experimental diffusivity data with predicted results from the available correlations for propene in N,N dimethyl formamide

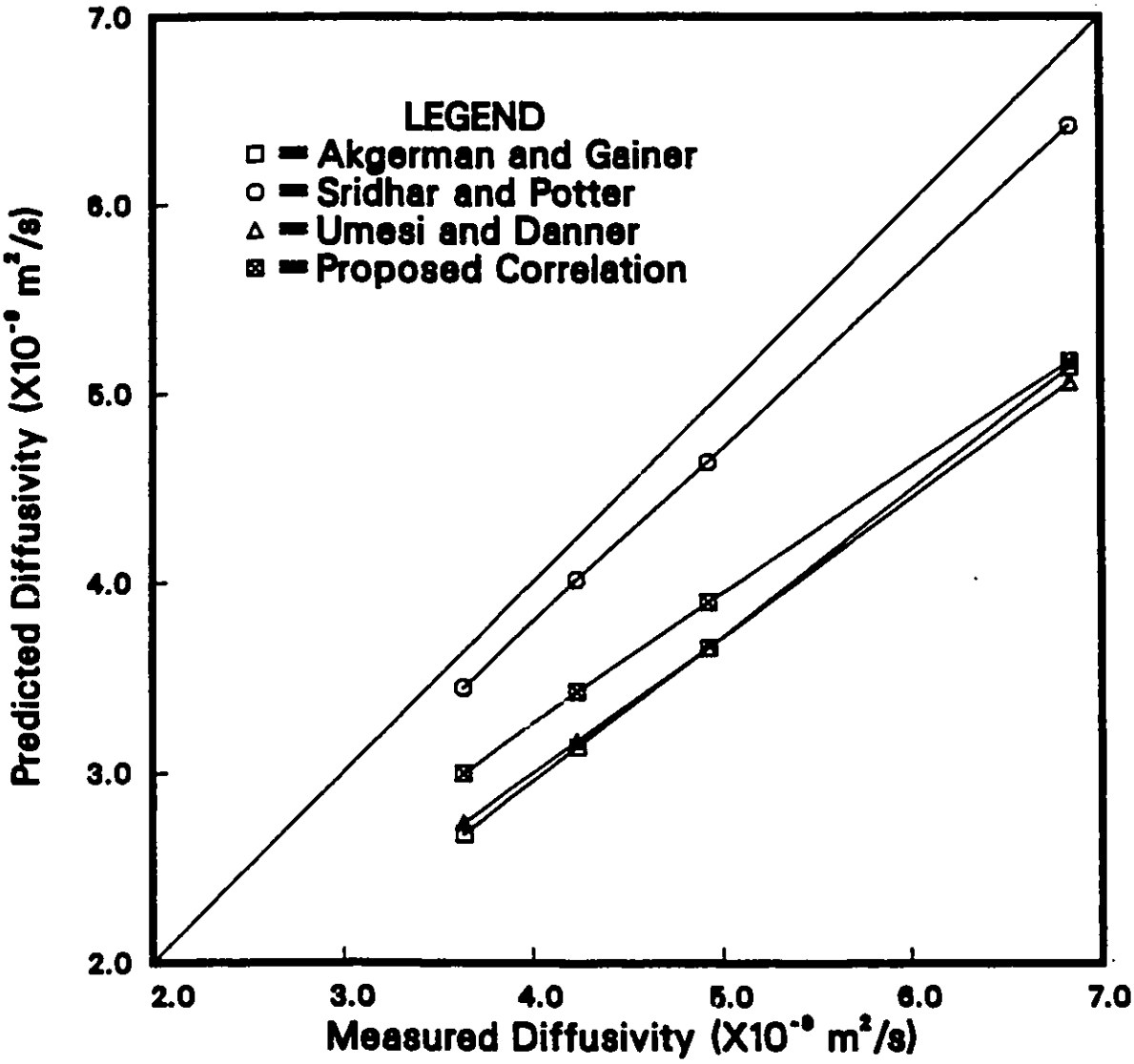

Figure G.5: Comparison of experimental diffusivity data with predicted results from the available correlations for propene in ethyl acetate

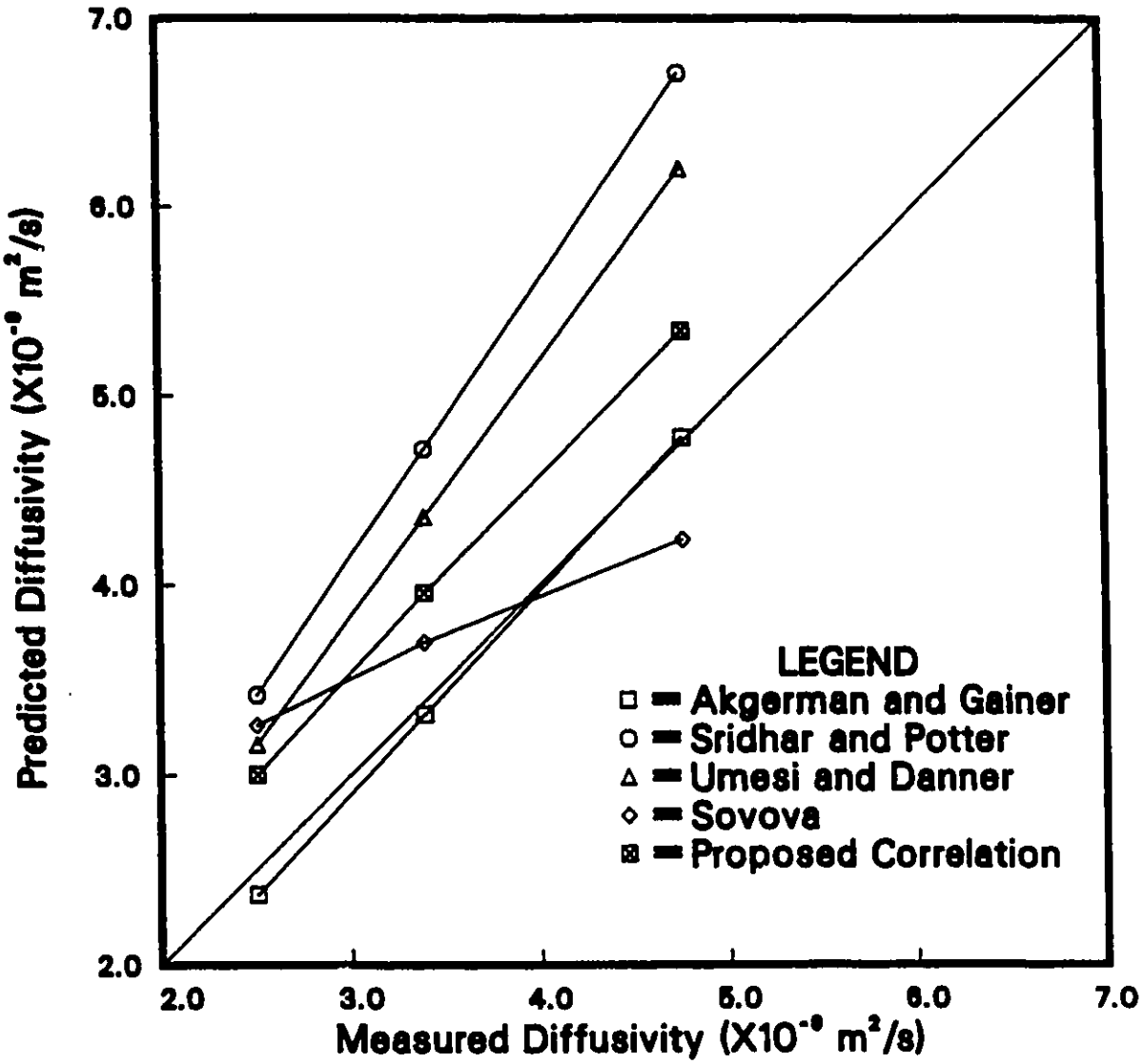

Figure G.6: Comparison of experimental diffusivity data with predicted results from the available correlations for propene in n-octane

Appendix H

Comparisons of Experimental Diffusivities in this Study with Predicted Values from the Diffusion Theories

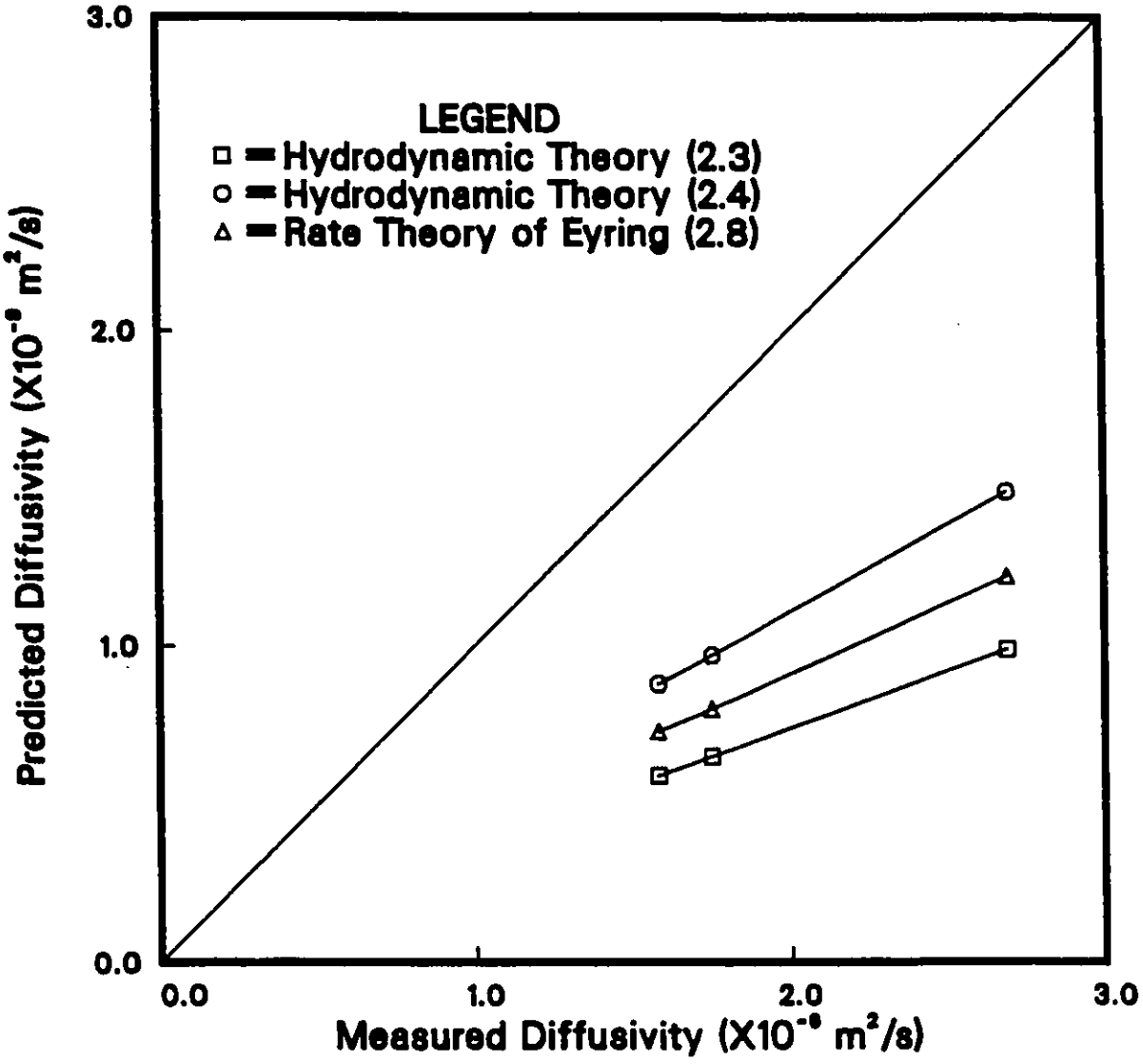

Figure H.1: Comparison of experimental diffusivity data with predicted results from the diffusion theories for propene in acetic acid

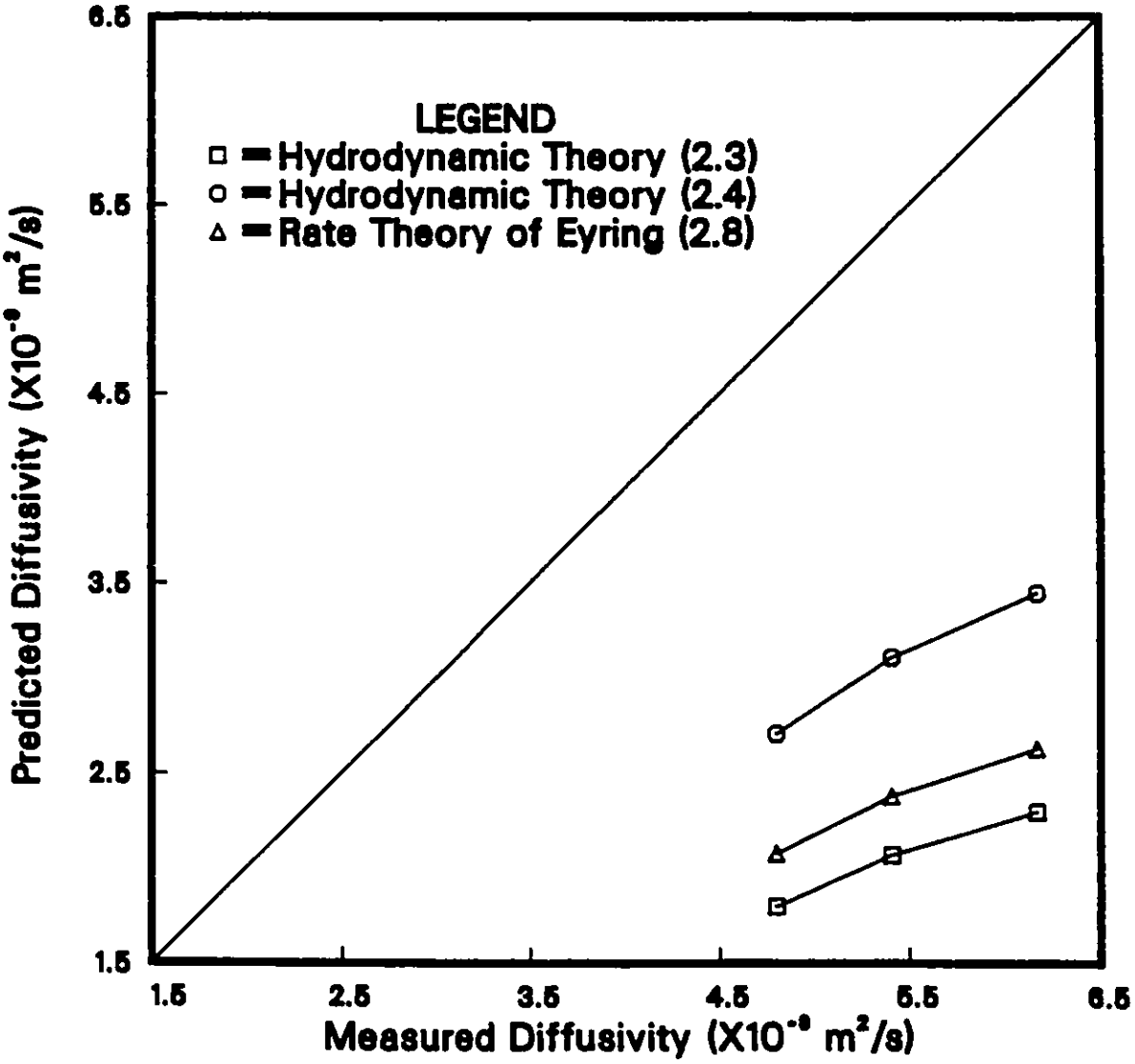

Figure H.2: Comparison of experimental diffusivity data with predicted results from the diffusion theories for propene in acetone

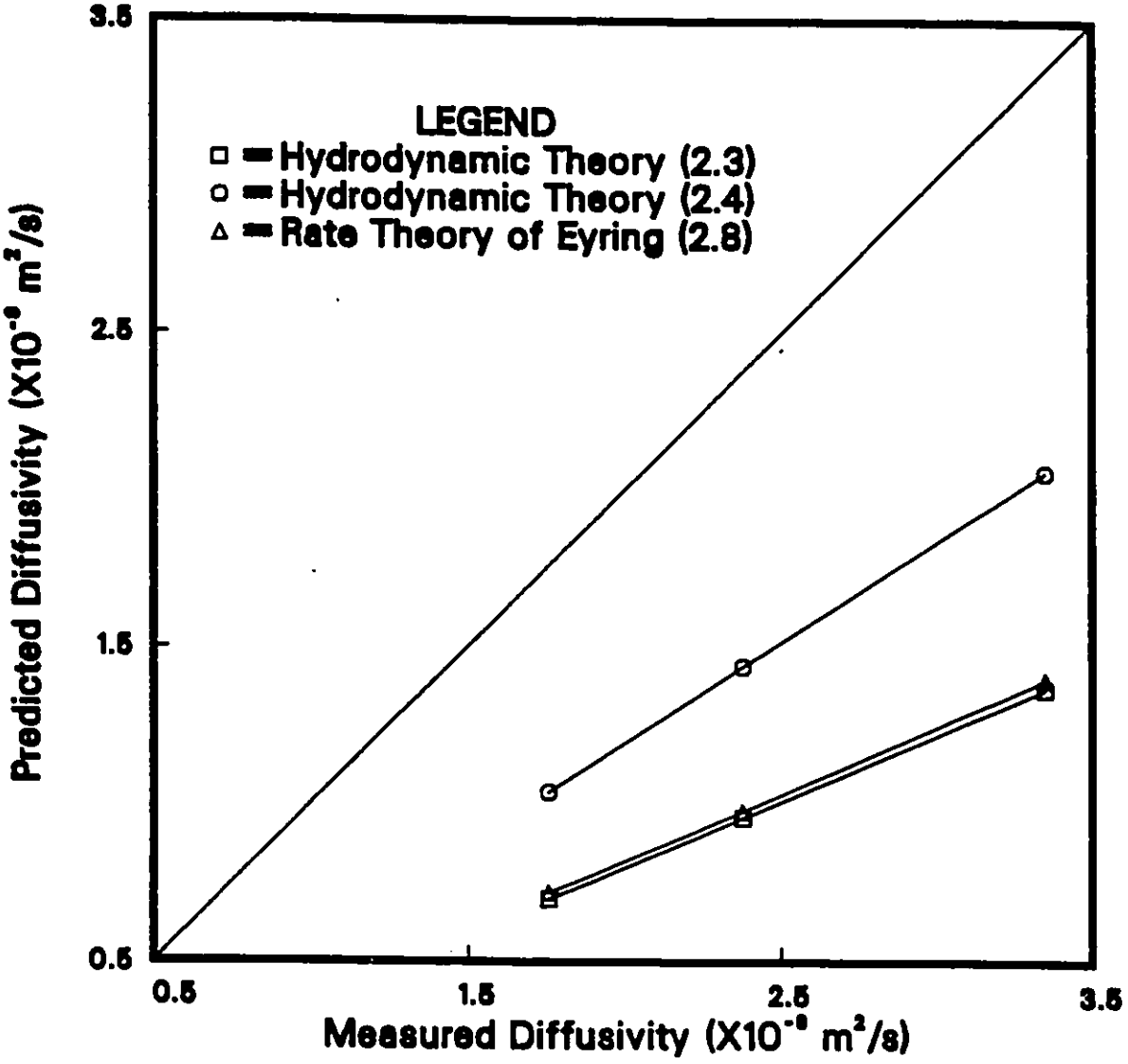

Figure H.3: Comparison of experimental diffusivity data with predicted results from the diffusion theories for propene in chlorobenzene

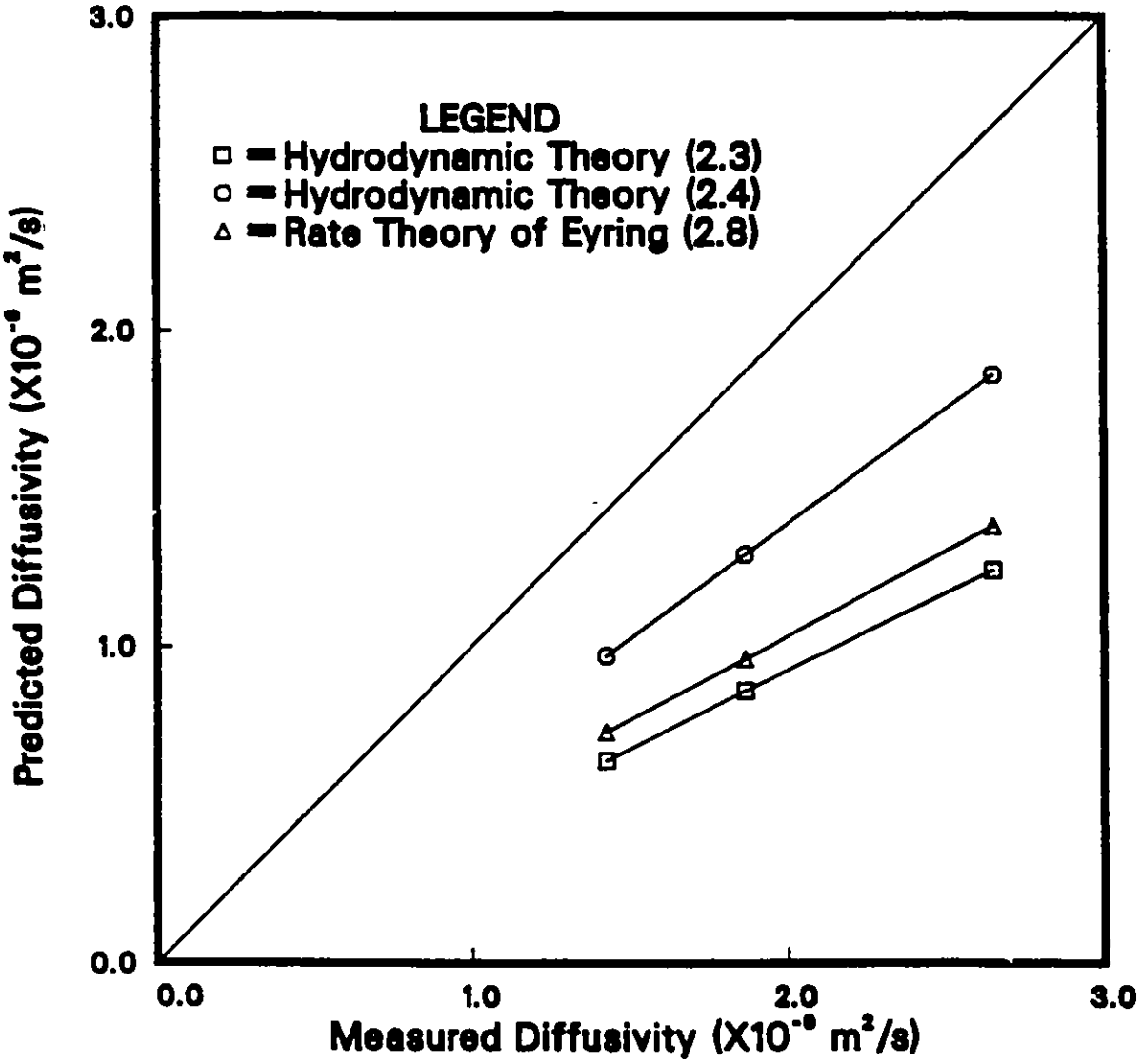

Figure H.4: Comparison of experimental diffusivity data with predicted results from the diffusion theories for propene in N,N dimethyl formamide

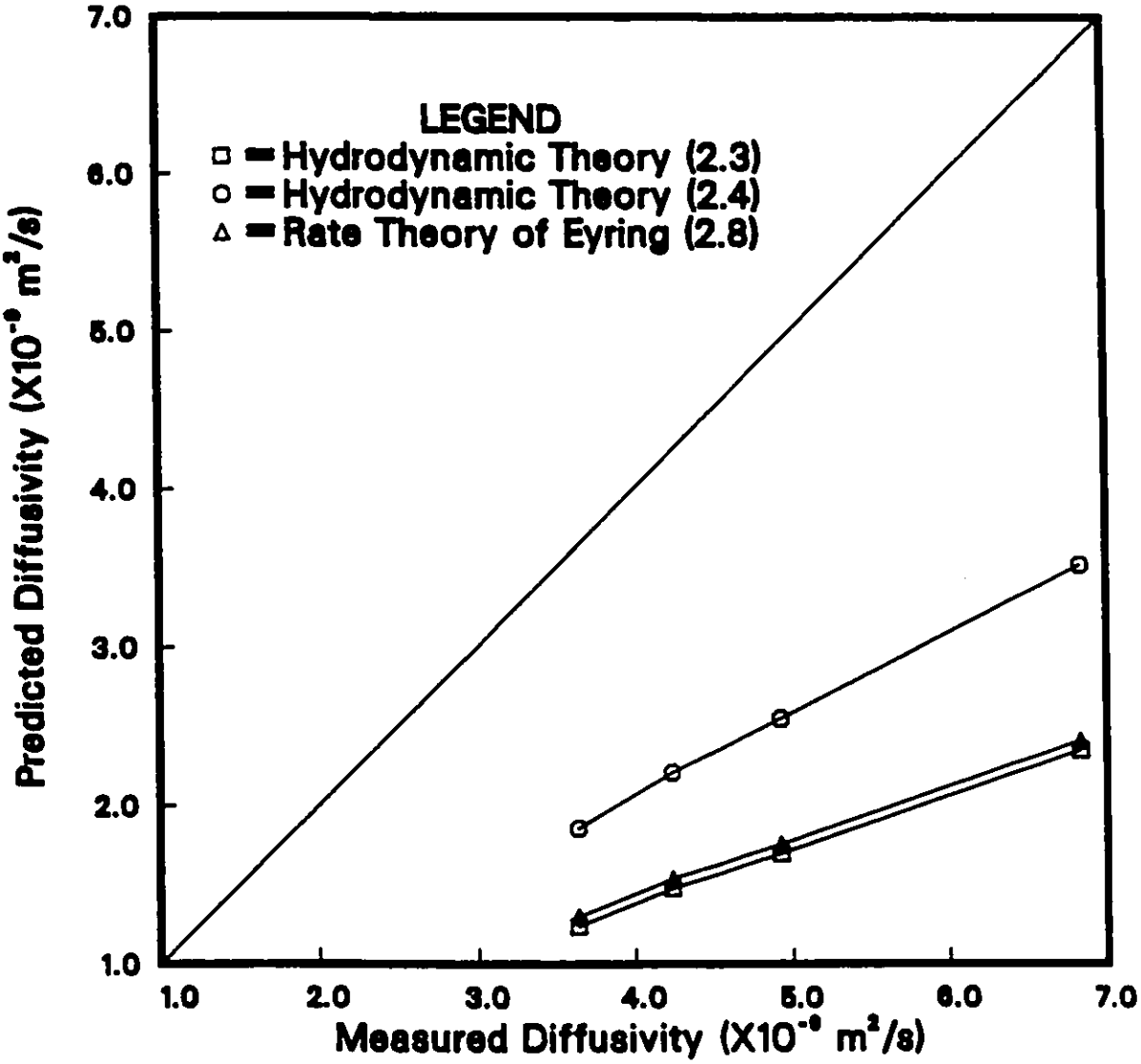

Figure H.5: Comparison of experimental diffusivity data with predicted results from the diffusion theories for propene in ethyl acetate

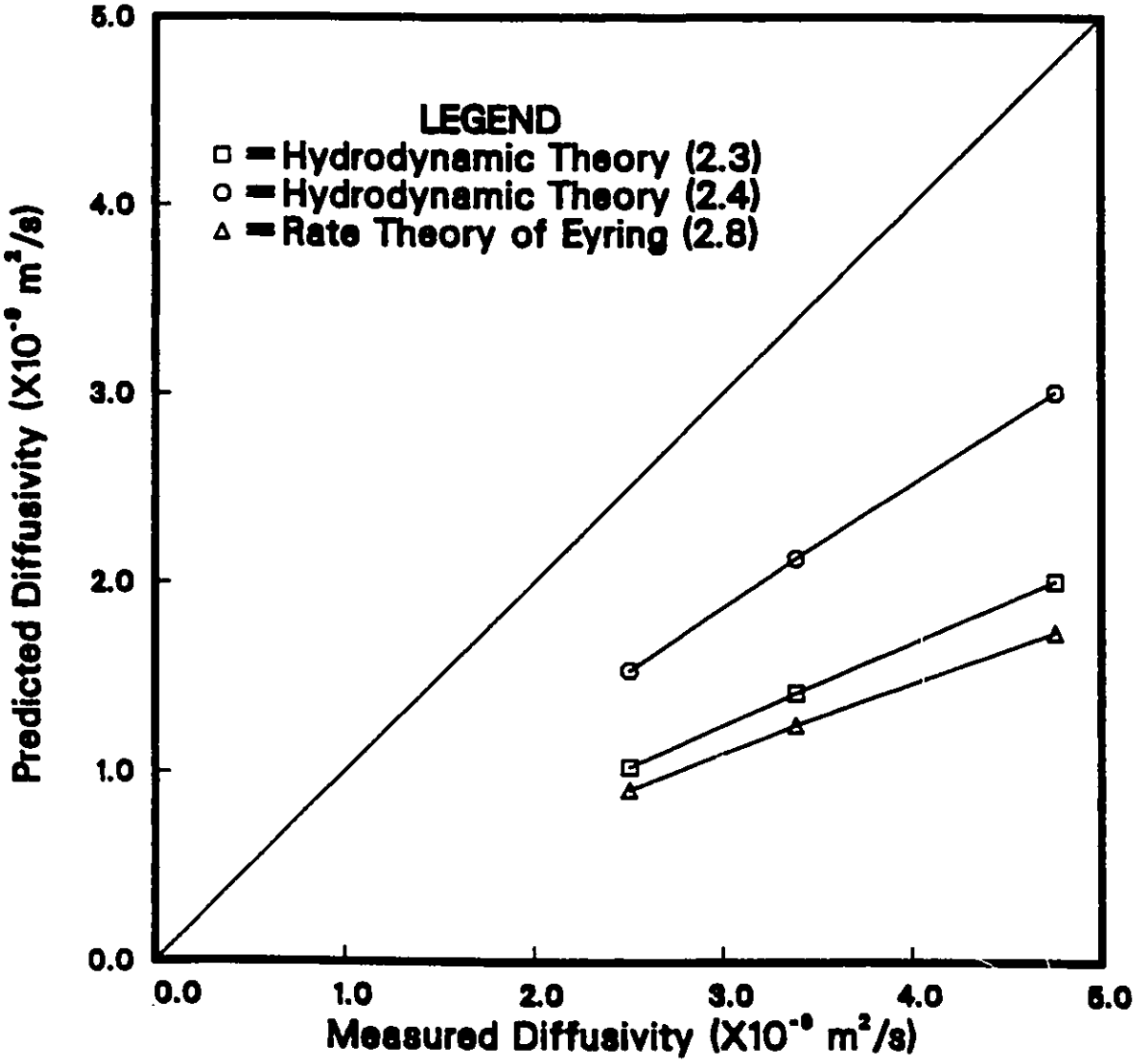

Figure H.6: Comparison of experimental diffusivity data with predicted results from the diffusion theories for propene in n-octane

Appendix I

Sample Calculation for the Determination of Diffusivity Measured by the Taylor Dispersion Method

A sample calculation to determine the diffusivity of propene in n-octane at 298.15 K and 103.4 kPa (15.0 psi) is illustrated as following:

- solute: propene (A)
- solvent: n-octane (B)
- experimental temperature: 298.15 K
- experimental pressure: 103.4 kPa (15.0 psi)
- radius of the capillary tube: 0.000380 m
- retention time t_R: 23448.5 sec
- width of half height $W_{1/2}$: 478.3 sec
- mean velocity of solvent v_m: 0.29 cm/s

The diffusivity of propene in n-octane measured by Taylor dispersion method is calculated by equation (5.45) as:

$$D^{\circ}_{AB} = 3.42 \times 10^{-9} m^2/s$$

Appendix J

Listing of the Solute-Solvent Systems Used for Development of a Correlation Based on the RHS Theory

SOLUTE	SOLVENT	TEMPERATURE(K)	REFERENCE
argon	n-butanol	298.15 - 433.15	[24], [27], [83]
	cyclohexane	298.15 - 415.85	[25], [83]
	decane	298.15 - 373.15	[26], [83]
	methanol	298.15 - 383.15	[27]
	n-octane	298.15 - 403.15	[26]
	n-octanol	298.15 - 430.15	[27], [83]
	tetradecane	298.15 - 430.15	[26], [83]
carbon dioxide	dodecane	304.15 - 567.15	[28]
	ethanol	279.55 - 303.15	[2], [5], [10], [71], [54]
	hexadecane	323.15 - 564.15	[28]
	toluene	298.15 - 323.15	[5], [148], [152], [153], [154]
carbon monoxide	dodecane	304.15 - 567.15	[28]
	n-heptane	298.15 - 427.15	[28]
	hexadecane	323.15 - 564.15	[28]
ethane	n-heptane	298.15 - 313.15	[54], [56]
ethylene	ethylene dichloride	288.15 - 303.15	[155]
	nitrobenzene	303.15 - 333.15	[155]
hydrogen	dodecane	303.15 - 567.15	[28]
	n-heptane	298.15 - 427.15	[28]
	hexadecane	323.15 - 564.15	[28]
krypton	n-butanol	298.15 - 433.15	[27], [83]
	cyclohexane	298.15 - 415.85	[25], [83]
	decane	298.15 - 433.15	[26], [11]
	methanol	298.15 - 383.15	[27], [83]
	n-octane	298.15 - 403.15	[26]
	n-octanol	298.15 - 430.15	[27], [83]
	tetradecane	298.15 - 374.15	[26], [83]
methane	n-butanol	298.15 - 433.15	[27], [83]
	cyclohexane	298.15 - 415.15	[25], [83]
	decane	298.15 - 433.15	[27], [83]
	dodecane	273.15 - 323.15	[57]
	n- heptane	277.15 - 311.15	[57], [98]
	methanol	298.15 - 383.15	[27], [83]
	n-octane	298.15 - 403.15	[26], [57]

SOLUTE	SOLVENT	TEMPERATURE(K)	REFERENCE
methane	n-octanol	298.15 - 430.15	[27], [83]
	tetradecane	298.15 - 430.15	[26], [83]
propane	n-butanol	273.15 - 323.15	[58], [140]
	chlorobenzene	273.15 - 323.15	[58]
propene	acetic acid	293.15 - 323.15	this work
	acetone	278.15 - 323.15	this work
	n-butanol	278.15 - 348.15	this work
	chlorobenzene	278.15 - 348.15	this work
	N,N dimethylformamide	278.15 - 323.15	this work
	ethyl acetate	278.15 - 323.15	this work
	ethylene glycol	298.15 - 348.15	this work
	n-octane	278.15 - 348.15	this work
xenon	n-butanol	298.15 - 433.15	[27], [83]
	cyclohexane	298.15 - 415.85	[25], [83]
	decane	293.15 - 433.15	[26], [83]
	methanol	298.15 - 383.15	[27], [83]
	n-octane	293.15 - 403.15	[26], [160]
	n-octanol	298.15 - 430.15	[27], [83]
	tetradecane	293.15 - 430.15	[26], [83]
chlorine	carbon tetrachloride	298.15 - 318.15	[35]

Table J.1: Experimental data used for development of a correlation based on the RHS theory